Sergey F. Sluzhenikin
Nadezhda A. Krivolutskaya
Viktor A. Rad'ko
Kreshimir N. Malitch
Vadim V. Distler
Valery A. Fedorenko

Ultramafic-mafic intrusions, volcanic rocks and PGE-Cu-Ni sulfide deposits of the Noril'sk Province, Polar Siberia

12th International Platinum Symposium

NORILSK NICKEL

Yekaterinburg
2014

Open Joint Stock Company «Mining and Metallurgical Company “NORILSK NICKEL”»
Joint Stock Company Noril’skgeologiya
Russian Academy of Sciences
Zavaritsky Institute of Geology and Geochemistry (IGG UB RAS)
Institute of Geology of Ore Deposits, Petrography, Mineralogy and Geochemistry (IGEM RAS)
Vernadsky Institute of Geochemistry and Analytical Chemistry (GEOKHI RAS)

Sergey F. Sluzhenikin,
Nadezhda A. Krivolutskaya,
Viktor A. Rad’ko,
Kreshimir N. Malitch,
Vadim V. Distler,
Valery A. Fedorenko

Ultramafic-mafic intrusions, volcanic rocks and PGE-Cu-Ni sulfide deposits of the Noril’sk Province, Polar Siberia

Edited by Oleg N. Simonov

FIELD TRIP GUIDEBOOK
July 31 – August 7, 2014

Yekaterinburg
2014

ББК 26.31

Sluzhenikin S.F., Krivolutskaya N.A., Rad'ko V.A., Malitch K.N., Distler V.V., Fedorenko V.A.

Ultramafic-mafic intrusions, volcanic rocks and PGE-Cu-Ni sulfide deposits of the Noril'sk Province, Polar Siberia. Field trip guidebook. 12th International Platinum Symposium (Edited by Simonov O.N.). Yekaterinburg: IGG UB RAS, 2014. 80 p.

ISBN 978-5-94332-111-5

This guidebook is dedicated to ultramafic-mafic intrusions, volcanic rocks and the world-class PGE-Cu-Ni sulfide deposits of the Noril'sk Province, Polar Siberia. The characteristics of geology, mineralogy and geochemistry of volcanic rocks and ore-bearing ultramafic-mafic intrusions are briefly outlined. The proposed excursion stops include inspection of the different volcanic and intrusive rocks, associated PGE-Cu-Ni sulfide ores from drill cores and bedrock outcrops. In addition, an open pit Medvezhy Ruchei and two mines (Oktyabrsky and Taimyrsky) collectively provide an overview of the Noril'sk-type intrusions and associated disseminated and massive PGE-Cu-Ni sulfide ores.

The materials of the guidebook are of a broad interest for geologists, earth scientists and students.

12th International platinum symposium is supported by Open Joint Stock Company «Mining and Metallurgical Company "NORILSK NICKEL"», Russian Foundation for Basic Research (grant 14-05-20091-g), and Federal Agency of Scientific Organizations (FASO)

ISBN 978-5-94332-111-5

TABLE OF CONTENTS

LIST OF FIGURES

LIST OF TABLES

INTRODUCTION

The Norilsk deposits occupy a very special place among igneous deposits associated with ultramafic-mafic complexes. Two main types, usually dissociated in natural objects, can be distinguished: essentially platinum-group element (PGE) deposits in large layered plutons (Bushveld, Great Dyke, Stillwater, etc.) and PGE-copper-nickel sulfide deposits (Sudbury, Voisey's Bay, Jinchuan, Duluth, etc.). The Norilsk deposits have both ore types combined within a single intrusive body (i.e., copper-nickel sulfide, also enriched with platinum group elements (PGE) and low-sulfide platinum). They are fundamentally different from the other magmatic deposits of the world by their younger age (the Early Triassic compared with the Proterozoic for most similar objects) and confinedness to relatively thin intrusions, as distinct from the usual association of this type deposits with large layered plutons.

Despite the fact that PGE-copper-nickel ores in the Norilsk area have been prospected since the early twenties of the last century (*Sotnikov*, 1919; *Kotulsky*, 1946; *Rogover*, 1959; *Godlevsky*, 1959; *Korovyakov*, *et al.,* 1963), and their processing provided the country with a strategically important metals during the war (the first nickel was obtained at the Norilsk plant in 1942), but only the discovery of the Talnakh and Oktyabrsky ore fields with unique deposits of sulfide ores with high PGE content brought former USSR in the early 60's to the leading position in the world platinum and nickel industry (*Egorov & Sukhanova*, 1963; *Vaulin & Sukhanova*, 1970; *Kravtsov*, 2003).

At present, Russia ranks second in the world in both reserves and production of platinum-group metals and nickel after Bushveld (South Africa), and Sudbury (Canada), respectively (*Naldrett*, 2004; *Butler*, 2012). The basis of the OJSC MMC Norilsk Nickel (that owns the main fields of the area) raw materials are sulfide Cu-Ni PGE ores of the Norilsk and Talnakh ore clusters. The Oktyabrsky, Talnakh and Noril'sk 1 ore bodies are being mined primarily to produce nickel and copper with PGE as a by-product. Currently, 96% of produced metals are extracted from ores of the Talnakh ore cluster (TOC) and only 4% from disseminated ores of the Norilsk ore cluster (NOC). The TOC ores are mined by five underground mines (i.e., Oktyabrsky, Taimyrsky, Komsomolsky, Skalisty and Mayak), while the NOC ores are mined in two mines (Zapolarny and Medvezhy Ruchey). Enrichment at metallurgical facilities in the Noril'sk-Talnakh area results in nickel, copper and pyrrhotite concentrates which are then converted to high-grade matte.

GEOLOGY AND MAGMATISM

General geology and deep structure of the Noril'sk district

The Norilsk ore district is located in the northweastern part of the Siberian platform (Fig. 1). In the west and north it is limited by the Enisei and Enisei-Khatanga troughs, and in the east by the Tunguska syneclise. In tectonic respect it forms an independent unit with a reduced thickness of the continental crust, consisting of crystalline basement and sedimentary-volcanogenic platform cover.

The geologic setting (Fig. 1), morphological, lithologic, petrographic and isotope-geochemical features of ultramafic-mafic intrusions and closely linked PGE-Cu-Ni deposits have been described in detail among others by *Godlevsky* (1959), *Distler et al.* (1988; 1999), *Likhachev* (1994), *Lyul'ko et al.* (1994; 2002), *Czamanske et al.* (1994; 1995), *Sluzhenikin et al.* (1994), *Walker et al.* (1994), *Komarova et al.* (2000; 2002), *Tuganova* (1991; 2000), *Turovtsev* (2002), *Tuganova & Shergina* (2003), *Arndt et al.* (2003), *Naldrett* (2004), *Yakubchuk & Nikishin* (2004), *Latypov* (2002; 2007), *Petrov et al.* (2009), *Malitch et al.* (2010a; 2010b) and *Krivolutskaya* (2014).

The insight of the deep territory structure is based on deep seismic profiles Vorkuta-Tiksi and Dikson-Khilok. Using seismic data (*Egorkin et al.*, 1984; *Malitch et al.*, 1987), a transition zone has been identified at the base of the crust in the Noril'sk region, with higher velocities of longitudinal waves (Vp; 7.3 km/s) than those typical for the crust (Fig. 2). This zone has been considered as a manifestation of ultramafic material injected in the subcrustal levels of the lithosphere (*Tuganova,* 1991). The thickness of this zone is 5-10 km, with a spatial extent of about 500 km at depths of 32-43 km. Most likely, a large volume of ultramafic-mafic material rich in sulfides preceded tholeiite-basaltic volcanism, which contributed to the removal of these bodies to form relatively small hybrid "layered" intrusions. It is noteworthy that the location of economic intrusions is restricted to the region above mentioned transition zone, which is considered a typical feature of the basal part of the crust from oceanic and continental paleorifts (e.g., *Ramberg & Morgan*, 1984; *Malitch et al.* 1987).

The analysis of the deep structure of the Noril'sk area (Fig. 2) suggest a connection between the formation of PGE-Cu-Ni deposits in paleorift structures and particular geological and geophysical parameters (*Tuganova*, 2000). These include high-gradient downfolds in the basement, a high abundance of horst-graben structures in the crust, large volumes of intruded mass of mantle material between the crust and mantle. In general, the deep structure of the Noril'sk area shows non-cratonic features with a differentiated crust of transitional type (*Malitch et al.*, 1988).

The platform cover in the Noril'sk-Igarka district is subdivided into several structural stages and substages (Fig. 3). The so-called transitional stage at its base consists of complexly deformed but only weakly metamorphosed Riphean sedimentary and volcanic rocks about 3500 m in apparent thickness dated back to 670-900 Ma. The medium-sized copper sandstone deposits are hosted in these rocks.

The plate stage is subdivided into three substages separated by structural and stratigraphic unconformities. *The lower substage* that corresponds to the Caledonian-Early Hercynian tectonic cycle comprises the Vendian-Lower Carboniferous marine sequences 3-8 km in total thickness. Carbonate rocks (dolomite, limestone, and marlstone) are predominant; terrigenous rocks (mudstone and siltstone) and evaporites (anhydrite and rock salt) are noteworthy. Anhydrite occurs in the Vendian, Middle Ordovician, Upper Silurian, and is abundant throughout the Devonian-Lower Carboniferous section (Fig. 3).

The Devonian-Lower Carboniferous rocks are represented by two types of sequences: sulphate-carbonate or halogenic-sulphate-carbonate of increased thickness, and carbonate of reduced thickness. The thick sequences are developed in the Noril'sk – Kharaelakh Trough in the west and the Lama-Khantaika Trough in the east. The sequences reduced in thickness are typical of the Dudinka Uplift close to the present-day Khantaika-Rybny Swell and somewhat shifted to the west of the latter.

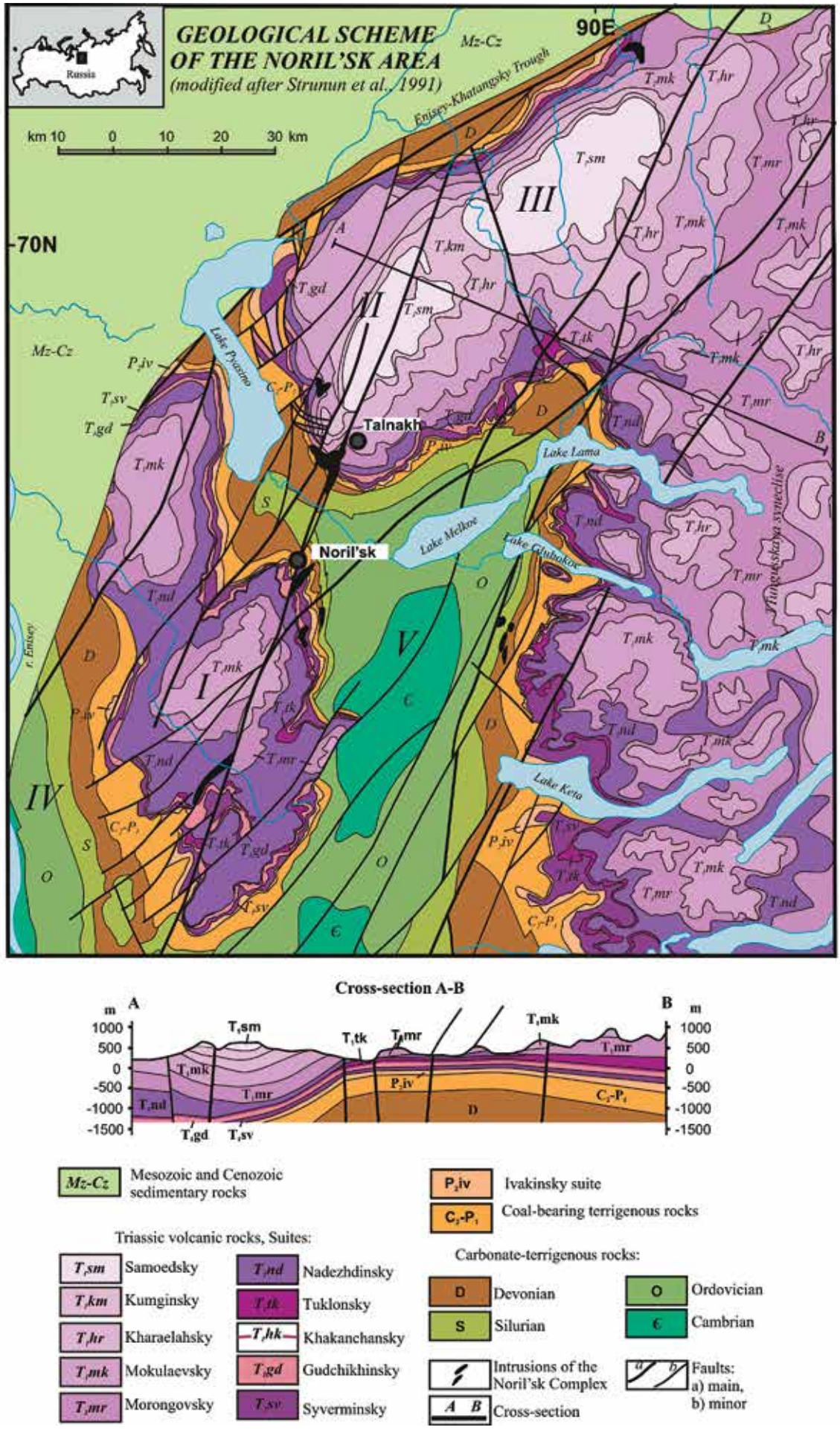

Fig. 1. Geological scheme of the Noril'sk area (modified after *Strunin et al*., 1991)

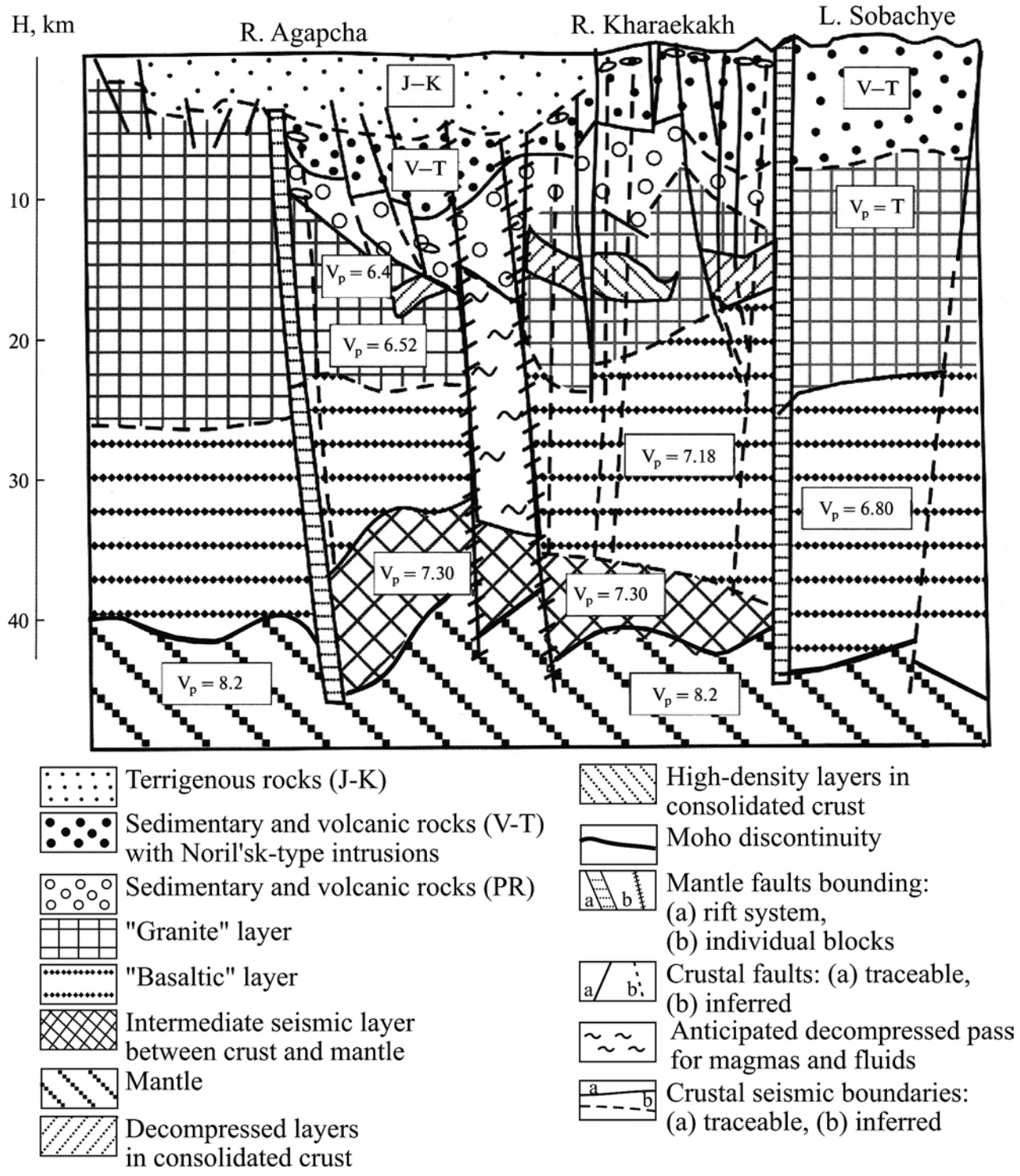

Fig. 2. Geoseismic section according to profile Dikson – Khilok (modified after *Egorkin et al.*, 1984; *Mitrofanov et al.*, 2013)

The second structural substage corresponds to the Late Hercynian tectonic cycle and comprises the sedimentary rocks of the Middle Carboniferous-Upper Permian Tunguska Group and flood basalts of the Late Permian-Early Triassic age; their total thickness reaches 4 km. The deposition of these sequences was related to the rifting that marked the onset of the formation of global systems of oceanic rifts. The rifting in the northwestern Siberian Platform was combined with dispersed rifting responsible for eruptions of flood basalts.

The Tunguska Group overlaps the underlying rocks of the lower structural stage with appreciable angular unconformity. The group consists of rhythmically alternating coal-bearing terrigenous rocks

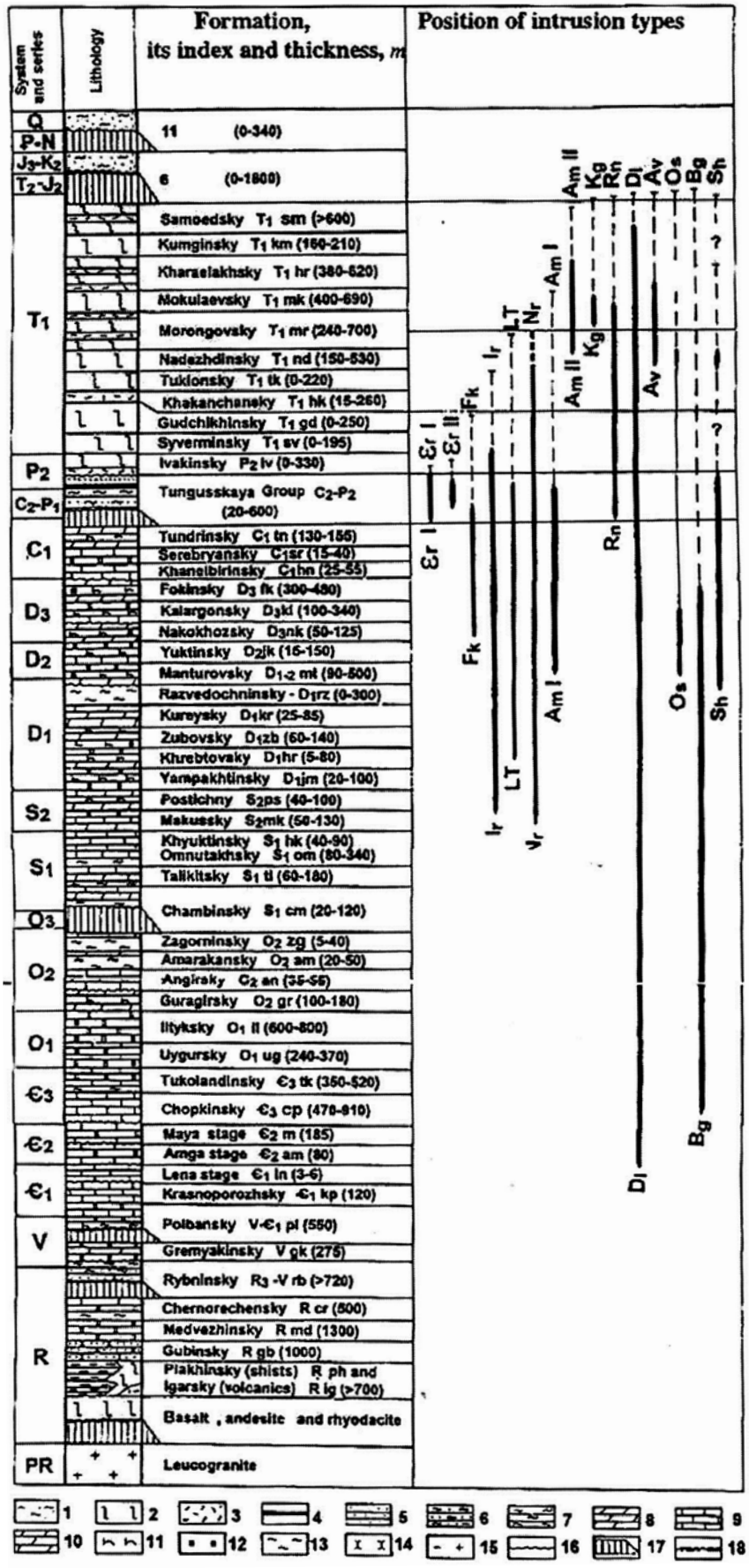

Fig. 3. Stratigraphic section of the Noril'sk ore district.
1 – terrigenous sediments; 2 – basalt; 3 – tuff; 4 – coal; 5 – sandstone; 6 – siltstone; 7 – mudstone and shale; 8 – marl; 9 – limestone; 10 – dolomite; 11 – anhydrite; 12 – salt; 13 – shist; 14 – quartz sandstone; 15 – leucogranite; 16 – erosion; 17 – angular unconformity; 18 – hiatus. Solid vertical lines on the right show position of intrusions in stratigraphic section; dashed lines show inferred relationships between volcanics and intrusions. See text for indices that denote intrusions

and coal seams with working thickness from 0.5 to 12-15 m, which make up the Noril'sk coal basin, one of the largest in Russia. The thickness of the Tunguska Group varies from 20-40 m at swell crests to 600 m in the axial zones of troughs.

The volcanic sequence from a few meters to 200-300 m thick overlies the Tunguska Group. The volcanic eruptions initiate the epoch of intense tectonic activity, which fell on the period from the Early Triassic to the Middle or Late Jurassic. The troughs and uplifts up to a few thousand meters in amplitude broadly inherited the Early Hercynian tectonic units, but became much more contrasting, complexly built, and dismembered. The main structural features include the Tunguska Syneclise, Kharaelakh, Vologochan, and Noril'sk synclines filled with sedimentary rocks of the Tunguska Group and younger volcanics. The Dudinka and Khantaika-Rybny swells and the Kayerkan-Pyasino Anticline are composed of the Lower and Middle Paleozoic rocks; the Riphean and Vendian rocks occur in the Igarka Inlier (Fig. 1). Most structural features (Khantaika-Rybny Swell, Kharaelakh and Noril'sk synclines, etc.) are NNE- and NE-trending. Some smaller features, e.g., the Kayerkan-Pyasino Anticline, are oriented in the NNW direction.

The numerous faults follow the same orientation. The Noril'sk-Kharaelakh Fault, the main ore-controlling tectonic line of the district, strikes in the NNE direction. Some faults, including the Noril'sk-Kharaelakh Fault, extend down to the lower crust and even transect the Moho surface (Fig. 2). At the same time, many auxiliary faults wane with depth. They commonly flatten in the units of plastic rocks (Tunguska Group, the Devonian Razvedochninsky Formation, and others) and are transformed into bedding-plane detachments. As a result, rootless grabens, or so-called sagging structures develop. They are especially characteristic of the Talnakh ore cluster.

The upper structural substage that corresponds to the Kimmerian tectonic cycle is composed of Jurassic and Cretaceous marine and continental terrigenous rocks overlapped by Quaternary sediments (Fig. 3). In the Noril'sk district, the Mesozoic section begins from the Upper Jurassic and reaches 1800 m in thickness. In the central West Siberian Plate and the Yenisei-Khatanga Trough, sedimentation started in the Early Jurassic, and total thickness of the Jurassic and Cretaceous sequences reaches 5 km. These sequences serve as repositories of the enormous petroleum resources of Russia. The northwestern part of the Siberian Platform was uplifted and underwent erosion throughout the Kimmerian cycle.

Flood basalts of the Noril'sk district

The Noril'sk district is a part of the world largest Siberian flood-basalt province that occupies about four million square kilometers. The Noril'sk district is distinguished by the Siberia greatest thickness of the volcanic sequence, which reaches 3500 m; lavas prevail over tuffs and intrusive trap rocks. The lavas and associated intrusive bodies, including ore-bearing ultramafic-mafic intrusions, are diverse in composition.

The volcanic sequence is represented by alternating lava flows and pyroclastic members in proportion of 9:1. More than 200 lava flows and about 30 tuff members are numbered. The thickness of separate flows varies from 1 to 100 m and is 15 m on average. The tuff members range in thickness from a few ten centimeters to 50-100 m (occasionally they are as thick as 200-400 m). The lava flows composed of the same rocks often group into packets from a few ten to a few hundred meters thick. Particular flows of such packets commonly pinch out for a short distance; however, some key flows are traceable for tens and a few hundred kilometers. Some pyroclastic units are as long as lava flows.

The comprehensive geochemical and isotopic characteristics of lavas are given *by Dyuzhikov* (1971), *Dyuzhikov et al.* (1988), *Zolotukhin et al.* (1978), *Ryabov et al.* (1977, 2000)*, Fedorenko* (1981), *Lightfoot et al.* (1990, 1993, 1994), *Naldrett et al.* (1992), *Wooden et al.* (1993), *Krivolutskaya* (2014) among others.

The lavas vary in composition from picrobasalt to trachybasalt and basaltic andesite. The ranges of major oxide contents are as follows (wt. %): 2-20 MgO, 45-55 SiO_2, 0.5-4.0 TiO_2, and 0.05-3.5 K_2O. The chemical composition of basaltic rocks in vertical sections of flows changes insignificantly; only volatile components concentrate in the upper portions of lava flows. The picrobasaltic flows reveal a more pronounced vertical differentiation. Plagioclase, clinopyroxene (augite and less abundant ferroaugite), and olivine are major rock-forming minerals in lavas. The volcanic glass amounts to 5–30 vol. % in massive lavas and to 50 vol. % and more in amygdaloid lavas.

The volcanic rocks are slightly altered under conditions of zeolite facies of metamorphism. Some flows in the lower part of the section, in particular, tholeiitic basalts underwent appreciable albitization. Volcanic glass is replaced by opacite and chlorite. Olivine is partly or completely replaced with iddingsite-boulingite and serpentine-chlorite; plagioclase is saussuritized and albitized; clinopyroxene is altered to the least extent.

The stratigraphic section of the volcanic sequence is represented in Fig. 3; its detailed description has been given *by Zolotukhin et al.* (1978). The sequence is divided into 11 suites (from bottom to top): Ivakinsky (Iv), Syverminsky (Sv), Gudchikhinsky (Gd), Khakanchansky (Hk), Tuklonsky (Tk), Nadezhdinsky (Nd), Morongovsky (Mr), Mokulaevsky (Mk), Kharaelakhsky (Hr), Kumginsky (Km), and Samoedsky (Sm); some of them are subdivided into subsuites.

The sections of volcanic sequence are persistent in the lateral direction; many suites and subsuites are traceable throughout the territory. The chemical composition of lavas belonging to the particular stratigraphic subdivisions commonly remains stable. Picrobasalts of the Upper Gudchikha Subsuite reveal a wide range of olivine fractionation.

The U-Pb age of zircon from leucogabbro of the Norilsk-I intrusion estimated at 248 ± 4 Ma (*Campbell et al., 1992*) and $^{40}Ar/^{39}Ar$ age of biotite from ore vein in the same intrusion measured at 248.7 ± 2.4 and 249.2 ± 2.4 Ma (*Dalrymple et al*., 1991) fit the Permian/Triassic boundary (251.4 ± 4 Ma). The $^{40}Ar/^{39}Ar$ ages of plagioclase fractions and whole rock samples of volcanic rocks from the Ivakinsky, Syverminsky, Gudchikhinsky, and Kharaelakh formations are virtually the same (243.5-245.3 Ma). Thus, the age of lavas cut through by the Norilsk-I intrusion (Ivakinsky-Nadezhdinsky formations) cannot be much younger than the Permian/Triassic boundary. The volcanic sequence overlies the sedimentary rocks of the Tunguska Formation with signs of unconformity; the depth of erosion varies from a few meters to 200-300 m. No levels of weathering are documented within the volcanic sequence. Moreover, the lavas buried so fast that the upper amygdaloid portions of flows are nearly always retained, often with clearly expressed upper crusts.

Judging by paleontological and geochemical evidence, the tuff-bearings units up to the middle of the Morongovsky Formation were deposited in the shallow-water lakes or marine lagoons (*Fedorenko,* 1991). The deposition was compensated completely by subsidence with maintenance of plain topography at the same level. Tuffs and lavas of the upper part of the volcanic sequence were formed under subaerial conditions. Some overcompensation of subsidence by accumulation of volcanic rocks took place during this period. However, the absence of distinct erosion landforms indicates that the overcompensation was not significant, and the plain topography was not modified. The high rate of compensated subsidence (3500 m over 1 Ma) was likely caused by exhausting of underlying magma chambers.

At present, the volcanic sequence fills the Tunguska Syneclise and a number of synclines that frames it in the north and west (Fig. 1). These structural units are postvolcanic, and originally the lavas covered the entire territory of the Noril'sk district, at least, to the west of the Yenisei River (*Fedorenko,* 1991). The initial attitude of volcanic rocks was markedly different from its present-day occurrence. The substantial structural rearrangements along with retention of the uniform tectonic regime are probably accounted for by relations of each volcanic association with self-dependent magma sources represented by near-horizontal transitional chambers localized within the crust (*Fedorenko,* 1994).

Intrusive complexes

The intrusive bodies occupy 6.6 vol. % of igneous rocks known in the Noril'sk district. They are similar to volcanic rocks in chemical and modal compositions. A single granodiorite stock in the western Vologochan Syncline and dikes of the peculiar mica lamprophyres in the northern Noril'sk Syncline are only exceptions.

The alkaline, subalkaline, and basic rocks are uniform in composition throughout intrusions, and only pegmatoid lenses enriched in Fe, Ti, and incompatible elements occur close to the upper contacts of thick bodies. The intrusions with elevated MgO content (8-10%) underwent fractionation with enrichment of their lower portions in olivine. Many layered intrusions contain sulfide disseminations and segregations of massive sulfides. The relative mass of sulfides is insignificant and commonly does not exceed hundredths of percent, however, amounts to 3-7 wt. % in the Talnakh and Kharaelakh ore-bearing intrusions (with account of massive ore). The uppermost portions of near-surface intrusions, both undifferentiated and layered, are enriched in amygdules.

Most intrusions are sheet-like. Undifferentiated intrusive bodies are largely represented by sills isometric in plan view; their thickness varies from a few meters to 100 and occasionally 150-220 m. In swells, the sills become laccolith-shaped. The separate sills extend for kilometers or a few tens of kilometers. The rocks of the same composition often fill several sills closely spaced in stratigraphic sections; the extent of such packets may be more than 150 km. The differentiated sheet-like intrusions are commonly ribbon-shaped in plan and extend as far as 20 km.

The sills residing in sedimentary sequences as if pull apart the country rocks, whereas the thick differentiated ore-bearing bodies eliminate the country rocks previously occupied their space. The nature of this phenomenon remains unclear, especially with allowance for absent of signs of crustal contamination of magma chambers except for their contact zones. The geochemical signatures of intrusions remain the same irrespective of lithology of country rocks.

Dikes are less abundant than sills. They are variously oriented and commonly steeply dipping; their thickness measured by meters and tens of meters. A dike as thick as 300 m and 10 km long is known in the core of the Kharaelakh Syncline. The maximum length of dikes reaches 50-70 km.

Some postvolcanic intrusions make up complex multistage systems, where sills pass from one stratigraphic level to another, being connected with steep dikes or inclined (20°-70°) conduits.

The dikes cut through the entire stratigraphic section from the Cambrian rocks to the uppermost volcanic units. Sills, with a few exceptions, are localized below the volcanic sequence; while appearing within this sequence they commonly propagates along tuffaceous units. The overwhelming majority of sills are localized in the upper part of sedimentary sequence at a distance no farther than 1-2 km below the sole of volcanic pile. No sills were penetrated by wells drilled for oil at deep levels of the sedimentary platform cover.

Classification of intrusions

Fifteen types of intrusions are recognized in the Noril'sk ore district by geochemical signatures, isotope ratios, and other featutres (*Fedorenko, 1981, 1994*). By composition, they make up four groups: granodiorite, mica lamprophyres, basic and differentiated ultramafic-mafic intrusions.

Granodiorite is represented by a single *Bolgoltokh type (Bg)*. The Bolgoltokh stock is located in the western Noril'sk district, where it cuts through the Lower and Middle Paleozoic sedimentary rocks. This stock 2.2-2.3 km in diameter is penetrated by boreholes to a depth of about 2 km. The rock contains (wt. %) 63-71 SiO_2, 3.0-4.5 Na_2O, 4.0-6.5 K_2O, and 0.2-0.7 P_2O_5. Granodiorite is characterized by very high Ce/Yb and La/Sm ratios, very low Yb/Gd ratio and low ε_{Nd}. The $^{40}Ar/^{39}Ar$ age of biotite equals 223.2 Ma. The Bolgokhtokh Granodiorite probably is the youngest igneous rock in the Noril'sk district.

Mica lamprophyres represent the *Ostrogorsky type (Os)* of igneous rocks known in the northern Noril'sk Syncline. They occur as near vertical dikes up to 1-2 m thick that cross the Devonian rocks, sedimentary rocks of the Tunguska Group, and volcanic sequence up to the Nadezhdinsky Suite. The rocks contain (wt. %) 45-52 SiO_2, 1.0-1.4 TiO_2, 5.6-8.0 MgO, 1.0-1.3 Na_2O, 5-8 K_2O, and 1-2 P_2O_5. They reveal anomalously high Ce/Yb and La/Sm ratios, low Yb/Gd ratio, and low ε_{Nd}. The ultrapotassic composition of these dikes together with high Cr concentrations (270-370 ppm) indicates that they are compositionally close to lamproites. The data on lamprophyre age are not available; dikes cut through the upper lava units and thus are probably postvolcanic.

Mafic intrusions are subdivided into eight types: *Ergalakh-I (Er-I),* alkaline, high-Ti basic rocks; *Ergalakh-II (Er-II)* and *North Kharaelakh (NKh),* subalkaline, high-Ti basic rocks; *Avamsky (Av),* basic rocks of normal alkalinity; *Irbinsky (Ir), Ambarninsky-I (Am-I), Ambarninsky-II (Am-II),* and *Daldykansky (Dl),* low-Ti basic rocks of normal alkalinity. Most intrusive rocks occur as sills and dikes (*Av* and *Am-II*) or their combinations (*Dl*). Position of intrusions in stratigraphic section is shown in Fig. 3.

Five of the above-listed types are comagmatic to certain lava units: Er-I type corresponds to trachybasalt Iv_1; Er-II type to Ti-augite basalt Iv_2; Ir type to Tk lava; Am-I to basalt Mr_2-Mk; Am-II type to basalts Hr-Sm. The comagmatic intrusive and volcanic rocks are identical to one another by concentrations of major and minor elements, ratios of incompatible elements, and by magnetic properties.

Differentiated mafic-ultramafic intrusions. Three groups of spatially and genetically related intrusions are distinguished by character of macroscopic and cryptic layering and bulk composition: (1) Noril'sk (Nr), or Noril'sk-Talnakh type of mesocratic intrusions with contrasting cryptic layering; (2) Zubovsky (Zb) and Kruglogorsky (Kg) types of leucocratic intrusions with poorly developed cryptic layering; and (3) Lower Talnakh (LT), Fokinsky (Fk), and Morongovsky (Mr) types of melanocratic intrusions.

The economic PGE-Cu-Ni sulfide deposits are related to the mesocratic intrusions of Nr type. The leucocratic differentiated intrusions of Zb and Kg types contain subeconomic PGE-Cu-Ni sulfide deposits and ore occurrences. The melanocratic differentiated intrusions of LT and Mr types contain sulfide mineralization devoid of economically valuable components and sporadic small occurrences.

The mesocratic and melanocratic intrusions, as well as leucocratic intrusions of the Kruglogorsky type are controlled by the Noril'sk-Kharaelakh Fault Zone in contrast to other leucocratic intrusions, which are widespread throughout the Norisl'sk district (Fig. 4).

The Noril'sk type (Nr). The Talnakh, Kharaelakh, and Norils'k-1 intrusions and associated economic PGE-Cu-Ni sulfide deposits belong to this group, as well as Norilsk-2, Chernogorsk (Chernaya Mountain), and probably Imangda intrusions with subeconomic ore mineralization. The completely differentiated bodies are accompanied by poorly differentiated offsets. Intrusions of this type are ribbon-shaped (length:width:thickness = 100:10:1). Their extent reaches 20 km, the width is 1-2 km, and thickness is 250-350 m.

Several groups of differentiated rocks are recognized in the mesocratic intrusions of the Noril'sk type. The *upper gabbroic group* comprises eruptive breccia, hybrid and contaminated rocks, contact gabbrodolerite, leucogabbro, chromite-bearing taxitic gabbro, and gabbrodiorite. The *main layered series* consists of quartz-bearing, olivine-free, olivine-bearing, olivine, olivine-biotite, and picritic gabbrodolerites. Horizon of so called picritic gabbrodolerites is represented by ultramafic rocks composed of sulfide-bearing werhlite, plagiodunite and troctolite. *The lower gabbroic group* is composed of taxitic and contact gabbrodolerites, quartz norite and gabbronorite, contaminated and hybrid-metasomatic rocks with hornfels xenoliths. Commonly taxitic-textured rocks are represented by olivine gabbro and troctolite together with "patches" of ultramafic rocks. Composition of the main layered series in different intrusions of the Noril'sk type varies insignificantly in contrast to the rocks of the upper and lower groups, the composition of which varies considerably depending on compositions of country rocks. The MgO content ranges from 3.5 to 28 wt. %, the weighted average value is 10-12 wt. %.

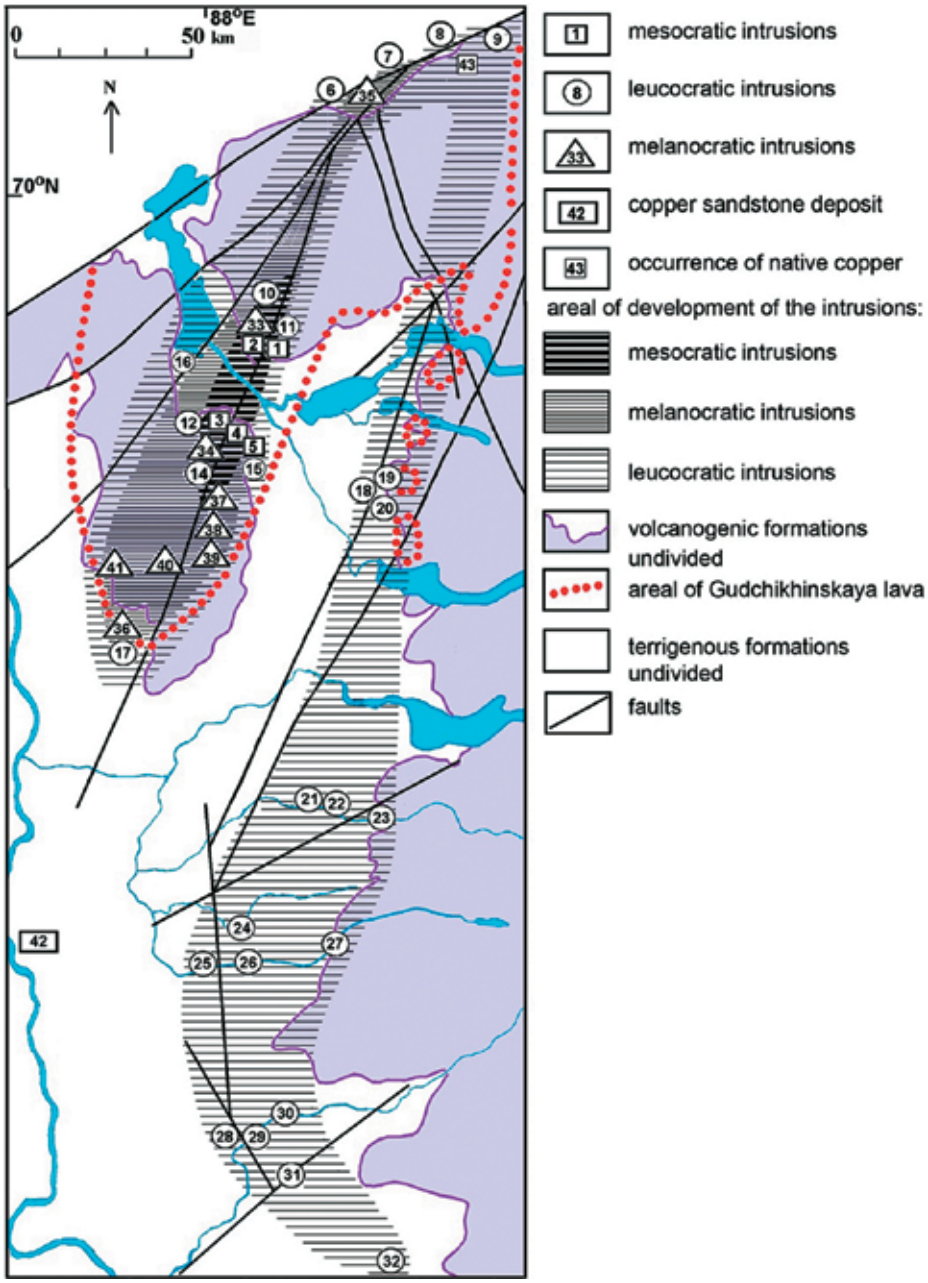

Fig. 4. Distribution of the mafic-ultramafic intrusions in the Noril'sk region.
Mesocratic ore-bearing intrusions: 1 – Talnakh, 2 – Kharaelakh, 3 – Norilsk 1, 4 – Norilsk 2, 5 – Chernogorsk; leucocratic weakly-mineralised intrusions: 6 – Tal'minsky, 7 – Ikonsky, 8 – Yttakhsky, 9 – Arylakhsko-Mastakhsalinsky, 10 – Tangaralakhsky, 11 – Gabbrovy, 12 – Zubovsky, 13 – Verkhneambarninsky, 14 – Verkhnebystrinsky, 15 – Kruglogorsky, 16 – Pyasino-Vologochansky, 17 – Burkansky, 18 – Imangdinsky, 19 – Manturovsky, 20 – Nakokhozsky, 21 – Verkhneiltyksky, 22 – Siluriisky, 23 – Kulyumbinsky, 24 – Brussky, 25 – Nizhnegorbyachinsky, 26 – Dzhaltulsky, 27 – Verkhnegorbyachinsky, 28 – Nizhny, 29 – Svetlogorsky, 30 – Second rapids of Kureika River, 31 – Okunevoozersky, 32 – Kotuisky; melanocratic barren intrusions: 33 – Nizhnetalnakhsky, 34 – Nizhnenorilsky, 35 – Klukvenny, 36 – Zelenogrivsky, 37– Picritovy Creek, 38 – Morongovsky, 39 – Magnitny Creek, 40 – Picritovaya Gora, 41 – Nizhnefokinsky, 42 – Sukharninskoe copper deposit; 43 – Arylakhskoe occurrence of native copper

The disseminated sulfide ores are confined to the lower portions of intrusions that are composed of picritic and taxitic gabbrodolerites. The low-sulfide PGE ore is confined to the upper contact zone. The layers of massive sulfides are localized near the lower contact largely in the country rocks and less frequently in the intrusion itself.

The intrusions of the Noril'sk type are distinguished by high Cr and K contents. The Cr content widely varies throughout the intrusions from the detection limit to a few percents. The K_2O contents vary from 0.2 to 2.0 wt. % and, in general, increase upward along with decrease in MgO content. The Noril'sk-type intrusions are close to the late tholeiitic lavas Mr_2-Sm in REE patterns, Th/U and Ta/La ratios but differ in elevated $^{87}Sr/^{86}Sr$ ratio.

The LT and Nr intrusions are close in age as indicated by the results of isotopic timing and geological relationships between intrusive bodies. The direct contacts of these intrusions in the Talnakh ore field are not accompanied by chilled margins, but the Nr intrusion is somewhat younger. The pegmatoid veins related to the Talnakh intrusion (Nr type) penetrate into the Lower Talnakh intrusion (LT type), and the ore mineralization related to the Talnakh intrusion is superimposed on the roof of the Lower Talnakh intrusion.

The intrusions of Nr type are accompanied by contact-metasomatic aureoles as thick as 250 m; the thickness of these aureoles is often greater than the thickness of intrusions themselves (*Turovtsev, 2002*). These aureoles are high-temperature metamorphic and metasomatic complexes that consist of hornfels and marble of spurrite-merwinite, pyroxene, amphibole, and muscovite facies of contact metamorphism subsequently replaced with alkaline metasomatic rocks, magnesian and calc-skarn, postskarn metasomatic rocks of various compositions, and products of low-temperature hydrothermal alteration.

The first U-Pb data for the Noril'sk-type intrusions [a SHRIMP study by *Campbell et al.* (1992) and an ID-TIMS study by *Kamo et al.* (1996)] analysed zircon and baddeleyite from pegmatitic leucogabbro of the Noril'sk-1 intrusion. The U-Pb data presented by *Campbell et al.* (1992) gave a range of $^{206}Pb/^{238}U$ ages from 243.8 ± 4.9 to 251.6 ± 5.0 Ma, with a mean of 248 ± 3.7 Ma. U-Pb results presented by *Kamo et al.* (1996) gave an even broader range of $^{206}Pb/^{238}U$ ages. These authors show (Fig. 2, p. 3508) that all the analyses (n=10) gave a maximum $^{206}Pb/^{238}U$ age of 256.5 ± 2.6 Ma, whereas nine tightly clustered analyses of zircon and baddeleyite produced an average $^{206}Pb/^{238}U$ age of 251.2 ± 0.3 Ma. The variability of the U-Pb ages obtained by both techniques on the same lithology is striking and could be due to the multistage growth nature of the zircon studied. A recent U-Pb study of baddeleyite and zircon from the main lithological units of the Noril'sk-1 intrusion (*Malitch et al.,* 2012) confirmed the polyphase nature of zircons and identified five age clusters that span from 290 ± 2.8 to 226.7 ± 0.9 Ma (i.e. 290 ± 2.8, 261.3 ± 1.6, 245.7 ± 1.1, 236.5 ± 1.8 and 226.7 ± 0.9 Ma). Multiple crystallization ages of baddeleyite and zircon were suggested to reveal several stages of protracted evolution of the ore-forming magma and/or to characterize interaction between isotopically distinct magmas during formation of the Noril'sk-1 intrusion. The oldest concordant $^{206}Pb/^{238}U$ age of 1914 ± 92 Ma (Fig. 5 in *Malitch et al.,* 2012) was for a zircon grain from the gabbro-diorite. This age suggests that zircon has been inherited from 1.9 Ga basement rocks, which may imply a deep-seated location of the chamber for the magmatic protolith.

The Zubovsky type (Zb) of differentiated intrusions comprises a large group of intrusive bodies in the central Noril'sk district, the northern Kharaelakh Syncline, and the Putorana Plateau. Some poorly studied intrusions in the Kulyumbe River and Kureika River basins are probably also related to this type. The intrusions of Zb type, having much in common with mesocratic intrusions of Nr type, are characterized by the following specific features:

(1) predominance of troctolite and limited occurrence of picritic gabbrodolerite units or their absence in the ultramafic zone;

(2) hanging position of picritic gabbrodolerite and troctolite units relative to the olivine and olivine-bearing gabbrodolerites, often with several horizons of olivine cumulus;

(3) poorly developed unit of taxitic gabbrodolerite or its absence;

(4) abundant leucocratic hybrid-metasomatic rocks and hybrid quartz- and cordierite-bearing norite and gabbronorite at the contacts with aluminosilicate sequences;

(5) low-grade ore disseminations hosted in troctolite and picritic units and virtually complete absence of massive ore;

(6) zonal aureoles of contact metamorphism commensurable with intrusions in thickness and insignificant occurrence of metasomatic alteration.

In general, the intrusions of Zb type are characterized by elevated silica content, enrichment in Fe and Ti in combination with low Mg content in comparison with Nr-type intrusions. The total of $Na_2O + K_2O$ is markedly elevated with prevalence of sodium in rocks of the main layered series and potassium in the upper gabbroic group as a result of metasomatic alteration at the late- and postmagmatic stages. The Cr_2O_3 content (<0.12 wt. %) in picritic gabbrodolerite is much lower than in similar rocks of the Nr-type intrusions.

The contact metamorphic aureoles related to the Zb-type intrusions bear many features similar to the aureoles of Talnakh and Lower Talnakh types but differ from the latter by a greater abundabce of amphibole hornfels and poorly developed superimposed metasomatic alteration. As a result, the hornfels and skarn mineral assemblages are retained better.

The Kruglogorsky type (Kg) combines the intrusions localized nearby the Noril'sk-Kharaelakh Fault Zone, largely in its eastern wall. The sill-like intrusions 10-30 m thick occupy rather large areas at flanks of the Noril'sk and Talnakh ore fields and in the North Kharaelakh and South Fokinsky areas.

The upper units of intrusions consist of leucogabbro, while the lower units, of olivine and olivine-bearing gabbrodolerites. Thin units of picritic gabbrodolerite with economic sulfide disseminations appear sporadically. The contact aureoles are characterized by a combination of pyroxene hornfels and skarn, and medium-temperature postskarn metasomatic alteration.

The Lower Talnakh type (LT) also termed as ***Nizhny Talnakh type*** is represented by high-Mg sulfide-bearing intrusions with low Cr and Ni content combined with enrichment in K. Such intrusions are localized solely in ore fields of the Noril'sk-Kharaelakh Fault Zone. The sheet-like intrusions with swells up to 400 m in thickness are framed at flanks by thin sills of olivine-bearing dolerite with 6-8 wt. % MgO. In cross-sections, the intrusions are differentiated from troctolite and picritic gabbrodolerite to olivine-bearing gabbrodolerite. The upper part of thick sections is occasionally composed of hybrid rocks that contain 65-75 wt. % SiO_2 and 2-3 wt. % MgO.

The chemical composition is characterized by depletion in TiO_2 and SiO_2 and enrichment in K_2O. The weighted average MgO content is 15-17 wt. % within a range of 7-28 wt. %. The Cr_2O_3 content does not exceed 0.03 wt. %. The low-grade sulfide disseminations systematically occur in differentiated segments of intrusions; Pd/Pt equals to 0.62.

The $\delta^{18}O$ value in rocks from central parts of intrusions is 5.5-6.0‰ and increases to 8.8-13.2‰ toward the upper and lower contact zones. The LT intrusions are enriched in LREE in comparison with ore-bearing intrusions; Yb/Gd ratio (0.54-0.66) is lower than in Nr intrusions (0.60-0.72); $(^{87}Sr/^{86}Sr)_{250}$ = 0.7075-0.7085; εNd is moderately low; the contents of radiogenic Sr and Pb isotopes are the highest among intrusive rocks of the district. The intrusions are accompanied by amphibole contact metamorphic and metasomatic aureoles. The thickness of these aureoles is commensurable with thickness of intrusions or is inferior to the latter.

The Morongovsky type (Mr) comprises high-Mg intrusions localized in sedimentary rocks of the Tunguska Group and in volcanic rocks from Iv to Mk formations in the central part of the Noril'sk Syncline. The intrusions are complex in morphology and differentiated from pegmatoid gabbrodolerite to troctolite and 'picrite' (Fo_{30-69}). The percentage of ultramafic rocks increases from north to south (50-100%). Near the Noril'sk-Kharaelakh Fault Zone, the Mr-type intrusions are steeply dipping, up to 400 m thick, and composed almost entirely of picritic gabbrodolerite. The coarse-grained pegmatoid rocks occupy the upper portion of the northernmost intrusions. The low-grade sulfide disseminations occur in the bottom zone. The Cu and Ni contents in sulfides are the same as in the Nr-type intrusions and approach them in PGE concentrations. The MgO content varies from 5 to 23 wt. %. The Mr intrusions are close to the LT-type by Cr_2O_3 content (0.002-0.030 wt. %) but differ by low K_2O content. The TiO_2 content is higher than in the LT- and Nr-type

rocks. By concentrations of incompatible minor elements and Sr-Nd isotopes, Mr type is indistinguishable from Dl type of postvolcanic basic intrusions. Both types are also close to each other in spatial distribution. The contact metamorphic aureoles of the Mr-type intrusions are generally identical to the aureoles of the Lower Talnakh type. They are much smaller in size relative to the thickness of intrusions.

The Fokinsky type (Fk) is represented by near-horizontal sills localized in the Devonian sedimentary rocks and the Tunguska Group in the southwestern Noril'sk and the northern Kharaelach synclines. The sills reach 135 m in thickness. The weighted average MgO content is 18-22 wt. %; the rocks are differentiated from picritic to olivine-free gabbrodolerites. The picritic and picrite-like varieties occupy about 80% of intrusions' volume. No sulfide mineralization has been detected. The high Cr content (380-1470 ppm) is the main characteristic feature of Fk-type intrusions. They are identical in chemical composition to picrobasalts of the Gd Suite. The contact aureoles are composed of metamorphic rocks pertaining to the muscovite hornfels facies. Alkaline metasomatic rocks, zones of skarnified, carbonated, and pyritized rocks are not abundant.

The internal structure of highly differentiated mesocratic ore-bearing intrusions of the Norilsk type

The classic geological and petrographic descriptions of ore-bearing intrusions by M.N. Godlevsky, I.A. Korovyakov and others published in the 1960s have not lost their significance until now. The monographs *by Dodin & Batuev* (1971), *Zolotukhin et al.* (1975; 1978), *Natorkhin et al.* (1977), *Dyuzhikov et al.* (1988; 1992), and *Turovtsev* (2002) supplemented the petrographic descriptions by geochemical data. The cryptic layering was studied *by Distler et al.* (1979); *Ryabov & Zolotukhin* (1977) presented a summary on mineralogy of rocks. *Czamanske et al.* (1994) characterized geochemistry of intrusive bodies, including Sr and Pb isotopic compositions. *Sukhanova* (1968), *Lyul'ko* (1971), *and* Stepanov (1985) developed models of lateral zoning of intrusions.

The geological structure of ore-bearing intrusions of the Noril'sk type, their petrography and mineralogy, and character of cryptic layering are demonstrated below by geological sections presented in the Guidebook and by mineralogical and petrographic sections of the Norilsk-1 (Fig. 5), Talnakh and Karaelakh intrusions. Three groups of rocks recognized in the ore-bearing intrusions (i.e., Norilsk-1 (Fig. 5), Talnakh and Karaelakh) are listed below.

1) The upper gabbroic group is composed of leucogabbro and anorthosite, i.e., plagioclase $An_{70–88}$ cumulus + clinopyroxene intercumulus, the amount of which is decreased down to 15 vol. %. The critical unit in the lower part of the upper gabbroic group is an alternation of picritic gabbrodolerite, olivine gabbro and irregular segregations of the rocks belonging to the underlying layered series. The amygdules filled with F- and CO_2-bearing hydrous silicates are a specific feature of the critical unit, which contains the low-sulfide PGE mineralization.

2) The main layered series is an example of classic fractionation of the high-Mg melt. Olivine is the major cumulative phase. Their accumulation at the base of the layered series gives rise to the formation of picritic gabbrodolerite, plagioclase-bearing peridotite, and troctolite. The intercumulus phases are represented by cotectic plagioclase-clinopyroxene assamblage and a small amount of orthopyroxene. Orthopyroxene appears as a product of buffer reaction that fixes an excess of silica.

The average composition of the lower unit is $Ol_{82}^{50} + Pl_{90}^{20} + Cpx_{26}^{5} + Sulf^{1-3}$.

The amount of olivine decreases upward, whereas amount of plagioclase and clinopyroxene increases in the same direction. The variation of rock composition and composition of minerals is described by the following series (from bottom to top):

- olivine and olivine-bearing gabbrodolerites ($Pl_{90-65}^{45-60} + Cpx_{30-27}^{20-30} + Ol_{56-78}^{5-25}$);
- olivine-free and quartz-bearing; gabbrodiorite and diorite ($Pl_{20-30}^{40-60} + Amph^{10-20} + Qtz^{5-25} + Or^{5-15}$).

The rocks of the layered group are characterized by the following specific features:

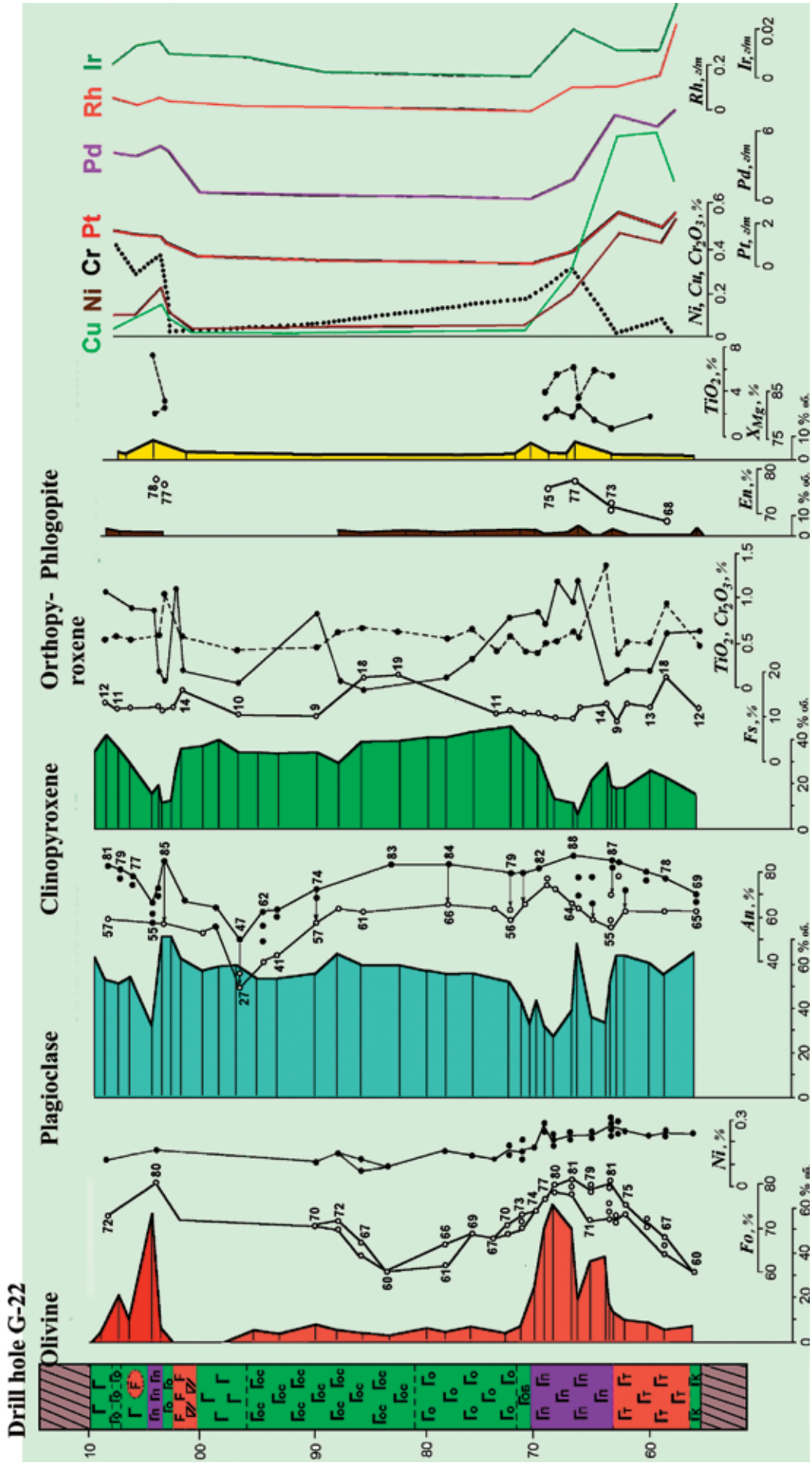

Fig. 5. Variations in the contents and chemical composition of rock-forming minerals, Cu, Ni, Cr_2O_3 (in wt.%), and PGE (in ppm) through a section of the Noril'sk 1 intrusion (drill hole G-22). Gabbrodolerites: Г – olivine-free, Гос – olivine-bearing, Го – olivine, F – leucogabbro, Гк – contact; Гп – ultramafic rocks, Гт – taxitic-textured rocks, F≥ –gabbrodiorite.

(1) sharp quantitative boundary in modal and chemical compositions between picritic and olivine (olivine-biotite) gabbrodolerite;

(2) decrease in amount of olivine cumulus from olivine to olivine-bearing gabbrodolerite; crystallization of the matrix is controlled by plagioclase-clinopyroxene cotectics;

(3) while plagioclase cumulus appears in the upper part of the layered series, olivine passes to intercumulus and then disappears;

(4) orthoclase + quartz assemblage crystallizes in the upper part of the layered group in addition to clinopyroxene + plagioclase assemblage that postdates the mass crystallization of plagioclase cumulus.

3) The lower gabbroic group. The ultramafic unit at the base of the layered series marks an extremum point in the vertical section of the differentiated intrusions, where quantities and compositions of major rock-forming minerals reach a maximum or a minimum. In the lower gabbroic group olivine passes into intercumulus, and Cr-spinel disappears as cumulus or intercumulus phase. Taxitic gabbrodolerite of the lower gabbroic group is one of the most important varieties of the rocks, typical only for the completely differentiated intrusions. The outer appearance of this rock is determined by large crystals of cumulative plagioclase in combination with clinopyroxene as an intercumulus phase. In contrast to the ultramafic unit, olivine is distributed nonuniformly and occurs either as an intercumulus phase or as a constituent of the fine-grained aggregate making up intergrowths with plagioclase and occasionally with Al-Mg-spinel.

The average composition of taxitic gabbrodolerite is $Pl_{40\text{-}80}^{35\text{-}70} + Cpx_{27\text{-}30}^{7\text{-}30} + Ol_{61\text{-}77}^{7\text{-}30} + Opx_{30}^{3\text{-}5}$. The equigranular gabbrodolerite is close in composition but olivine is absent. The contact rocks have the following composition: $Pl_{50}^{60} + Cpx_{30}^{15} + Ol_{56}^{15}$.

The cryptic layering in intrusions of the Noril'sk type consists in the upward decrease in amount of cumulative olivine together with its decreasing Mg# from $Fo_{79\text{-}85}$ to Fo_{60}; anorthite content of cumulative plagioclase decreases in the same direction from $An_{78\text{-}88}$ to $An_{47\text{-}63}$. The Fs content of intercumulus clinopyroxene increases in the same direction from 10-8 to 19-11 mol. %. The amount of cumulative olivine and its Mg# abruptly changes at the olivine gabbrodolerite/picritic gabbrodolerite boundary. The amount of intercumulus olivine and its Mg# reach their maximums in the upper picritic unit; a peak of anorthite content of plagioclase cumulus falls in leucogabbro unit.

The internal structure of differentiated leucocratic intrusions

The differentiated leucocratic intrusions are distinguished from the completely differentiated intrusions by prevalence of mafic rocks over ultramafic rocks. The mafic units repeat several times, whereas the thickness of ultramafic units does not exceed 5-10% of total intrusion thickness. These units are commonly composed of olivine gabbrodolerite and less abundant troctolite or picritic gabbrodolerite. As in the highly differentiated intrusions, taxitic gabbrodolerite occurs at the bottom, they give way to equigranular olivine gabbrodolerite. Silicic rocks, up to granodiorite and less frequent granite, often occur in the uppermost units. The general trends in layering of highly differentiated and differentiated leucocratic intrusions are close to each other.

The compositions of rocks from leucocratic intrusions are as follows:

- granite and granodiorite ($Pl^{30\text{-}40} + Amph^{10\text{-}20} + Qtz^{10\text{-}20} + Or^{5\text{-}15} + Mc^{5\text{-}10}$);
- diorite and gabbrodiorite ($Pl^{50\text{-}60} + Amph^{10\text{-}20} + Cpx^{5\text{-}10} + Qtz^{5\text{-}10} + Mc^{5}$);
- gabbrodolerite ($Pl^{50\text{-}60} + Cpx^{20\text{-}30} + Amph^{5\text{-}10}$).

The character of cryptic layering in the differentiated leucocratic and highly differentiated intrusions is identical. Olivine in units of olivine gabbrodolerite corresponds to $Fo_{70\text{-}74}$; $Fo_{76\text{-}79}$ occurs in troctolite and picritic gabbrodolerite. Olivine in taxitic and equigranular gabbrodolerites corresponds to $Fo_{67\text{-}75}$.

The internal structure of differentiated melanocratic intrusions

Prevalence of troctolite over picritic gabbrodolerite is the main characteristic feature of this type of intrusions. The following units change one another in the vertical section (from top to bottom): leucocratic silicic rocks varying from quartz diorite to granodiorite; gabbrodiorite; amphibole-bearing gabbrodolerite; olivine-free, olivine-bearing, and olivine gabbrodolerites; troctolite; and picritic gabbrodolerite. The rocks of these units are close to the respective varieties in the highly differentiated intrusions but differ in thickness and occupy less than 1/4 of their total thickness. The troctolitic-picritic unit occupies the main volume of intrusions in their central portions and pinches out at flanks. The rocks of this unit are uniformly fine- and medium grained with sporadic more leucocratic coarse-grained variety. The boundary with overlying rocks is rather sharp and is emphasized by change of structure and decrease in amount of dark-coloured minerals, mainly olivine. In contrast to the highly differentiated intrusions, the panidiomorphic and allotrimorphic textures are typical of the ultramafic rocks; the ophitic texture is less abundant. The thickness of contact gabbrodolerite does not exceed a few meters. This unit consists of the fine-grained ophitic and occasionally porphyritic rocks.

The differentiated melanocratic intrusions differ from the completely differentiated sills by one-directional variation of composition of rock-forming minerals combined with asymmetric structure. The Ol^{30-50} + Pl^{30-50} + Cpx^{10-20} mineral assemblage is prevalent. Depending on proportions of these minerals, the rocks are classified as troctolite or picritic gabbrodolerite. Orthopyroxene and subcalcic augite are limited in abundance. Phlogopite is a characteristic mineral. In contrast to picritic gabbrodolerite from completely differentiated intrusions, the rocks are devoid of Cr-spinel, and accessory minerals are represented by magnetite and ilmenite.

The following modal compositions: Pl^{45-60} + Cpx^{20-30} + Ol^{5-15}, Pl^{50-60} + Cpx^{20-25} + $Amph^{5-10}$ +Mc^{1-3}, Pl^{40-60} + $Amph^{10-20}$ + Q^{5-25} + Or^{5-15}, and Pl^{40-50} + Cpx^{20-40} + Ol^{15-20} are typical of gabbrodolerite, gabbro and gabbrodiorite, diorite and granodiorite, and lower contact gabbrodolerite, respectively.

Olivine retains a constant composition (Fo_{78-81}) in most part of vertical section that form olivine and olivine-bearing gabbrodolerites to the lower contact; a less magnesian olivine (down to Fo_{75}) occurs only in the contact zone. Clinopyroxene is represented by augite varying in a narrow range of composition from Fs_{19} in core of crystals to Fs_{21} in the outer zone. Variations in Al and Ti are also limited. The characteristic homogeneous grains of subcalcic augite occur throughout the intrusions and occupy the same structural position as the common augite. Orthopyroxene is extremely rare in the picritic-troctolitic unit and is more magnesian (Fs_{25}) in comparison with other types of intrusions.

PGE-Cu-Ni SULFIDE DEPOSITS

The PGE-Cu-Ni sulfide deposits of the Noril'sk ore district are spatially and genetically related to the layered intrusions. All known deposits and occurrences group into ore zones controlled by lineaments and axes of volcanotectonic troughs. Ore clusters within the ore zones are the areas occupied by multistage layered intrusions with massive, stringer-disseminated, and disseminated sulfide ores. Localization of ore types and their lateral and vertical zoning are controlled by morphology of layered intrusions and tectonic features that form the medium of ore deposition.

The Noril'sk, Talnakh, North Kharaelakh, South Noril'sk, and Imangda ore clusters are recognized (Fig. 1). The promising occurrences of Cu-Ni ore mineralizations were found recently in the territory of South Taimyr that adjoins the Yenisei-Khatanga Trough.

The deposits of the Noril'sk ore district are represented by units of sulfide-bearing rocks localized at various levels of the differentiated intrusions of the Noril'sk type. The disseminated ore is confined to the lower units composed of picritic and taxitic gabbrodolerites. The massive ore is localized in metamorphic and metasomatic rocks that immediately underlie the lower contacts of intrusions

or in contact zone of intrusive rocks. The vienlet-disseminated ore occurs as haloes around the massive ore in the lower and less frequently upper contact zones.

The Noril'sk ore cluster combines several deposits at the northern centroclinal closure of the Noril'sk Syncline that are hosted in the Noril'sk-1, Noril'sk-2, Zubovsky, and Chernogorsk intrusions. The Norilsk-1 deposit (Fig. 6) resides in the differentiated intrusion of the same name. The intrusion extends in the northeastern direction and gradually plunges to the southwest. Its northern part is sandwiched between the flows of tholeiitic basalts belonging to the Sv-Iv suites, while its southern part is located between plagiophyric basalt and sedimentary rocks. The main ore mass concentrates in the northern portion of the intrusion, where it is hosted by picritic and taxitic gabbrodolerites and underlying basalts and Ti-augite dolerite, where massive ore occurs. The intensity of ore mineralization markedly drops down the dip of intrusion. The high-grade sulfide ore hosted in picritic gabbrodolerite is traceable as a continuous tract, whereas only isolated sulfide-rich lenses are known in taxitic gabbrodolerite.

The disseminated ore of the Noril'sk-1 deposit is currently mined in the open pit of the Medvezhy Ruchei (Bear Creek) Mine and in the underground Zapolarny (Transpolar) Mine. The Talnakh

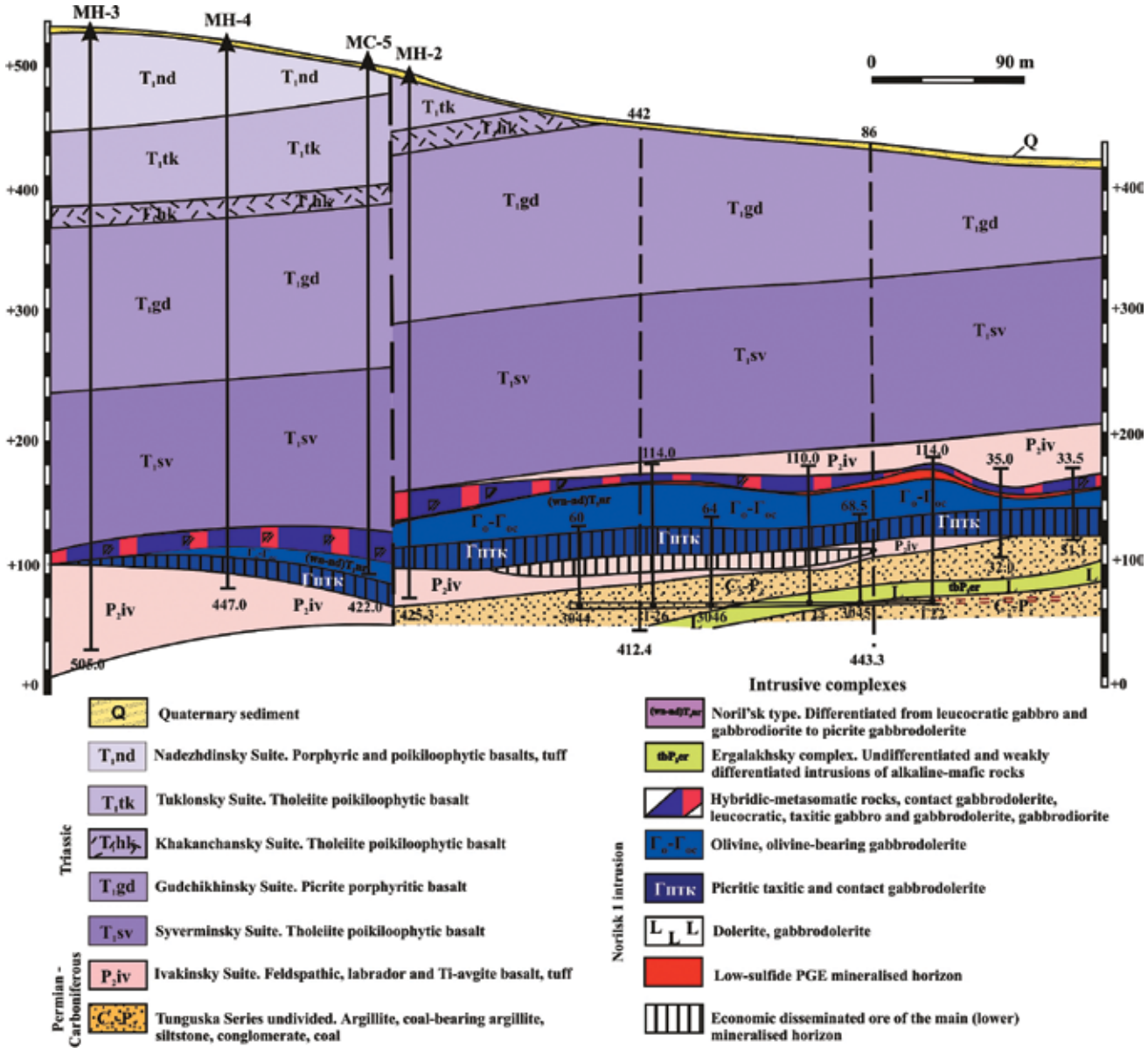

Fig. 6. Geological cross-section through volcanic rocks and location of the ores within the Noril'sk 1 intrusion

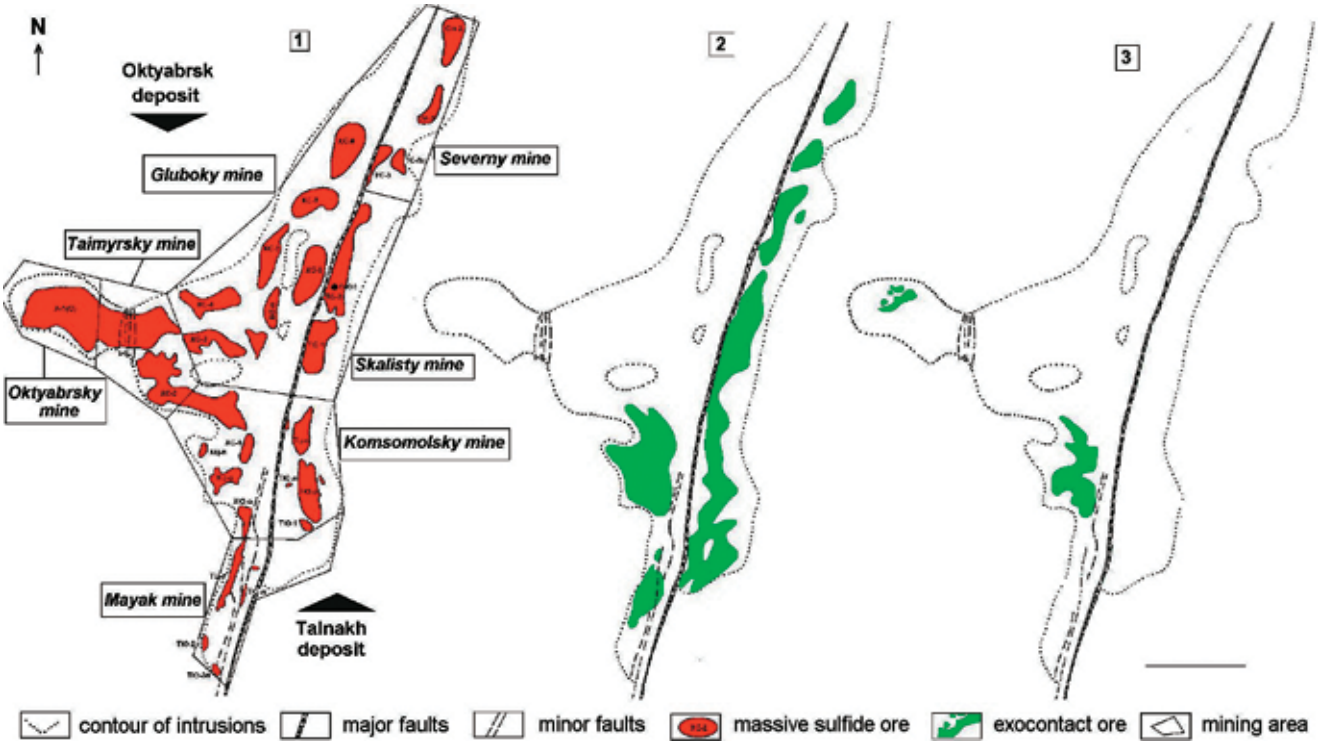

Fig. 7. Distribution of massive (1) and veinlet-disseminated ores in metamorphic and metasomatic rocks of the basal (2) and upper (3) exocontacts of the Talnakh and Kharaelakh intrusions

ore cluster combines the Talnakh and Oktyabrsky deposits (Figs. 7, 8). The former is related to the northeastern and southwestern branches of the Talnakh intrusion. The northeastern branch extends for 20 km in the eastern wall of the Noril'sk-Kharaelakh Fault, while the southwestern branch (also known as Kharaelakh intrusion) is situated in the graben to the west of this fault. The intrusions are sheetlike in section (Figs. 7, 8) and gently plunge northward. The central parts of the intrusions are sagged down to the Upper Devonian carbonate rocks.

The ore units are simple in structure. The disseminated ore in picritic and taxitic gabbrodolerites are traced over the virtually entire extent of the intrusion. The sheetlike and lenticular bodies of massive ore are located in the axial zones of intrusions (Fig. 9) having a variable thickness. The minimal thickness of 1 m is constrained by the existing mining standards, and the maximal thickness reaches 40 m. The zonal massive ore lode of the southwestern branch with a talnakhite ore has been mined out by the Mayak Mine. The talnakhite and cubanite ores of the Southern lode in the eastern part of the Komsomol'sky Mine is also exhausted. At present, the pyrrhotite ore of the marginal part of the Southern lode and the Central lode are mined. The Skalisty Mine started to mine the massive ores of the Northern-1 and Northern-2 lodes.

The veinlet-disseminated ore is traced at the base of the northeastern branch over its entire extent. The ore units lying under and above the massive ore lodes are recognized. The maximum thickness of these lodes (up to 10-12 m) is confined to the axial zone of the ore-bearing intrusion, where they are localized in the metasomatically altered carbonate rocks of the Devonian age.

The Oktyabrsky deposit is related to the Kharaelakh intrusion. The large and complexly built intrusion plunges to the northeast at angles 12°-15°. The intrusive sheet is complicated by numerous swells and pinches controlled by morphology of country rocks. In some places, the intrusion is split into a series of near-parallel offsets. The morphology of intrusion is especially complex in the extreme west, where numerous offsets alternate with parts of metasedimentary rocks. The more

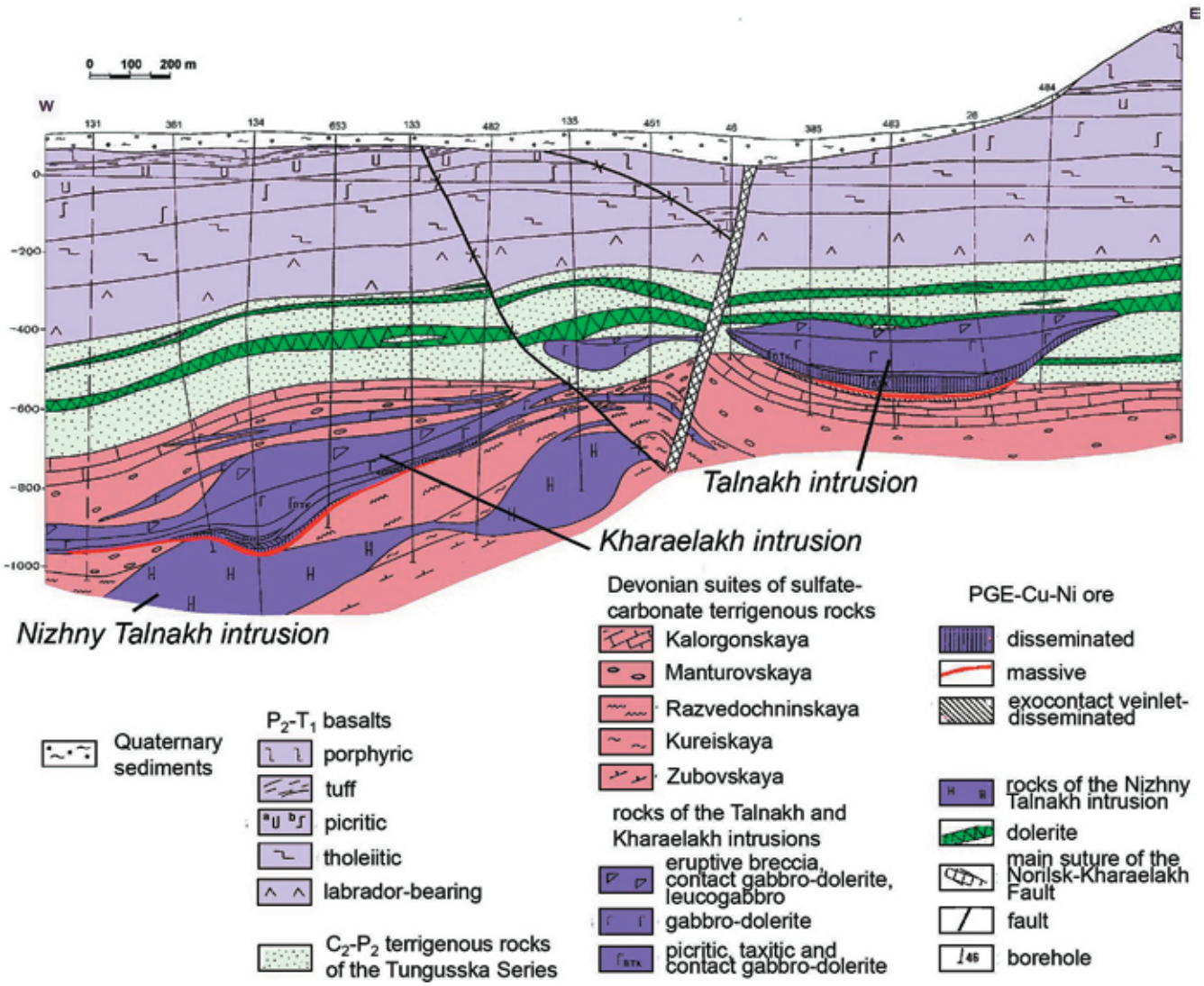

Fig. 8. Geological cross-section of the Talnakh ore field. Intrusions are not to scale

complex morphology of intrusion leads to the complication of ore bodies, which become discontinuous in the flank zone.

The massive ore lodes at the Oktyabrsky deposit are most extended. The main Kharaelakh lode extends for hundreds of meters and reaches 45 m in thickness. The Kharaelakh, Northern-4, -5, and -6 ore bodies reveal a zoning with chalcopyrite and cubanite ores (Fig. 9). The massive ore of the western portion of the Kharaelakh lode is currently mined by the Oktyabrsky Mine; its eastern portion is mined by the Taimyr Mine; and the Central, Southern, and Northern-1 lodes are mined by the Komsomolsky Mine.

The veinlet-disseminated ore hosted in the country rocks of the outer contact zone is of economic importance only at the roof of the southeastern part of the Kharaelakh intrusion, where the Upper Devonian metamorphic and metasomatic rocks are mineralized. The so-called brecciated ores (from low-grade disseminated to massive) are localized between numerous offsets of the Kharaelakh intrusions in its western portion.

The PGE-Cu-Ni deposits of the Noril'sk district comprise a set of ore units diverse in composition and internal structure that occupy a certain position relative to the differentiated intrusions of the

Table 1

Percentage of reserves of different ore types in the Noril'sk
(after Lyul'ko et al., 2002)

Ore type	*Reserves, %*				*Average grade*		
	Ore	*Ni*	*Cu*	*PGE*	*Ni, %*	*Cu, %*	*PGE, ppm*
Massive copper-nickel	10.3	41.7	31.8	20.6	3.21	4.57	10.76
Veinlet-disseminated copper	7.4	8.1	13.3	0.88	3.33	9.82	
Other type	82.3	50.2	51.8	66.1	1.49	0.93	4.34
	100.0	100.0	100.0	100.0			

Noril'sk type (*Genkin et al.,* 1981; *Distler et al.,* 1979; *Naldrett,* 2004). They differ in relative amounts of sulfides, structural patterns, and character of host rocks. The disseminated ore hosted in intrusive rocks, stringer-disseminated ore in the country rocks adjoining the intrusions, massive PGE-Cu-Ni, and low-sulfide PGE ores are distinguished (Table 1).

The disseminated ore is confined to the lower units of the differentiated intrusions composed of picritic and taxitic gabbrodolerites (Figs. 7, 9). The structure of disseminated ore bodies is completely controlled by morphology of host rocks. The greatest thickness (up to 40-50 m) of ore bodies is established in the thickest parts of the layered intrusions. The disseminated ore is rather persistent in grades of Cu and Ni (~1.5 wt. % in total and Cu:Ni = 2:1). The sulfur content is 2.0-3.7 wt.% (Table 2).

In picritic gabbrodolerite, sulfides occur as small (less than 2 mm across) interstitial segregations and larger (up to 2-3 cm in diameter) droplets, often layered: their upper portion consists of chalcopyrite, while the lower portion, of pyrrhotite. The relatively large (1-3 cm) xenomorphic sulfide segregations dominate in taxitic gabbrodolerite along with fine interstitial disseminations and shclieren of irregular, lenticular, and veinlike shapes that reach 10-15 cm in size.

The disseminated ore reveals the vertical zoning expressed in systematic variation of proportions of major ore minerals and their compositions. Such a zoning is especially pronounced in picritic gabbrodolerite. The ore in the central parts of picritic gabbrodolerite units consists of troilite, cubanite, Fe-rich pentlandite, and talnakhite. The latter mineral occurs as regular intergrowths with thin chalcopyrite plates. Cubanite is represented by both tabular and grained varieties.

Upward and downward from the units of low-sufide assemblages, chalcopyrite appears instead of talnakhite. In approaching the upper and lower contacts of picritic gabbrodolerite unit, the amount of cubanite decreases to its complete disappearance. The homogeneous troilite gives way to its intergrowths with hexagonal pyrrhotite in various quantitative proportions and further, to the intergrowths of hexagonal and monoclinic pyrrhotites. The homogeneous monoclinic pyrrhotite occurs in picritic layers sporadically and only in their marginal parts. The Ni content increases from trolilite (practically devoid of Ni) to monoclinic pyrrhotite. In the intergrowths of hexagonal and monoclinic pyrrhotites, the proportion of Ni in these phases commonly equals 1:2. Such perfect zoning is developed only in the section where both intrusions and ore units reach their greatest thickness. The assemblage (troilite + hexagonal pyrrhotite) + tabular cubanite + chalcopyrite + Fe-bearing pentlandite commonly occurs in the central parts of picritic units. The local inhomogeneity of sulfide ore mineralization is also developed in picritic gabbrodolerite. As a rule, the large sulfide droplets are composed of higher-sulfuric assemblages than the interstitial disseminations. For instance, the interstitial segregation may be composed of troilite, cubanite, chalcopyrite, and Fe-rich pentlandite, whereas a droplet situated nearby, of hexagonal pyrrhotite, chalcopyrite, and Fe-bearing pentlandite. The taxitic gabbrodolerite hosts high-sulfuric assemblages of sulfides. Troilite and cubanite appear only in the upper parts of taxitic units; commonly, iron monosulfides are represented by intergrowths of monoclinic and hexagonal pyrrhotites with similar Ni content. The homogeneous monoclinic pyrrhotite is often the sole monosulfide

Table 2

Contents of Ni, Cu, Co, S and noble metals in PGE-Cu-Ni sulfide ores of the Talnakh and Oktyabrsky deposits

Ore type	*Ni*	*Cu*	*Co*	*S*	*Pt*	*Pd*	*Rh*	*Ir*	*Ru*	*Os*	*Au*	*Ag*
Talnakh												
Northeastern branch												
Disseminated	0.50	0.92	0.026	3.73	0.65	2.50	0.03	0.03	0.28	0.02	0.17	0.15
Southwestern branch												
Massive pyrrhotite	4.74	3.57	0.142	31.31	2.35	9.98	0.52	0.20	0.20	0.28	0.26	9.04
Disseminated	0.54	0.95	0.026	3.09	1.47	4.13	0.07	0.02	0.12	0.04	0.24	3.48
Massive pyrrhotite	4.05	4.41	0.153	30.0	3.50	13.40	1.24	0.16	0.26	0.12	0.50	7.52
Oktyabrsky												
Massive cubanite	4.20	9.20	0.080	28.3	3.40	23.10	0.50	0.08	0.14	0.08	2.12	42.6
Massive talnakhite	4.48	21.8	0.060	30.2	24.20	101.80	0.02	0.09	0.12	0.06	5.50	96.2
Veinlet-disseminated	0.65	3.21	0.022	5.73	2.40	7.54	0.06	0.03	0.30	0.03	0.50	9.44
Disseminated	0.45	1.40	0.025	5.41	0.98	3.34	0.02	0.01	0.14	0.03	0.24	5.98
Massive pyrrhonte	3.01	5.59	0.124	29.04	2.32	10.58	0.12	0.03	0.12	0.04	0.45	8.01
Massive cubanite	2.99	12.64	0.108	29.82	4.90	20.88	0.07	0.03	0.11	0.03	1.51	38.0
Massive mooihoekite	2.36	21.14	0.068	29.29	10.01	41.46	0.02	0.02	0.09	0.05	5.02	83.0
Veinlet-disseminated	1.11	5.05	0.040	13.51	2.64	9.17	0.05	0.02	0.11	0.02	0.72	13.3

Note. Contents of Ni, Cи, Co and S are given in wt. %; other elements in ppm

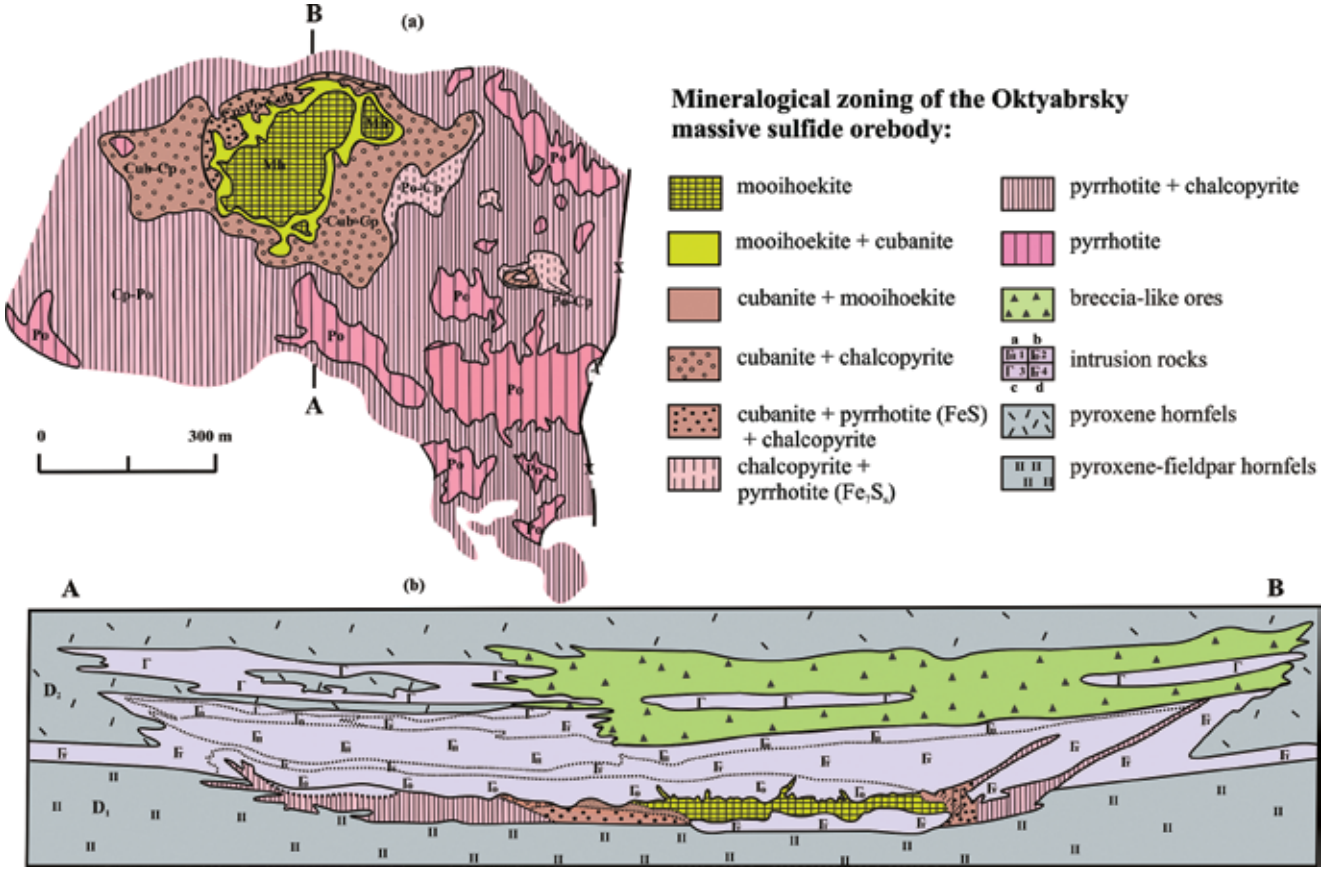

Fig. 9. Mineralogical zoning of the Oktyabrsky massive sulfide body: (1) mooihoekite, (2) mooihoekite + cubanite, (3) cubanite + mooihoekite, (4) cubanite + chalcopyrite, (5) cubanite + pyrrhotite (FeS) + chalcopyrite, (6) chalcopyrite + pyrrhotite (Fe_7S_8), (7) pyrrhotite + Chalcopyrite, (8) pyrrhotite, (9) breccia-like ores, (10) intrusion rocks, (11) pyroxene hornfels, (12) pyroxene-feldspar hornfels

in this ore. The disseminated ore hosted in taxitic units is distinguished by enrichment in copper contained in chalcopyrite.

The disseminated ore is characterized by the lowest bulk PGE concentrations, but their highest concentrations recalculated to the mass of sulfides. The PGE concentrations (in ppm) are as follows:

0.4-1.5 Pt, 3.0-5.0 Pd, 0.02-01.14 Rh, 0.003-0.06 Ir; Pt/Pd = 0.25-0.35;

(Pt + Pd)/(Rh + Ir + Ru + Os) = 7.6-22.4.

As in all ore types, PGE occur in the disseminated ore as solid solutions in sulfides and as platinum-group minerals (PGM). The contribution of each species to the total PGE content is different for specific elements. In the disseminated ore of the Talnakh deposits, 90-95% Pt concentrates in sperrylite. The Pt content in pyrrhotite and pentlandite is below 1.2 ppm. At the same time, 90-95% Pd concentrate in pentlandite, where its content amounts to 50-1000 ppm, whereas only <0.1 ppm Pd are detected in pyrrhotite and chalcopyrite. The rare Pd minerals in the disseminated ore are represented by arsenides, arsenostibnides, and arsenostannides. Rh, Ir, and Os make up solid solutions in pyrrhotite and pentlandite (1.1 ppm Rh, 0.2 ppm Ir). These elements also occur as admixture in sperrylite (up to 1.5% Rh).

The massive ore is the most economically important type. In the Talnakh ore cluster, the area of massive ore occurrence is comparable with area of differentiated intrusions and related units of disseminated ore (Fig. 7). The lateral extent of massive ore lodes reaches a few hundred meters; their thickness varies from centimeters to 45 m. In most cases, the bodies of massive ore are localized in country metamorphic and metasomatic rocks adjoining the ore-bearing intrusions from below. The barren zone between the sole of intrusion and the roof of the massive ore lode varies in thickness from a few centimeters to seven meters. The sheet-like and flattened lenticular ore bodies hosted in the metasedimentary rocks are typical. The character of orebody boundaries depends on competence of host rocks. The ore bodies localized in rigid fine-grained hornfels after the Paleozoic terrigenous rocks are bounded by sharp rectilinear contacts, whereas the tortuous boundaries and xenoliths of country rocks are typical, where the latter are represented by coarse-grained metamorphic rocks and metasomatically altered carbonate–sulphate sequence of the Devonian age.

In the rare cases, the massive ore is localized within the ore-bearing intrusions as veins, fill of free space, and always bears indications of active effects on the host rocks. The blocks and stockwork zones of complexly branching veins occur here in addition to the sheet-like and lenticular bodies.

The complete series of paragenetic sulfide assemblages in the Fe-Ni-Cu-S system was identified in the massive ore at the Noril'sk and particularly Talnakh deposits. The spatial distribution of these assemblages exhibits the zoning and cryptic layering of orebodies. Most ore bodies are composed of prevalent pyrrhotite with Cu/Ni ~ 0.8, i.e., almost twice as lower as in the disseminated ore. The massive ore consists by 60-65% of pyrrhotite and contains 15-20% of chalcopyrite, 10-15% of pentlandite, and 5% of magnetite. The chalcopyrite content increases to 30-40% in outer zone; homogeneous hexagonal pyrrhotite and its intergrowths with trolilite are replaced in the same direction with monoclinic pyrrhotite and its intergrowths with hexagonal variety. This zoning is stressed by the outward enrichment of pyrrhotite in Ni.

The ore bodies that reveal distinct zoning are localized at the bottom of intrusions; this zoning is especially clear in the western part of the Kharaelakh lode at the Oktyabrsky deposit (Fig. 9). The ore composed of minerals of chalcopyrite group: talnakhite, mooihoekite, putoranite (55-60%), cubanite (10-15%), pentlandite (20-25%), troilite (up to 5%), and magnetite (5%) occurs in the center and at the upper contact of the intrusion and is rimmed by several ore varieties with variable proportions of ore minerals but always with cubanite (30-50%) associated with minerals of chalcopyrite group (20-40%), troilite (5-20%), pentlandite 10-15%, and magnetite (5%). Further outward, the low-S minerals of chalcopyrite group disappear and only tetragonal chalcopyrite becomes stable; iron monosulfides are represented by Fe hexagonal pyrrhotite as intergrowths with troilite and then without troilite. The chalcopyrite-cubanite, cubanite-chalcopyrite, and cubanite-chalcopyrite-pyrrhotite ores become typical. They grade into the ores with sulfide assembalges described for ore bodies of simple structure. This zoning is emphasized by cryptic layering expressed in variation of chemical composition of pent-

landite and Ni content in iron monosulfides. In the ore with low-S assemblages, the Ni content falls to 28 wt. % and rises to 36 wt. % in the pyrrhotite ore. Thereby, the Ni content in pyrrhotite varies from hundreths fractions of percent (in troilite) to 1.6 wt. % in monoclinic pyrrhotite. The Ni/Cu ratio equals 0.23-0.45 in the cubanite ore, 0.11 in the mooihoekite ore, and 0.20 in the talnakhite ore; the variation of Ni/Cu ratio is determined by variable Cu content at the virtually constant Ni content.

The pyrrhotite ore is characterized by a rather stable PGE contents, ppm: 1.5-2.0 Pt, 7-9 Pd, 0.6-1.2 Rh, 0.2-0.3 Ru, 0.06-0.10 (up to 0.2) Ir, and 0.03-0.05 Os. The ore bodies are enriched in Pt and Pd toward their margins in compliance with enrichment in Cu. The pyrrhotite ore contains the highest concentrations of Rh, Ir, Ru, and Os. The Rh content is occasionally comparable with that of Pt. The (Pt + Pd)/(Rh + Ir + Ru + Os) ratio is 1-20; Pt/Pd = 0.23-0.35.

The highest variability of PGE concentrations is inherent to the zonal orebodies. The Pt and Pd contents abruptly increase in the talnakhite and mooihoekite ores along with depletion in Rh, Ir, Ru, and Os; the (Pt + Pd)/(Rh + Ir + Ru + Os) ratio increases to 285-470. The Pt and Pd contents in these ores equal 10-25 and 40-100 ppm and more; the Pt/Pd = 0.24-0.30. The cubanite ore is characterized by intermediate PGE concentrations, ppm: 3.40-4.90 Pt, 19-23 Pd, 0.05-0.10 Rh, 0.01-0.08 Ir, 0.09-0.14 Ru, and 0.01-0.08 Os; Pt/Pd = 0.23-0.24.

Rh, Ir, Ru, and Os in massive ore are completely concentrated as solid solutions in sulfides, largely in pyrrhotite and pentlandite. The Rh content in pyrrhotite and pentlandite is 0.2-1.6 and 0.4-1.8 ppm, respectively. The high-S pyrrhotite is richer in Rh than the low-S variety. The abrupt depletion of high-grade Cu ore in Rh is caused by replacement of high-S pyrrhotite with troilite and then complete disappearance of iron monosulfides. Rh also concentrates in sperrylite (up to 1.5%) and very rarely forms its own mineral – hollingworthite. The Ir content in pyrrhotite and pentlandite is 0.05-0.25 ppm. As in the case of Rh, its content abruptly falls in the ore with prevalence of low-S sulfides. The Ru contents were estimated at 0.13-0.45, 0.06-0.32, and 0.06-0.43 ppm in pyrrhotite, pentlandite, and chalcopyrite, respectively. The respective Os concentrations are 0.06-0.25, 0.02-0.05, and 0.03-0.08 ppm. A partial solubility of Ru and Os in minerals of chalcopyrite group causes a not so drastic depletion of ore composed of low-S sulfides in these elements.

Palladium forms solid solutions in sulfides, largely in pentlandite. In the massive ore with pyrrhotite, as in the disseminated ore, pentlandite, which contains 50-300 ppm of this element, is the main concentrator of Pd. In other sulfides, the Pd content is as high as 5 ppm. The Pd arsenides, stibioarsenides, and stannoarsenides are very rare minerals.

In ores largely consisting of low-S minerals of chalcopyrite group (talnakhite, mooihoekite, and putoranite) and cubanite, the Pd content in pentlandite decreases to 5-30 ppm. Numerous minerals in the Pd-Pt-Cu-Sn system: stannopalladinite, taimyrite, cabriite, and atokite-rustenburgite series Pd_2Sn-Pt_2Sn; Pd plumbides: zvyagintsevite and plumbopalladinite; tellurides and bismuthides: kotulskite, sobolevskite, froodite, michenerite, and merenskyite; stibnides: stibiopalladinite, mertieite, and sudberryite; plumbobismuthides: polarite and urvantsevite; arsenides: mayakite, palladoarsenide, $Pd_2(Sn, As)$, and vincentite; and paolovite as a tannide $Pd_2(Sn, Sb)$ are the Pd concentrators in this ore.

Platinum has the lowest solubility in sulfides. Its concentration in pyrrhotite and pentlandite does not exceed 0.5 ppm. This element forms its own minerals: sperrylite in the pyrrhotite ore and tetraferroplatinum, rustenburgite. maslovite, moncheite, and niggliite in the ore enriched in copper. Sperrylite and tetraferroplatinum permanently contain an admixture of Rh, Ir, and Ru.

The veinlet-disseminated ore hosted in metamorphic and metasomatic rocks at contacts with ore-bearing intrusions form outer haloes around massive ore lodes. The separate lenticular and sheet-like ore bodies within such haloes are conformable with country rocks. Their thickness commonly is not greater than 2-3 m, however, at the lower contact of the northeastern branch of the Talnakh intrusion these ore bodies hosted in metasomatically altered carbonate rocks reaches more than 10 m.

The structural pattern of stringer-disseminated ore is determined by structure of host rocks and intensity of ore mineralization. The banded structure is caused by alternation of mineralized and barren laminas. The thickness of massive sulfide bands varies from 1 mm to a few centimeters.

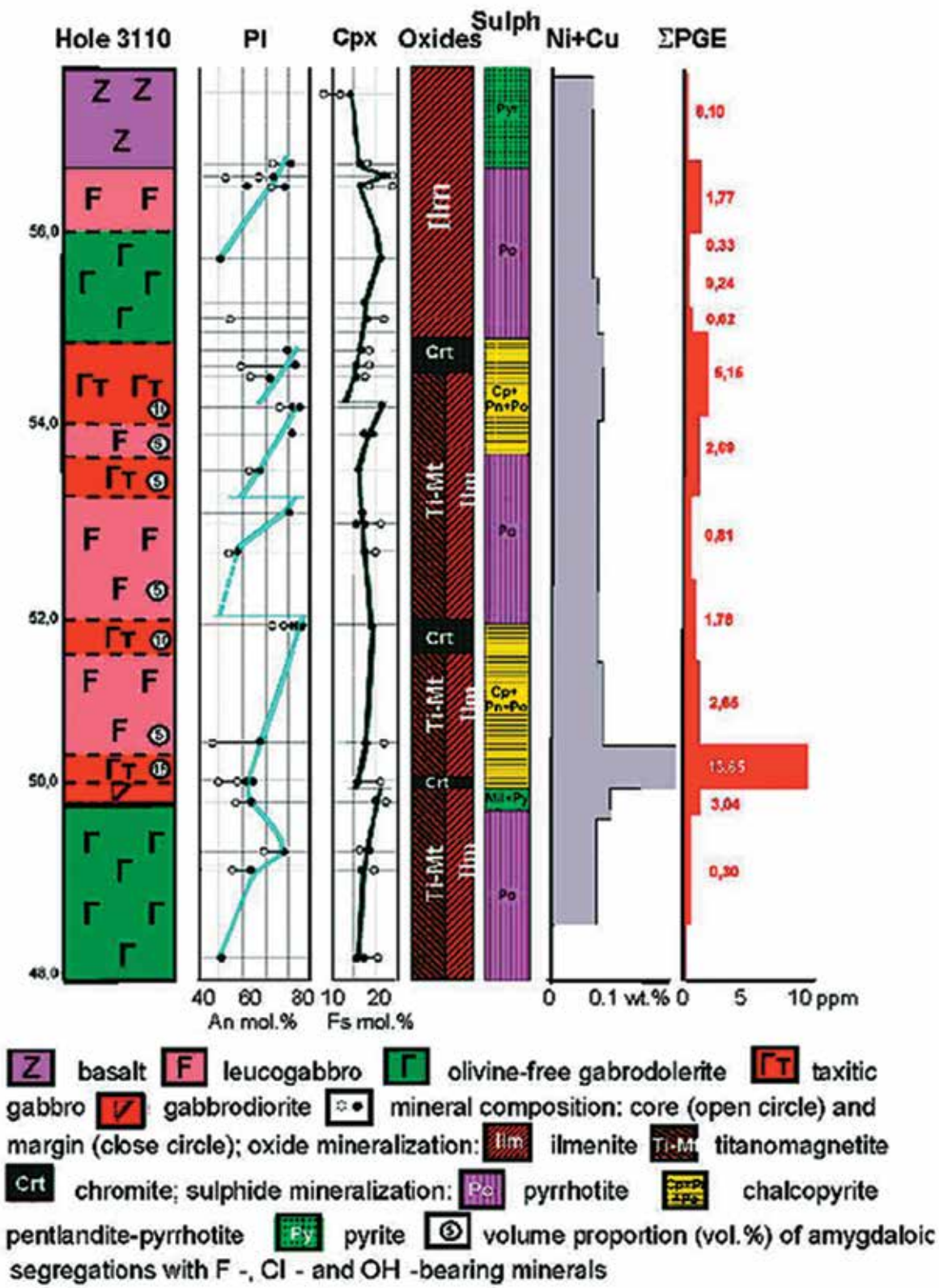

Fig. 10. Variations in the contents and composition of rock-forming, oxide and sulphide minerals, Cu, Ni and PGE contents through the upper contact zone that hosts the low-sulfide PGE horizon in the Noril'sk 1 intrusion (drill hole 3110)

A specific breccia-like ore occurs in the roof of the Kharaelakh intrusions at its western termination. The "fragments" in this ore are finely impregnated with sulfides, and the matrix is commonly composed of massive ore.

The vienlet-disseminated ores are the most diverse in modal composition among all ore types. The ore bodies demonstrate a distinct zoning. The zones that adjoin the massive pyrrhotine ore or the sole of intrusion consist of pyrrhotite, chalcopyrite, and pentlandite. Moving apart from this zone, one may observe that percentage of chalcopyrite increases at the expense of pyrrhotite, and the latter finally disappears giving way to the chalcopyrite + pentlandite and then to the chalcopyrite + millerite + pyrite assemblages. The outermost zone is composed of the chalcopyrite + millerite + bornite assemblage. The complete zonal column is observed only in the section with the greatest thickness of stringer-disseminated ore, e.g., at the footwall of the northeastern branch of the Talnakh intrusion and at the roof of the Kharaelakh intrusion, where the ore is hosted in metasomatically altered carbonate rocks of the Upper Devonian age. In most cases, the zoning is reduced and limited by pentlandite-chalcopyrite assemblage.

In the back zone of the zonal column of stringer-disseminated ore, pyrrhotite is represented by homogeneous hexagonal modification only rarely; the intergrowths of hexagonal and monoclinic pyrrhotites or only homogeneous monoclinic pyrrhotite commonly occur. The Ni content in pyrrhotite increases with distance from massive ore and reaches a maximum of 1.6 wt. %. The Ni content in pentlandite also rises and reaches a maximum of 46 wt. %. These are the Ni-richest pentlandites of all ore types and varieties.

The cubanite-bearing mineral assemblages in the stringer-disseminated ore hosted in metaterrigenous rocks are not abundant. The stringer-disseminated ore is enriched in sphalerite, galena, and djerfisherite. The latter mineral locally occupies 10-15% of sulfide volume. The stringer-disseminated ore is severely affected by secondary alteration, and the primary sulfide assemblages are often replaced completely. Pyrrhotite is replaced with pyrite, marcasite, magnetite and valleriite; chalcopyrite is replaced with pyrite, valleriite, and vyalsovite, while pentlandite, with violarite, polydymite, millerite, and pyrite. Sulfides are often replaced with chlorite, serpentine, prehnite, vesuvianite, and hydrogarnet. The compositions of minerals from the djerfisherite and valleriite groups are determined by the primary chemical composition of ore.

The high percentage of tetragonal chalcopyrite determines the high Cu grade of the vienlet-disseminate ore, which was called cupriferous in economic classification of ores. The Ni/Cu ratio is not higher than 0.2. The veinlet-disseminated ore is enriched in PGE proportionally to its enrichment in Cu. As a result, despite the lower total amount of sulfides, the bulk PGE grade turns out to be not lower and often even higher than in the massive pyrrhotite ore. The PGE (ppm)/S (wt. %) ratio is 0.9-1.9; (Pt + Pd)/(Rh + Ir + Ru + Os) = 20-60. The own minerals of Pt and Pd are detected not only in the vienlet-disseminated ore enriched in Cu, but also in the pyrrhotite ore that contains arsenides, stibioarsenides, arsenostannides, and stibiostannides of Pt, Pd, and Ni. Kotulskite and moncheite are typical of the ore enriched in chalcopyrite. The ore bearing millerite and bornite are the richest in PGE, whereas the ores with pyrrhotite and chalcopyrite are depleted in Pt and Pd sulfides. The Pt, Fe, Ni, and Cu sulfides of the kharaelakhite type with variable proportions of these metals were found in the pyrrhotite-chalcopyrite ore in addition to cooperite, braggite, and vysotskite. Tellurides are represented not only by kotulskite but also by telargpalite and sopcheite; silver sulfides and selenides are associated with Ag-Pd, Pd-Ag-Pb, and Pd-Ag-Bi selenosulfides. Sperrylite is a common mineral.

The low-sulfide (LS) PGE mineralization. This type of mineralization was discovered in the Noril'sk ore district as a result of joint investigations carried out by the Geological Survey of the Noril'sk Integrated Works and Russian Academy of Sciences *(Sluzhenikin et al., 1994; Distler et al., 1999)*. As has been shown by exploration of the LS Reef at the Zapolarny Mine, which mines PGE-Cu-Ni sulfide ore of the Noril'sk-1 deposit, that the PGE grade of the low-sulfide ore is sufficiently high (7.1 ppm on average) and PGE reserves are comparable with those at the main ore levels.

The low-sufhide PGE-bearing horizon occupies a special position in the section of the Noril'sk-1 intrusion in its upper contact zone. This horizon is separated from the underlying sulfide ore by

barren rocks 50 m thick (Fig. 6). The upper contact zone is composed of eruptive breccia; olivine-free, olivine-bearing, and olivine gabbrodolerites; gabbrodiorite; leucogabbro; and taxitic chromite-bearing gabbro. The olivine-rich rocks close in composition to the lower picritic and troctolitic gabbrodolerites are of subordinate importance. Leucogabbro and especially taxitic chromite-bearing gabbro are the main host rocks (Fig. 10).

The leucogabbro does not form a continuous layer near the roof of intrusion but occurs as lenses varying from a few meters to a few hundred meters in length and from a few meters to 25 m in thickness. They either come into contact with country rocks or are separated from the latter by marginal gabbrodolerite, gabbrodiorite, and eruptive breccia. The taxitic gabbro occurs within the leucogabbro as several zones, the main of which is located at the base of leucograbbro unit (Fig. 10). The taxitic and leucocratic gabbro grade via a transitional zone that has several centimeters in thickness.

The PGE contents in all rocks of the upper contact zone of the Noril'sk-1 intrusion exceed 0.3 ppm in total. The contents from 0.3 to 2.0 ppm may be regarded as an ordinary background range. The PGE contents in ore are above 3 ppm and commonly range from 3 to 12 ppm, locally reaching 20-40 ppm and 60 ppm in some hand specimens. By the grade and PGE proportions, the low-sulfide ore at the Noril'sk-1 is close to the J-M Reef in the Stillwater pluton.

The Cu and Ni contents in LS ore at the Noril'sk-1 is commonly less than 0.20-0.25%. The ratio of total PGE contents (ppm) to sulfur content (wt. %) in the LS unit is always above 5 and reaches 40-70, whereas this index for disseminated ore at the Talnakh deposit is as high as 1.2 and equals 1.0- 3.5 at the Noril'sk deposit. The Pt/Pd ratio ranges from 0.23 to 0.63 and is approximately equal to that in the PGE-Cu-Ni ore of the main ore units; the prevalent Pt/Pd ratio is 0.33-0.50.

The PGE are distributed in the LS unit nonuniformly both in the lateral and vertical directions. The lateral variations are mainly caused by distribution of leucogabbro, although elevated (as high as 5 ppm) PGE contents are also detected in eruptive breccia and gabbrodolerite. Several maximums of PGE contents were established in the section of LS unit; they are related to the taxitic gabbro enriched in mineral bearing volatile components and chrome and to the productive sulfide assemblages (Fig. 10). The direct correlation exists between PGE grade and relative amounts of H_2O-, Cl-, and F-bearing minerals. The highest PGE contents are detected at the base of LS unit and less frequently elsewhere (Fig. 10).

In contrast to the disseminated ore at the main ore levels, the PGE solid solutions in sulfides make only a small contribution to the total of PGE in the LS unit. The PGE concentrations in Ni, Co, and Fe arsenides and sulfoarsenides-nickeline, maucherite, Co-gersdorffite, and Ni-cobaltite are higher: up to 0.41 wt. % Pt, 0.89 wt. % Pd, and 0.44 wt. % Rh.

The main mass of PGE in low-sulfide ore is related to their own minerals, including intermetallides, Fe–Pt alloys, sulfides, and sulfoarsenides.

The platinum minerals are mainly represented by sperrylite (15%), Pt-Fe alloys (15%) and Pt-atokite (25-35%). The wide isomorphism of both PGE and ligands is typical of A_3B, A_5B_2, and A_8B_3 compounds, where A is Pt and Pd and B is Sn, As, Sb, and occasionally Te. Minerals of composition Pd_2B comprise paolovite Pd_2Sn, palladoarsenide Pd_2As, and phases $Pd_2(Sn,As)$ and $Pd_2(As,Sb)$ with variable proportions of Sn, As, and Sb. Bismuthotellurides are represented by PdTe–PdBi series, Bi-merenskyite and Bi-moncheite. Pt and Pd sulfides comprises cooperite, braggite, vysotskite, and Pt, Pb, Cu, Ni, and Fe sulfides that correspond to kharaelakhite in composition. Hollingworthite is a single mineral of rare PGE identified in the LS ore.

The PGM are 3-90 μm in size; the size of 5-40 μm is predominant. PGM and PGE-bearing arsenides and sulfoarsenides are related to the H_2O-, Cl-, and F-bearing minerals that replace sulfides, often to the contact between sulfides and secondary silicates.

FIELD TRIP STOPS

STOP 1: Drill core yard of the JSC Noril'skgeologiya

The participants will be shown drill cores of the ore-bearing intrusions and associated PGE-Cu-Ni sulfide ores from Talnakh, Oktyabr'sky and Maslovsky deposits. The Talnakh ore junction is represented by drill cores OUG-2 (Fig. 11), SF-11 (Fig. 12) and EM-6 (Fig. 13) from the Talnakh deposit, whereas drill cores RT-7 (Fig. 14), ZF-37 (Fig. 15) and ZF-23 (Fig. 16) characterize the Oktyabrsky deposit. Breccia-type Cu-rich ores from apophyses of the Kharayelakh intrusion (Oktyabrsky deposit, drill cores ZF-23 and ZF-37) and massive copper-rich ores of the Mayak mine (Talnakh deposit, dril core EM-6) will be also studied. Maslovsky deposit will be exemplified by drill core OM-1 (Fig. 17). The section through the Ivakinsky to Morongovsky tuff-lava sequence will be demonstrated by drill core OM-3 (Fig. 18).

The Talnakh intrusion extends in the meridional direction for nearly 20 km, with a width of about 2 km. Its thickness varies from 100 to 350 m (Figs. 7, 8). Disseminated sulfide ores occur within the lower part of intrusion, composed of ultramafic rocks (so called picritic gabbrodolerites) and taxitic-textured mafic rocks with "patches" of ultramafic rocks. Massive ores occur in the bottom part at the contact with the host rocks or separated from the intrusion by a 2-meter thick screen of terrigenous-carbonate sediments of the Devonian or carbonaceous-terrigenous rocks of the Tunguska series (C2-P1). The internal structure of the Talnakh intrusion exemplified by the drill core OUG-2 has been studied in great detail. This information will be given in the next subchapter of the guidebook. Low-sulfide mineralization in the section of the Talnakh intrusive can be observed in the drill hole SF-11 (Fig. 13). Massive sulfide ores of the South 2 deposit will be demonstrated by the example of the drill hole EM-6 (Fig. 14), where significant chalcopyrite ores with high content of platinum-group elements have been revealed. The average contents of copper and nickel for individual ore bodies are shown in Figs. 12-17.

The largest Oktyabrsky deposit (Figs. 7-9) with unique sulfide deposit (2 x 4 x 0.4 km) is confined to the Kharaelakh intrusion. The structure of the Kharaelakh intrusion will be demonstrated by its different parts: the northern part (dril hole RT-7, Fig. 15) and the western part where the intrusive body is divided into a number of apophyses (i.e., drill hole ZF-37, Fig. 16 and dril hole ZF-23, Fig. 17). The Maslovsky deposit forms the southern part of the ore-bearing Norilsk 1 intrusion. It was thoroughly explored by geologists of JSC Norilskgeologiya in recent years. Due to this work a substantial increase in the reserves of nickel, copper and platinum-group elements for Polar Division of Norilsk Nickel was gained. Mineralogical and geochemical characteristics of the rocks and ores are given in publications (*Krivolutskaya et al.,* 2011; *Krivolutskaya et al*., 2012). The thickest intrusive body in the Northern part is represented by the drill hole OM-1 (Fig. 18), where main lithologies typical for the ore-bearing intrusions can be observed. The drill core OM-3 (Fig. 19) will show the cross-section of the lower volcanic suites (from Ivakinsky to Morongovsky).

Composition of lithological units and associated PGE-Cu-Ni sulfide ores of the Talnakh and Kharaelakh intrusions in cross-sections of drill holes OUG-2 and RT-7

The sections consist of the lower contact, taxitic, and picritic gabbrodolerites, olivine, olivine-bearing, and olivine-free gabbrodolerites, gabbrodiorite, prismatic-grained gabbrodolerite, the upper contact gabbrodolerite, quartz diorite, and eruptive breccia (Figs. 19, 20).

The contact gabbrodolerite occurs in the lower and the upper marginal zones as a grey, very fine- and fine-grained massive rock with microdoleritic, ophitic, and poikoloophitic textures of the groundmass and sporadic plagiocalse phenocrysts (An_{70}) incorporated therein. The rock contains olivine (Fo_{64}) and ore minerals. The average modal composition (vol. %) is as follows: 50-60 Pl, 30-40 Cpx, 5-10 Ol, and 5-15 ore minerals; amphibole, biotite, apatite, and titanite are noted.

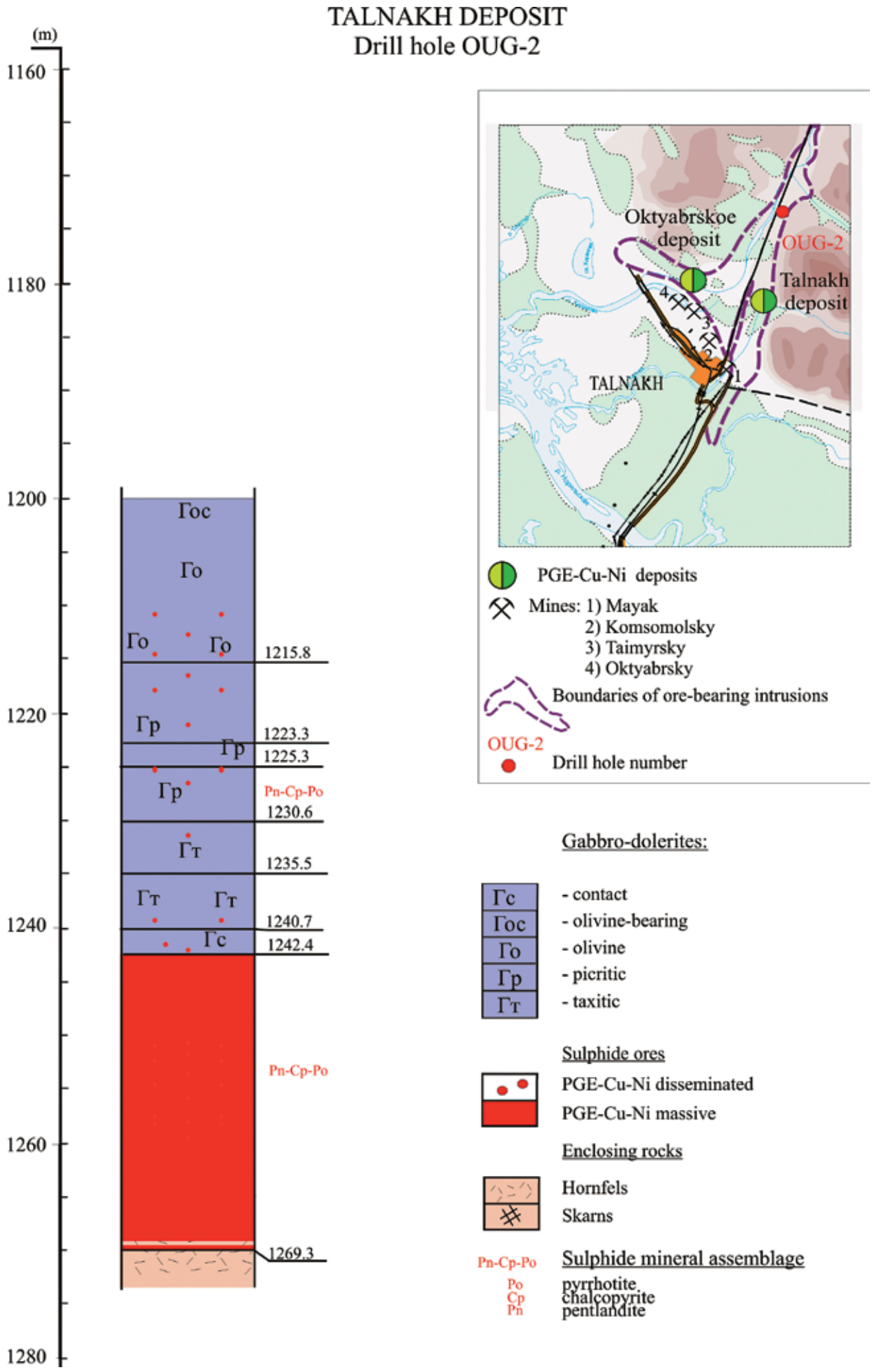

Fig. 11. Location and rock section of drill hole OUG-2, Talnakh deposit

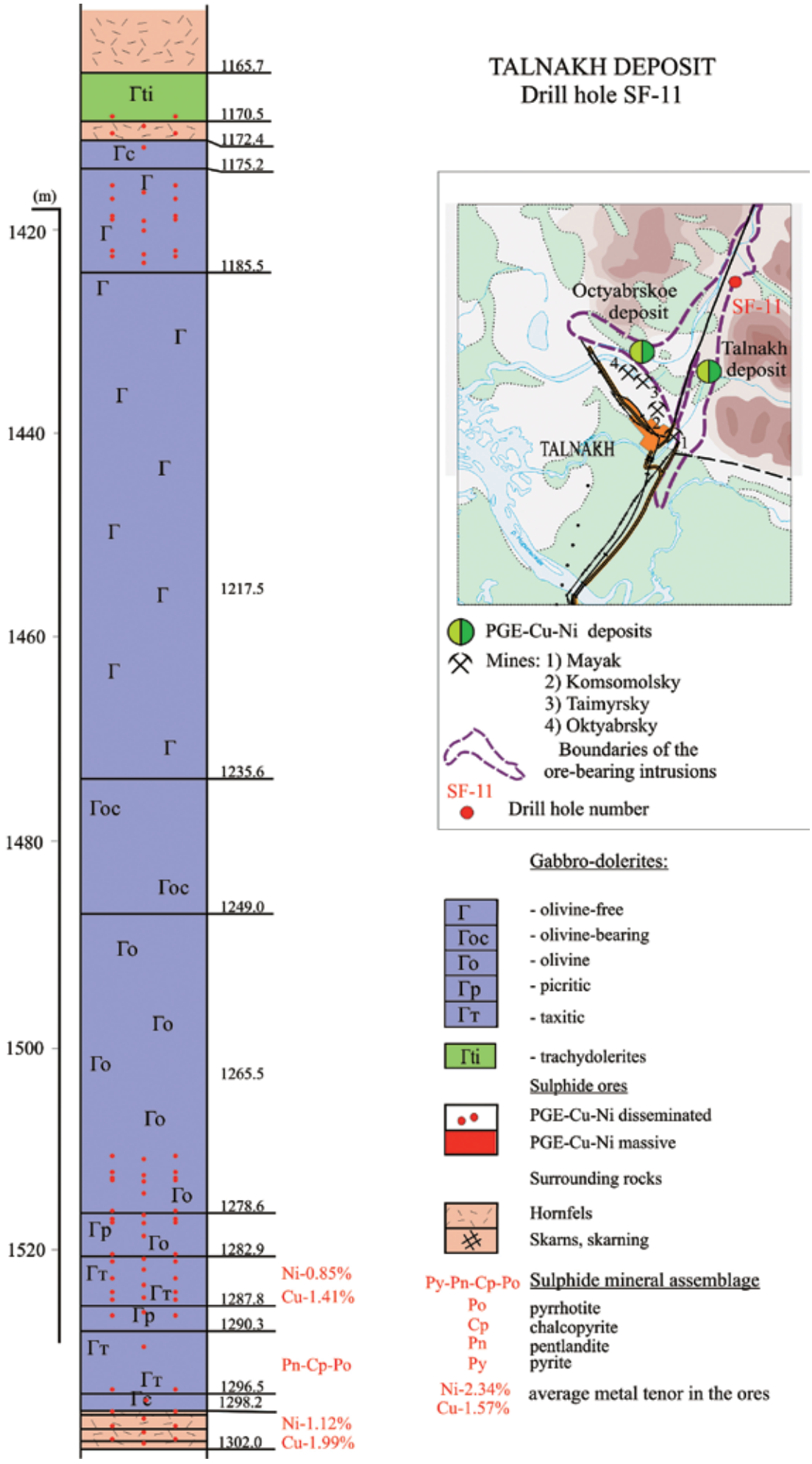

Fig. 12. Location and rock section of drill hole SF-11, Talnakh deposit

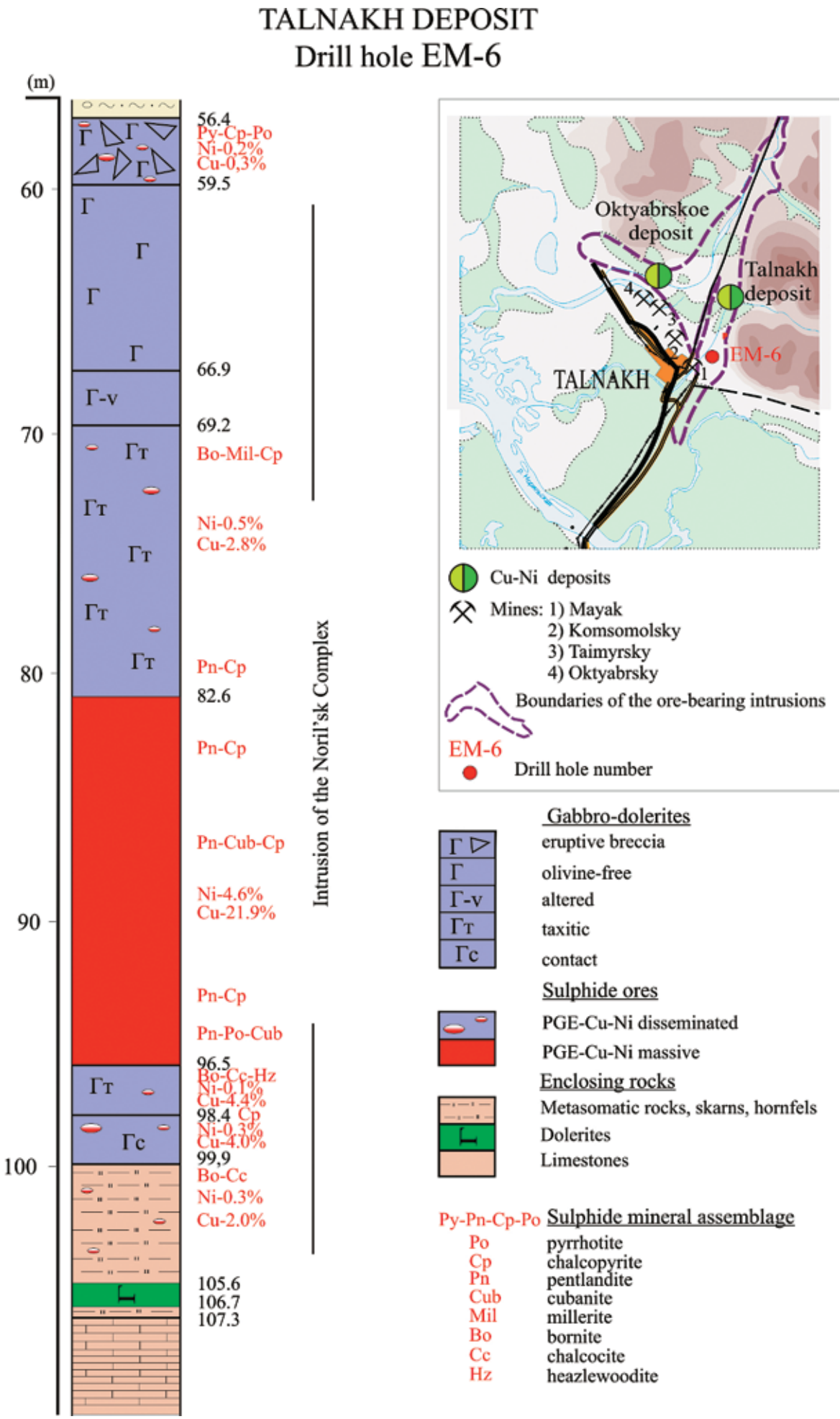

Fig. 13. Location and rock section of drill hole EM-6, Talnakh deposit

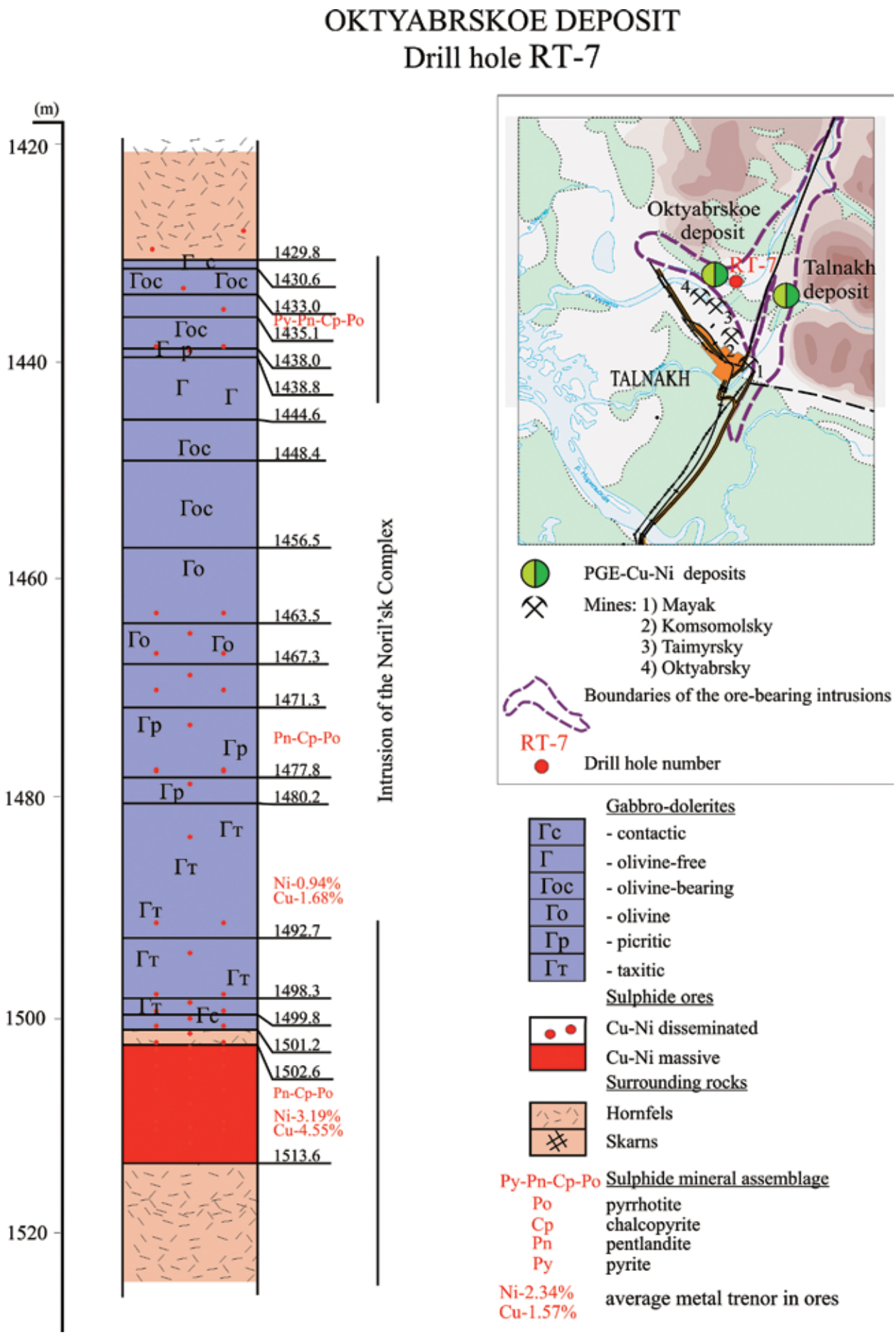

Fig. 14. Location and rock section of drill hole RT-7, Oktyabrskoe deposit

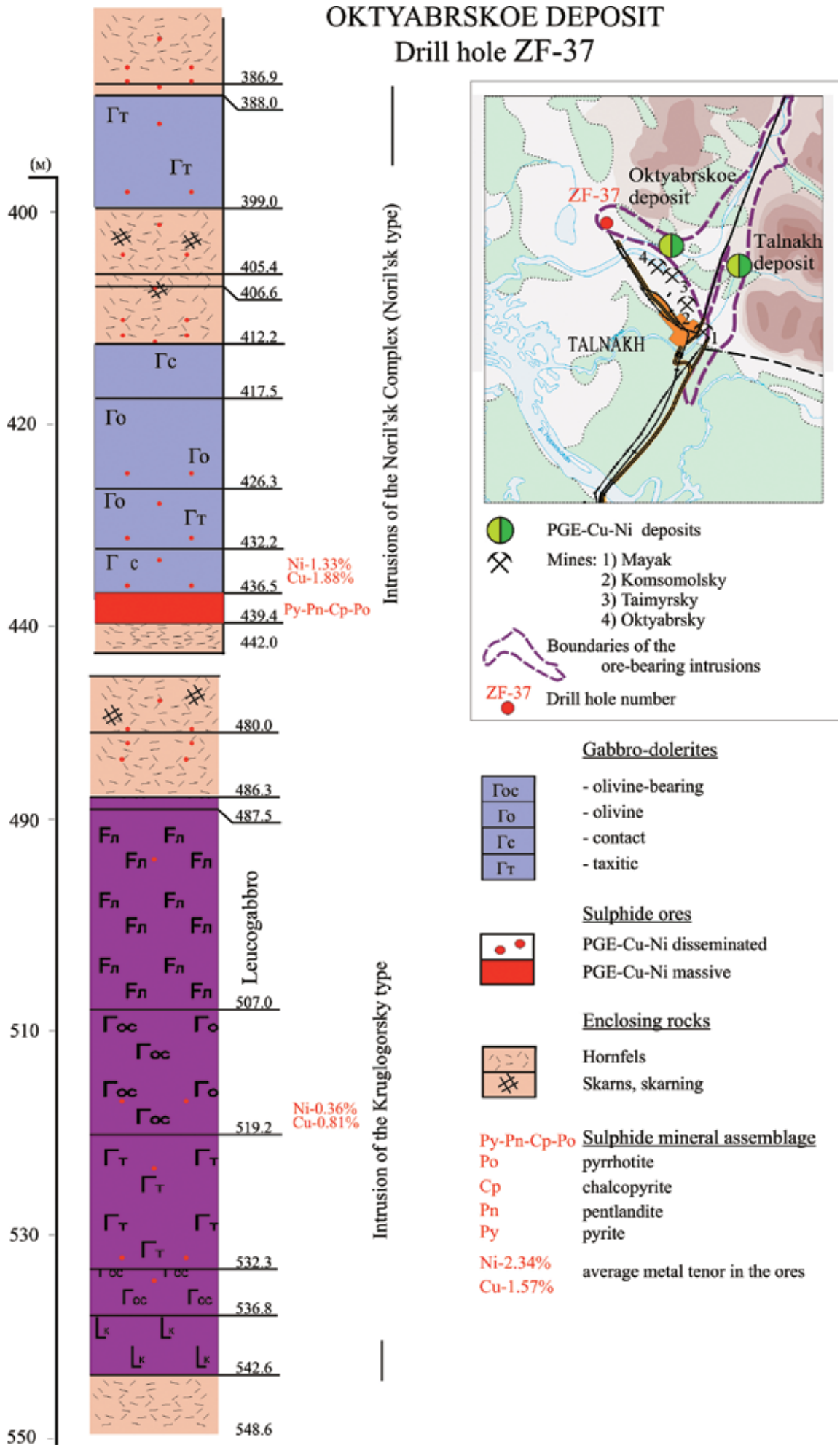

Fig. 15. Location and rock section of drill hole ZF-37, Oktyabrskoe deposit

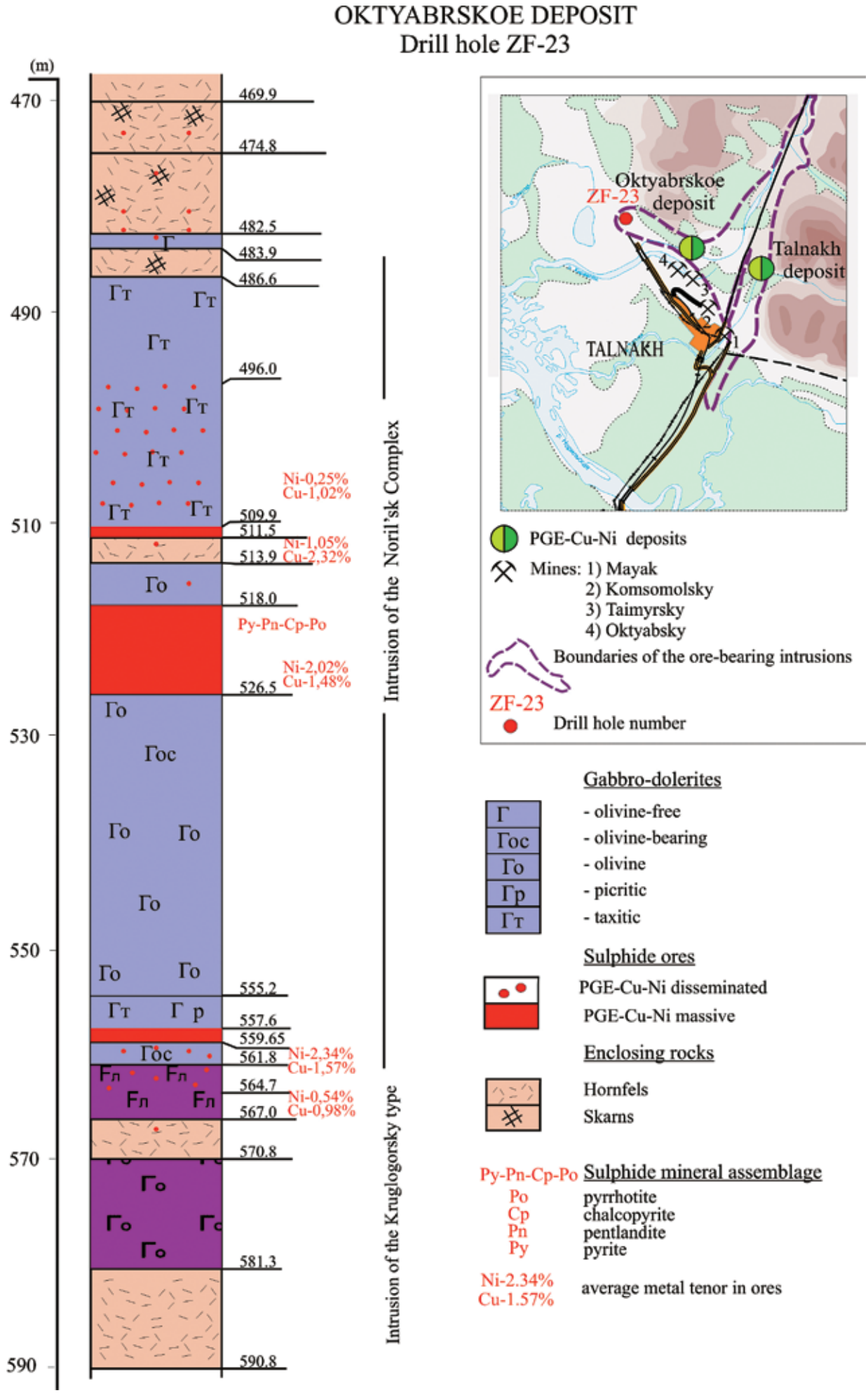

Fig. 16. Location and rock section of drill hole ZF-23, Oktyabrskoe deposit

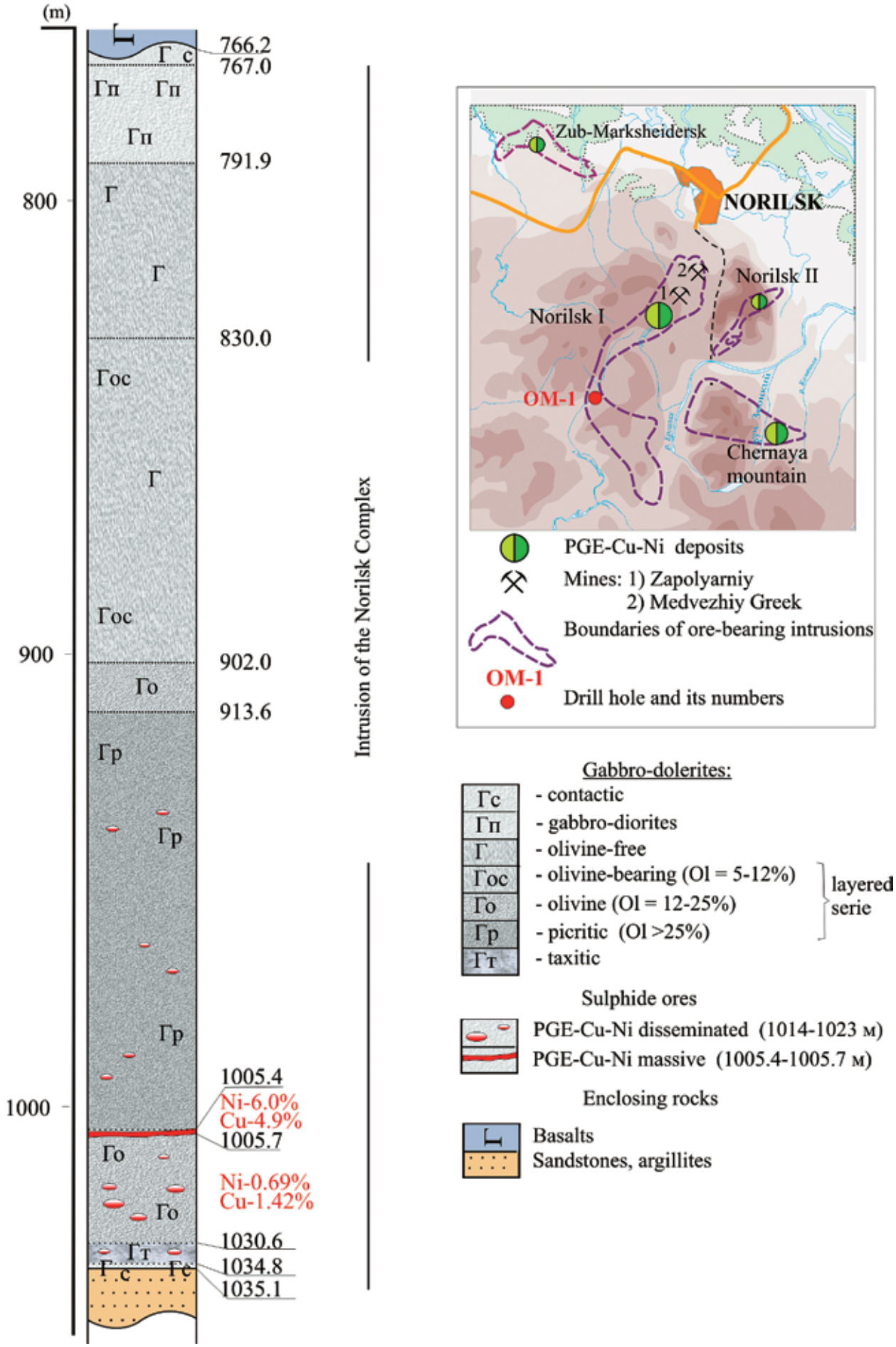

Fig. 17. Location and rock section of drill hole OM-1, Maslovsky deposit

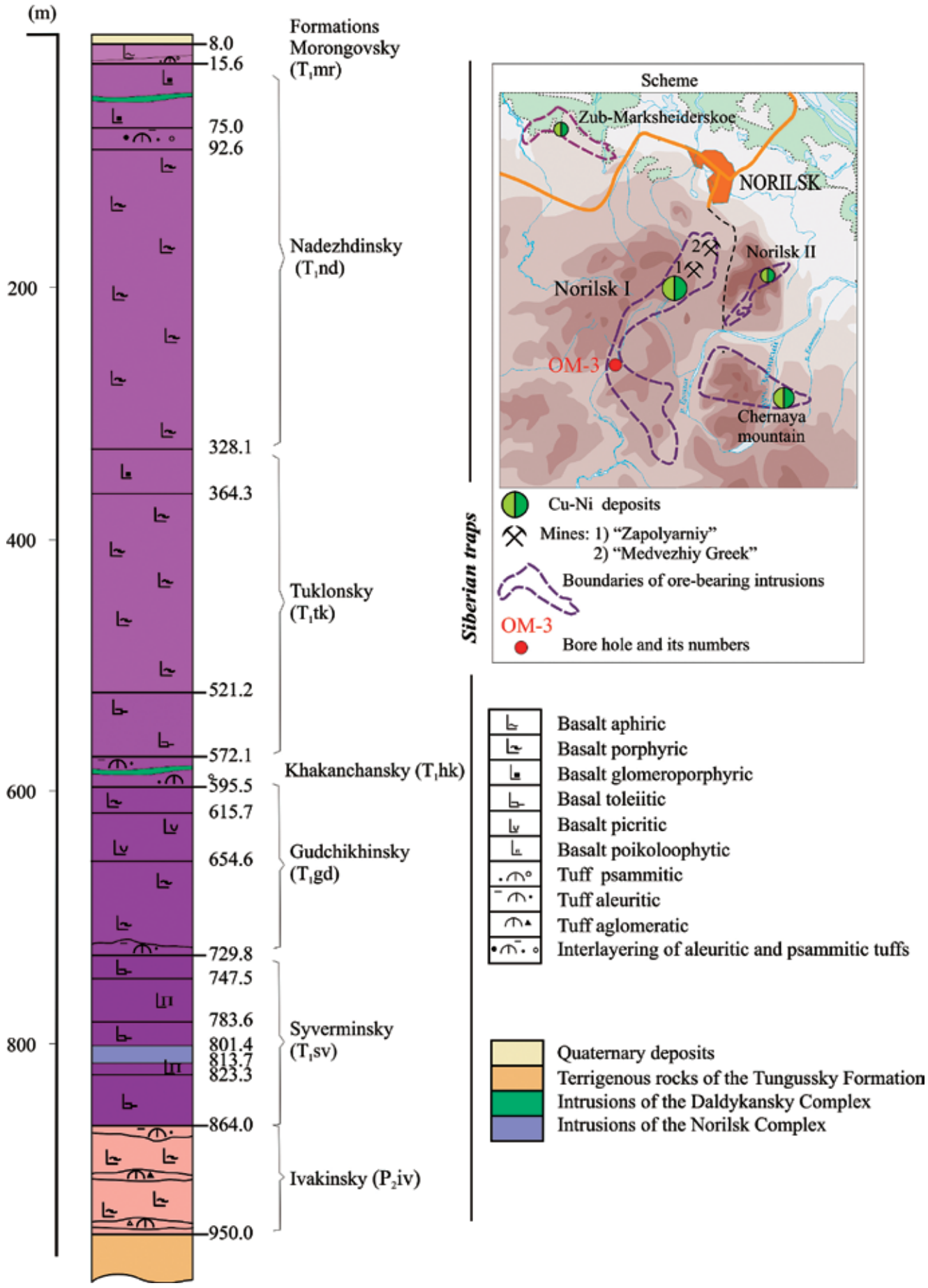

Fig. 18. Location and rock section of drill hole OM-3, Maslovsky deposit

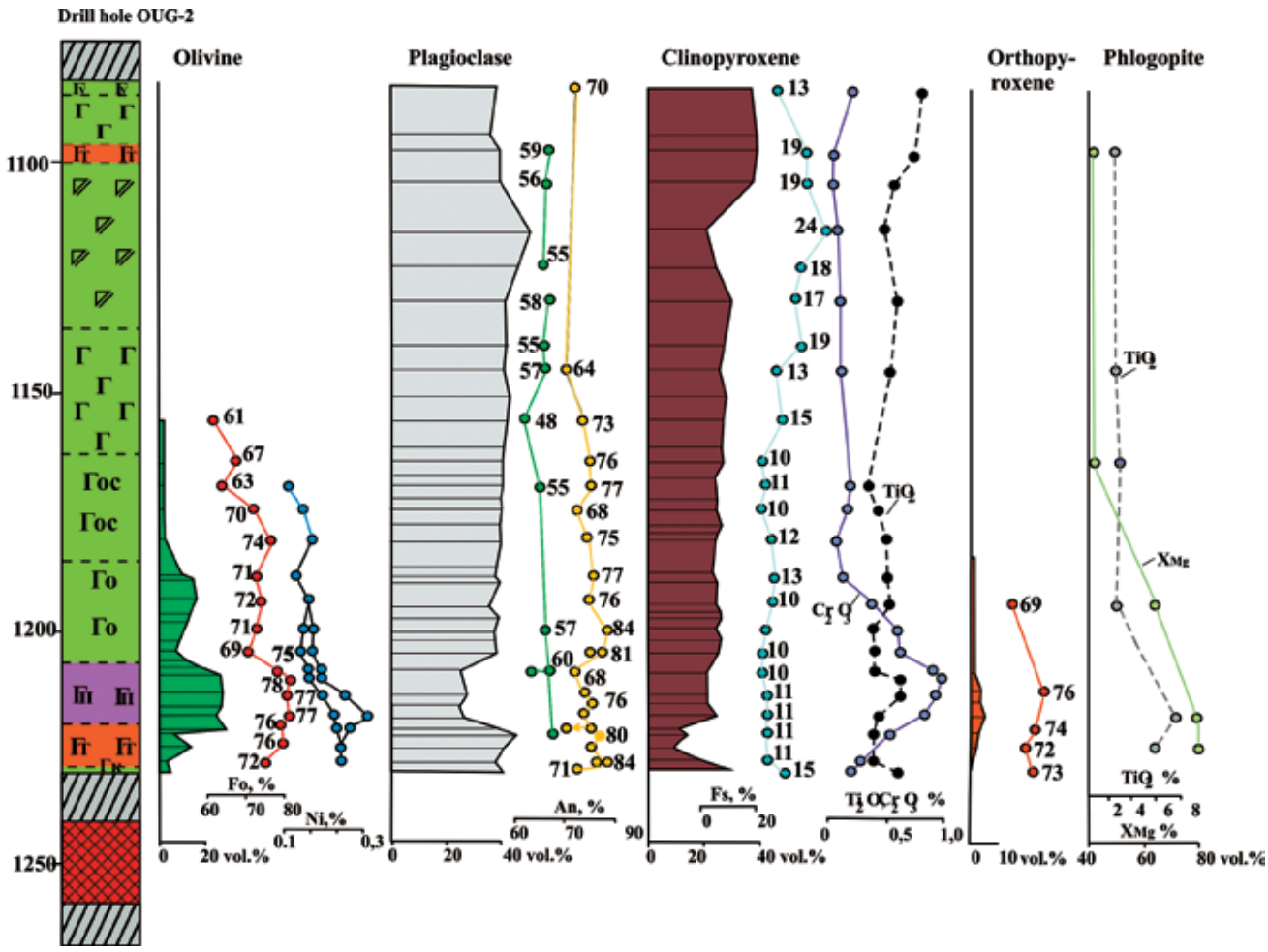

Fig. 19. Variations in the contents and chemical composition of rock-forming minerals through a section of the Talnakh intrusion (drill hole OUG-2). Gabbrodolerites: Г – olivine-free, Гос – olivine-bearing, Го – olivine, F – leucogabbro, Гк – contact; Гп – ultramafic rocks, Гт – taxitic-textured rocks, F≥ – gabbrodiorite.

The taxitic gabbrodolerite is a light grey, coarse-grained rock with clearly expressed taxitic texture. The modal composition is variable (vol. %): 35-75 Pl (two generations – An_{83-76} and An_{66-51}), 10-30 Cpx (Fs_{10-19}), 5-25 Ol (Fo_{82-62}) and up to 5 Opx (Fs_{21-30}).

The structural pattern of rock is determined by large (3-5 mm) zonal tabular plagioclase crystals (An_{83-76} and An_{66-57}) with outer rims of An_{30} incorporated in aggregate of xenomorphic clinopyroxene grains up to 5 mm in size. Clinopyroxene, in turn, contains small (<1 mm) plagioclase laths and olivine grains and reveals zoning: internal zones are green, while the outer zones are brownish.

The coarse-grained domains are combined with the fine-grained domains with distinct ophitic and gabbroic textures. Small, up to 1-2 cm in size, lenticular segregations are composed of the fine-grained olivine and plagioclase, occasionally with an admixture of Al-Mg-spinel; this aggregate corresponds to troctolite in composition. As a rule, olivine is xenomorphic and includes tabular plagioclase crystals.

Titanomagnetite and ilmenite occupy up to 5% of rock volume. The taxitic and picritic gabbrodolerite make up an ore-bearing unit with 10-15 vol. % of sulfides. The ore minerals occur as large (up to 5 cm across) xenomorphic segregations and schlieren. The secondary alteration consists in saussuritization of plagioclase, replacement of clinopyroxene with amphibole, and biotite replaced with chlorite. The taxitic gabbrodolerite grades upward into the picritic gabbrodolerite.

The picritic gabbrodolerite is a unit with a sharp upper boundary. The dark grey, medium- and fine-grained massive rock contains 25-75 vol. % of olivine. The texture is poikiloophitic, poikilitic, and locally panidiomorphic. The average modal composition is as follows (vol. %): 25-30 Ol (Fo_{78-72}), 30-35 Pl (An_{21-72} and An_{66-53}), 30-35 Cpx (Fs_{9-12}), <5 Opx (Fs_{20-23}), and 5-7 Bi. Apatite and titanite are accessory minerals.

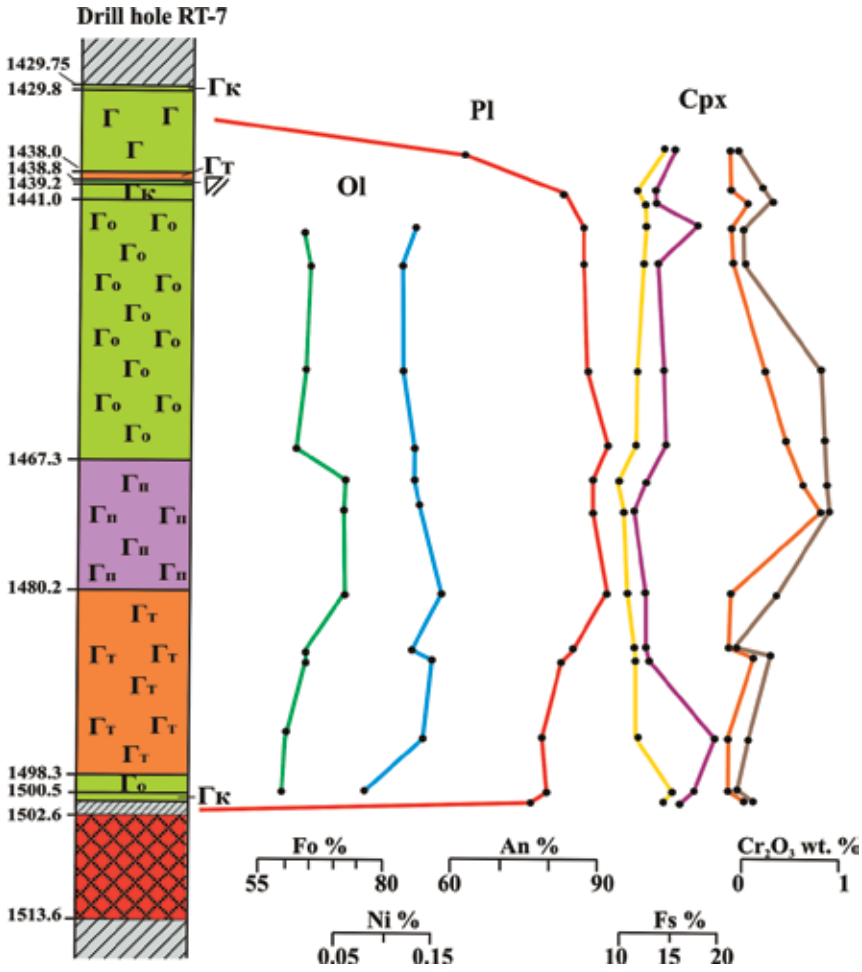

Fig. 20. Variations in the contents and chemical composition of rock-forming minerals through a section of the Kharaelakh intrusion (drill hole RT-7)

Olivine is distributed rather uniformly as euhedral grains 0.3-1.0 mm in size, partly serpentinized. Plagioclase occurs as large (up to 1.5 mm) tabular crystals with included euhedral olivine crystals, as well as xenomorphic zonal grains. The clinopyroxene oikocrystals (1-5 mm across) contains small olivine grains and plagioclase laths. Titanomagnetite, ilmenite, chrome-magnetite, and chromite occupy 3-5% of rock volume. The sulfide content reaches 5-8 vol. %. In the upper part of the picritic unit, sulfides occur as fine (<2 mm) interstitial disseminations, while ovoid segregations as large as 25 mm across are predominant in the middle and lower parts of the unit. Clusters of large plagioclase grains appear in the zone of transition to the taxitic gabbrodolerite; their amount increases downward where these clusters merge, and the rock acquires typical taxitic appearance.

The olivine gabbrodolerite is a grey medium-grained massive rock with poikiloophitic and ophitic textures. The transition to the underlying picritic gabbrodolerite is rather sharp; the transition zone is 0.1-0.3 m thick. The modal composition of olivine gabbrodolerite is as follows (vol. %): 10-15 Ol (Fo_{75-67}), 40-50 Pl (An_{90-75} and An_{60-57}), 25-30 Cpx (Fs_{11-13}), 3 Opx (Fs_{26}). The boundary zone between olivine gabbrodolerite and picritic gabbrodolerite is enriched in biotite (up to 6-7 vol. %) and sulfides.

The olivine-bearing and olivine-free gabbrodolerites overlie the olivine gabbrodolerite via a zone of gradual transition. The amount of olivine progressively decreases upward up to its complete disappearance. The rocks consist of plagioclase (An_{83-62} and An_{57-55}), clinopyroxene (Fs_{10-19}), olivine (Fo_{71-61}), orthopyroxene, and quartz that appears in the upper portion of the unit. Oxides and dispersed sulfides are noted.

Gabbrodolerite and gabbrodiorite are greenish and pinkish grey medium- and coarse-grained rocks with prismatic granular and ophitic textures, pegmatoid schlieren, and interlayers of titanomagnetite gabbro. The rocks consist of 50-70 vol. % of plagioclase (An_{59-56}) and 20-30 vol. % of clinopyroxene (Fs_{17-24}).

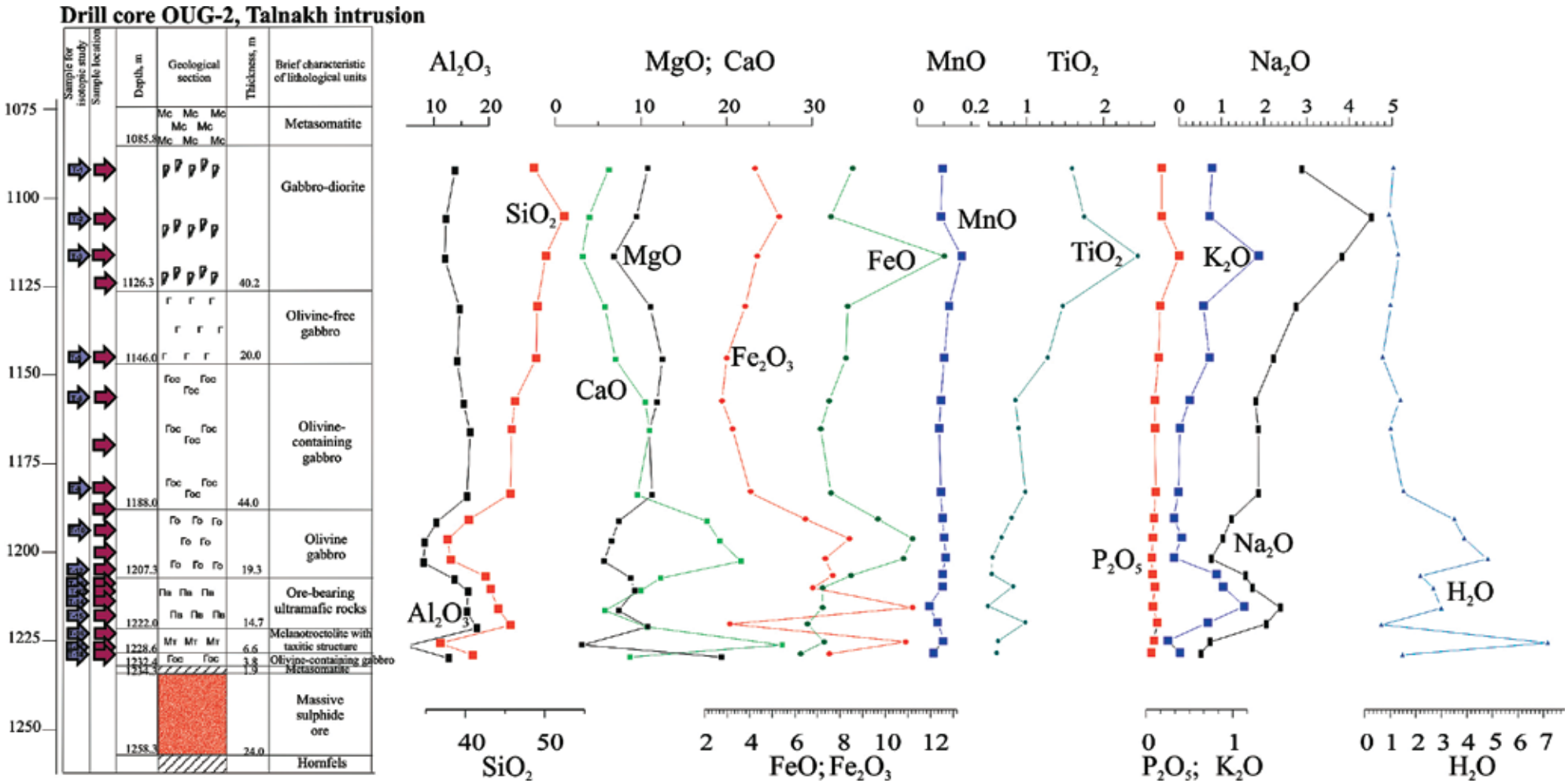

Fig. 21. Variations in the contents of Cr_2O_3, MgO, FeO, Fe_2O_3, Na_2O, K_2O, TiO_2, CaO, Al_2O_3, SiO_2, P_2O_5 through a section of the Talnakh intrusion (drill hole OUG-2)

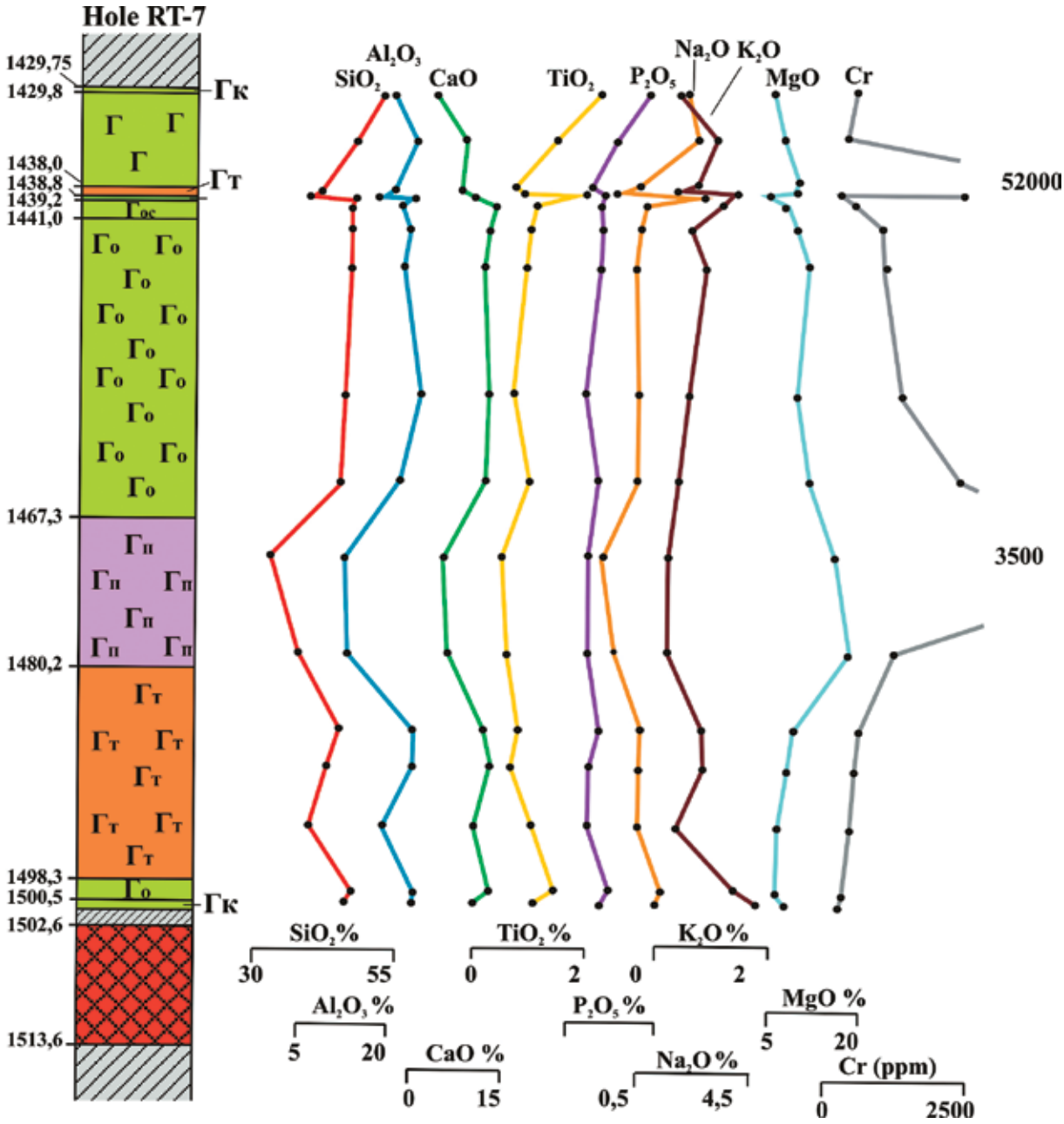

Fig. 22. Variations in the contents of SiO_2, Al_2O_3, CaO, TiO_2, P_2O_5, Na_2O, K_2O, MgO (in wt.%) and Cr (in ppm) through a section of the Kharaelakh intrusion (drill hole RT-7).

Quartz diorite of the uppermost unit is a leucocratic rocks with sharply delineated and shadow xenoliths of the country sandshale rocks.

In the section of drill hole RT-7 at the upper endocontact of the Kharaelakh intrusion an upper taxitic gabbro with low-sulfide PGE ores has been identified (Fig. 20). The horizon has thickness 0.8 m. The rock composed of idiomorphic plagioclase tables and xenomorphic clinopyroxene grains (Fs_{12}). Olivine (20% of the rock volume) forms isometric rounded crystals. Plagioclase completely replaced by fine-grain chlorite, whereas olivine replaced by magnesium- and iron-bearing hydrosilicates. Clinopyroxene is intensively replaced by hornblende and actinolite. The rock contains a large amount of amygdaloid phases up to 2 cm, composed of phlogopite, chlorite, and actinolite. High chromium content (5.2 wt.%) is supported by abundant chromite that form small (less than 40 microns) grains unevenly distributed in the rock.

The variation of major and ore components in the sections of drill holes OUG-2 and RT-7 are shown in Figs. 21 and 22, respectively. The following systematic trends may be pointed out:

(1) The unit of picritic gabbrodolerite is characterized by the highest MgO content with a peak in the upper third of the unit. The MgO content decreases upward and downward from this level as a result of depletion in olivine. Another maximum of MgO content, which appears elsewhere in this intrusion, is related to the appearance of olivine-bearing rocks in the upper contact zone. In the borehole sections the MgO content ranges from 22.41 to 5.11 wt. %.

The curve of Cr_2O_3 distribution mimics that of MgO virtually completely except the upper part of the olivine gabbrodolerite unit where chrome-magnetite disappears abruptly against the gradual decrease in olivine content. In general, the Cr_2O_3 content varies from the detection limit (<0.007 wt. %) to 0.77 wt. % in the upper part of picritic unit due to the high Cr content in clinopyroxene and large segregations of chrome-magnetite and chromite. The Cr_2O_3 contents decrease up- and downsection from this level in compliance with decreasing amounts of oxides and falling Cr content in clinopyroxene.

(2) The FeO and Fe_2O_3 distributions are identical. Their highest concentrations (7.6 and 11.45 wt. %, respectively) are related to the picritic unit enriched in olivine and clinopyroxene at the expense of plagioclase and to the uppermost unit, where gabbrodiorite contains up to 10-15 vol. % of titanomagnetite. The minimum of Fe contents falls on the boundary between picritic and olivine gabbrodolerite.

(3) Maximums of CaO and Al_2O_3 contents (12.21 and 19.18 wt. %, respectively) fall on olivine and olivine-bearing gabbrodolerites enriched in calcic plagioclase. The taxitic gabbrodolerite is close to the above rocks in this respect. The picritic gabbrodolerite characterizes by low CaO and Al_2O_3 contents (4.96 and 5.59 wt. %, respectively) owing to the enrichment in olivine and depletion in plagioclase.

(4) P_2O_5, TiO_2, MnO, K_2O, and Na_2O are gradually increased from bottom to top of the section in contrast to CaO and Al_2O_3. Local peaks of MnO contents are caused by enrichment in olivine that contains up to 0.65 wt. % MnO. The elevated Na_2O content in the upper part of the section is related to albitization of plagioclase.

(5) Concentrations of Ni, Co, and Cu are largely related to sulfides that occur in the ore-bearing picritic and taxitic gabbrodolerites.

Oxygen isotope compositions

The rocks of the middle part of the Talnakh intrusive section have the $\delta^{18}O$ value within the limits typical for unaltered mantle rocks (Fig. 23). The rocks of the upper and lower parts of the intrusion have elevated $\delta^{18}O$ values (i.e., 8-13), whereas ultramafic rocks have low $\delta^{18}O$ values (4-6). Enrichment can be explained both by the assimilation of crustal material at the magmatic stage, and by hydrothermal alteration of the already crystallized rocks. The prononced $\delta^{18}O$ variations, from 4.6 to 13.2 ‰, are characteristic of the Kharaelakh intrusion. The rocks in the central part of the massif have $\delta^{18}O$ values close to that of the mantle rocks. In the upper part of the intrusion (60 m), composed of gabbro diorites and leucogabbro with low-sulfide PGE mineralization, the rocks do not differ greatly in their oxygen isotopic composition from the metamorphosed and metasomatized sedimentary rocks surrounding the massif. The rocks at the bottom of the intrusion show isotopic and petrological features for contamination that took place at the present location site. Norites and quartz norites occurring near the contact with argillaceous rocks are not typical for the Norilsk type intrusions.

Strontium and neodymium isotope compositions

A considerable variation in $^{87}Sr/^{86}Sr$ values is observed for different rocks of the Talnakh massif (Fig. 24). Minimum values are characteristic of olivine-containing and olivine gabbro dolerites. $^{87}Sr/^{86}Sr$ are distinctly different in the marginal zones of intrusion. This type of pattern is similar to the

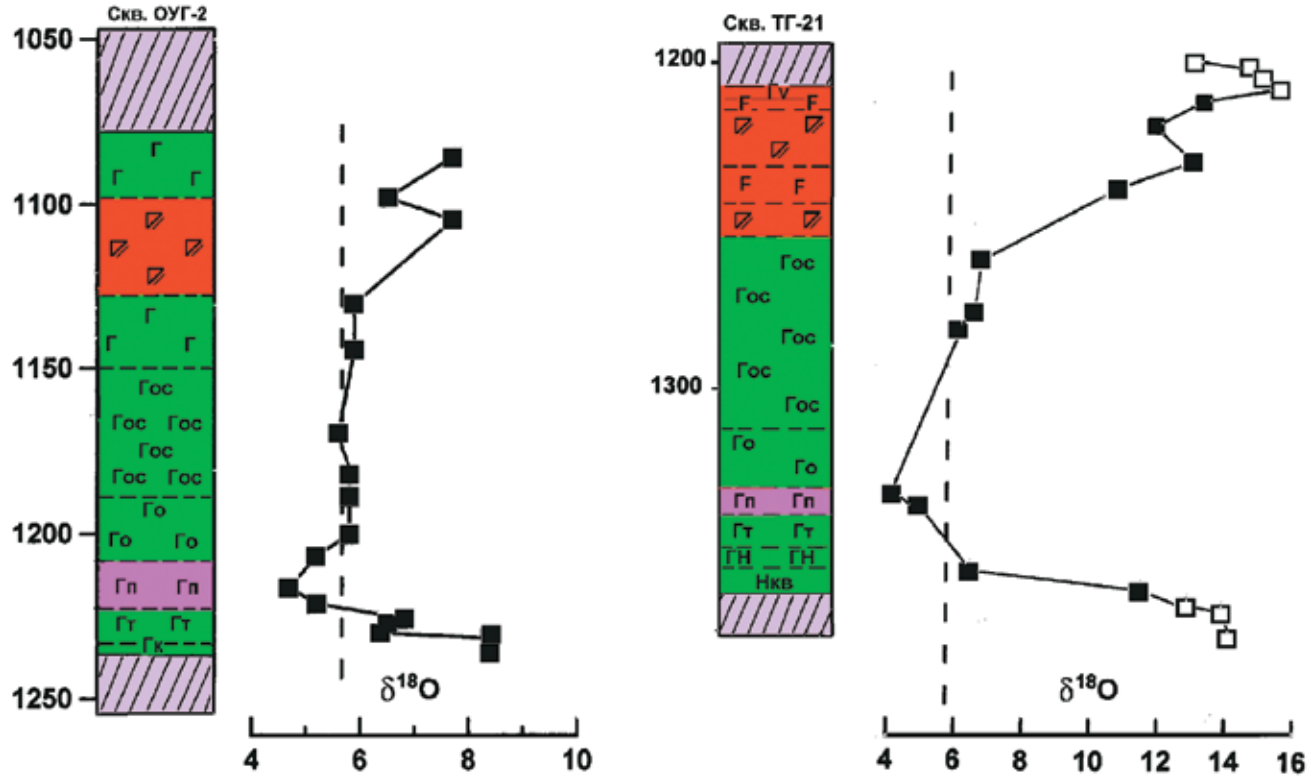

Fig. 23. Variations in the oxygen isotope composition through a section of the Talnakh (drill hole OUG-2, left) and Kharaelakh (drill hole TG-21, right) intrusions

distribution of $\delta^{18}O$. These results can be governed by several factors, such as contamination, with minimum values of $^{87}Sr/^{86}Sr$ and $\delta^{18}O$ in the central parts of the intrusion, or by involvement of post-magmatic processes. Contamination does not necessarily have to occur at present location site of the intrusion, but rather during the interaction within deep-staging chamber(s).

For most ore-bearing intrusions, including Talnakh and Kharayelakh, εNd values show a restricted range (around +1). This is in contrast to melanocratic massifs of the Lower Talnakh type, with negative εNd values from -4 to -5 and highly radiogenic strontium. In contrast to $^{87}Sr/^{86}Sr$ values no significant variations of εNd values have been observed in different rock lithologies of the Talnakh intrusion (Fig. 24).

Sulfur and copper isotope compositions

All three types of PGE-Cu-Ni sulfide ores occur in drill holes OUG-2 and RT-7 (Figs. 19, 20, 25). The disseminated ore is hosted in picritic and taxitic gabbrodolerites and is represented by chalcopyrite-pyrrhotite variety. In the upper part of the picritic unit, iron monosulfides are represented by intergrowths of troilite and Fe-rich hexagonal pyrrhotite. Cubanite (10% of sulfide mass) is represented by its tabular variety. Downsection, troilite disappears, and pyrrotite is represented by both hexagonal and monoclinic modifications. The PGE-Cu-Ni massive ore occurs as a thick layer hosted in hornfels. The chalcopyrite-pyrrhotite ore contains hornfel xenoliths. A halo of veinlet-disseminated ore surrounds the body of massive ore. In low-sulfide PGE ores sulfides are represented by assemblages of pentlandite + chalcopyrite and millerite + pyrite + chalcopyrite.

The massive ores of the Talnakh intrusion (Fig. 26) have $\delta^{34}S$ values ranging from 7.8 to 12.1‰ with a mean of 10.88‰ and a standard deviation of 0.77 (n=40), which are similar to the disseminated ores with $\delta^{34}S$ values of 9.9 to 12.0‰ and a mean of 10.97 ‰ and a standard deviation of 0.44 ‰ (n=40).

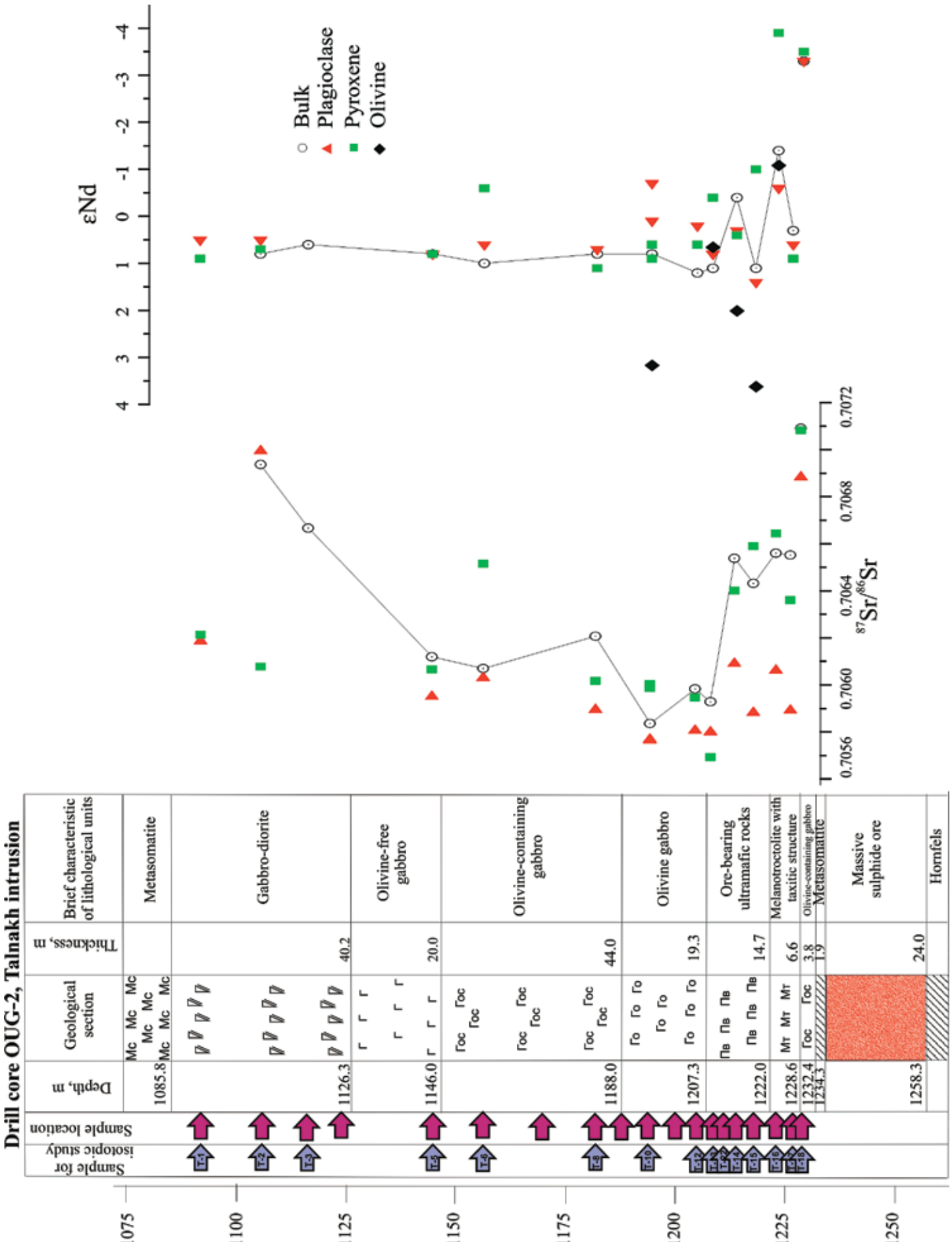
Drill core OUG-2, Talnakh intrusion
Sample for isotopic study
Sample location
Depth, m
Geological section
Thickness, m
Brief characteristic of lithological units
Metasomatite
Gabbro-diorite
Olivine-free gabbro
Olivine-containing gabbro
Olivine gabbro
Ore-bearing ultramafic rocks
Melanotroctolite with taxitic structure
Olivine-containing gabbro
Metasomatite
Massive sulphide ore
Hornfels
1085.8
1126.3
1146.0
1188.0
1207.3
1222.0
1228.6
1232.4
1234.3
1258.3
40.2
20.0
44.0
19.3
14.7
6.6
3.8
1.9
24.0
1075
1100
1125
1150
1175
1200
1225
1250
εNd
4 3 2 1 0 -1 -2 -3 -4
Bulk
Plagioclase
Pyroxene
Olivine
$^{87}Sr/^{86}Sr$
0.7056 0.7060 0.7064 0.7068 0.7072

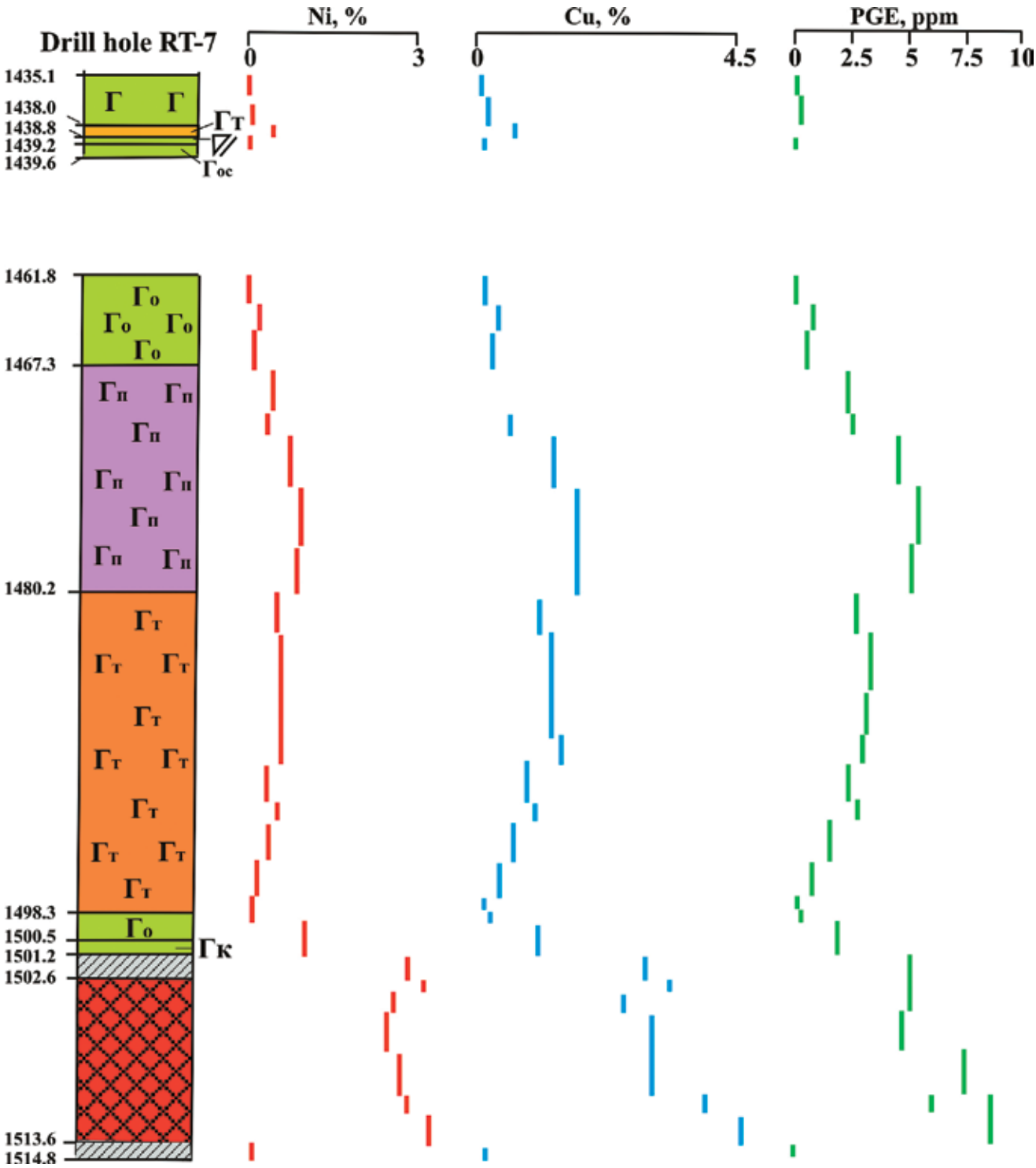

Fig. 25. Variations in the contents of Ni, Cu (in wt.%) and PGE (in ppm) through the upper contact zone that hosts the low-sulfide PGE horizon in the Noril'sk 1 intrusion (drill hole 3110)

Fig. 24. Strontium and neodymium isotope variations in rocks and minerals through a section of the Talnakh intrusion (drill hole OUG-2)

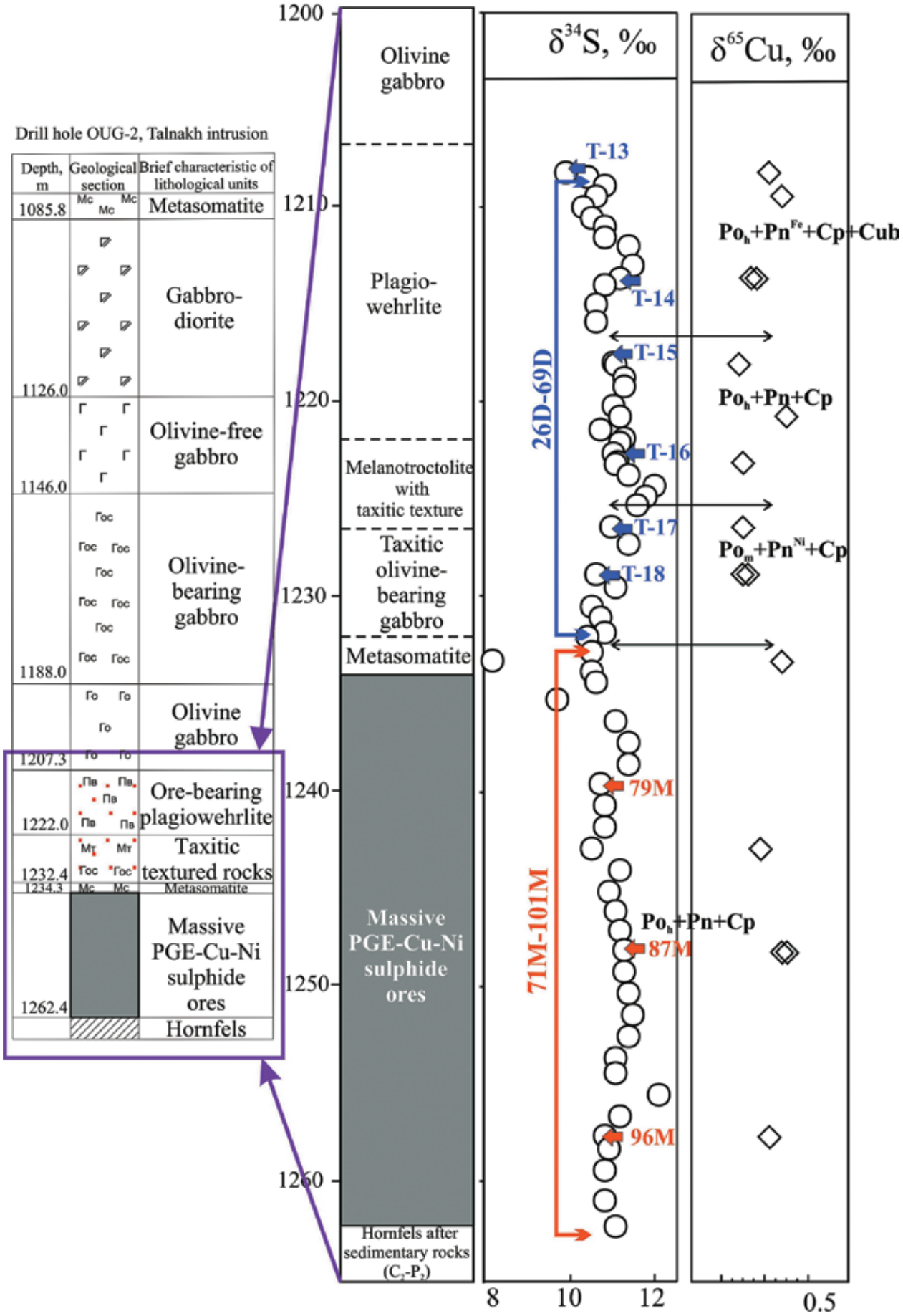

Fig. 26. Variations in the sulfur and copper isotope compositions through a lower sulfide-bearing part of the Talnakh intrusion (modified after *Malitch et al.,* 2014). Red points in geological section refer to disseminated PGE-Cu-Ni sulfide mineralization

The disseminated and massive ores of the Talnakh intrusion (Fig. 26) have Cu isotopic compositions with δ^{65}Cu values ranging from -1.1 to 0 ‰. The disseminated ores have a mean δ^{65}Cu value of -0.70 ‰ and a standard deviation of 0.40 ‰, whereas the massive ores have a mean δ^{65}Cu value of -0.24 ‰ and a standard deviation of 0.25 ‰.

Samples from the different intrusions in the Noril'sk Provinve have overall δ^{65}Cu values ranging from -2.9 to 1.0‰ and δ^{34}S values from -0.7 to 13.8‰ (*Malitch et al*., 2014). Sulfide ores from the economic Kharaelakh, Talnakh and Noril'sk-1 intrusions have different mean δ^{65}Cu values of -1.56 ± 0.27‰, -0.55 ± 0.41‰ and 0.23 ± 0.28 ‰, respectively (Fig. 27). The variation of δ^{65}Cu values is interpreted to represent a primary feature of the ores, although assimilation of external source at Kharaelakh cannot be ruled out.

Sulfide ores from the three economic intrusions have distinct but restricted ranges of δ^{34}S values with a mean of 12.66 ± 0.49‰ for Kharaelakh, 10.92 ± 0.62‰ for Talnakh and 9.20 ± 1.82‰ for Noril'sk-1. The variations of δ^{34}S values are most likely due to the addition of different amounts of crustal sulfur to mantle-derived magmas during their residence in deep-staging chambers.

The ores of the subeconomic Chernogorsk intrusion have homogenous δ^{34}S values of 10.86 ± 0.43‰, in contrast to the highly variable S isotopic compositions for those in the Vologochan and Zub-Marksheider intrusions (5.1-8.5 ‰ and -0.7-3.9 ‰, respectively) and sulfide accumulations from the non-economic Nizhny Talnakh intrusion (1.8-7.6 ‰) (Fig. 28).

Given the Zub-Marksheider and Kharaelakh intrusions are located at the same stratigraphic level, their contrasting S isotopic compositions indicate that the immediate country rocks may have little impact on the S isotopic composition of sulfide ores of the intrusions, whereas the interaction of magma with host rocks that took place deeper before final emplacement may be the major control (*Malitch et al*., 2014).

The observed negative correlation of S and Cu isotope compositions and a restricted range of δ^{34}S and δ^{65}Cu values for an individual intrusion may be a useful indicator of the potential for hosting Ni-Cu-PGE sulfide deposits.

STOP 2: Field trip to the upper section of the Mokulaevsky tuff-lava sequence

Structure of the tuff-lava strata along the Mokulaevsky creek

The structure of the upper section part of the tuff-lava strata can be demonstrated on the example of the volcanite section exposed along the sides of the Mokulaevsky creek (Fig. 29). The geological section of the upper rock formations is shown in Fig. 30. The section begins in the middle of the Nadezhdinsky Suite and ends by the Kumginsky Suite.

The Nadezhdinsky Suite (T_1nd)

The Nadezhdinsky Suite in this section is represented by 19 lava flows and a tuffaceous horizon. The thickness of flows varies from 5 to 65 m (with an average of 15-20 m). The upper formation boundary goes along the sole of the tuff interlayer at the basis of the Morongovsky suite. The total thickness of the Nadezhdinsky suite is about 440 m. Basalts have a typical aphyric or porphyric structure. The most characteristic is oligoglomeroporphyric (poliphiric) structure with the presence of 1-2 phenocrysts per one square cm. An aphyric structure is rare for basalts. A typical poliphyric structure is characterized by the presence of intratelluric plagioclase, clinopyroxene and olivine phenocrysts along with fine-grained microdoleritic, tholeiitic and intersertal groundmass. Porphyry and glomeroporphyry structures are characterized by a significant predominance of plagioclase in the phenocrysts composition. The maximum number of porphyry phases (6-15%) was found in the basalts of the upper section part. According to their composition phenocryst plagioclases (An_{55-75}) correspond to labrador-bytownite. The bulk rocks comprise 35-55% plagioclase (An_{45-60}), 25-32% clinopyroxene (Mg# 71-84), 3-8% olivine (Fo_{43-56}), 5-18% devitrified glass and 1-4% ore minerals.

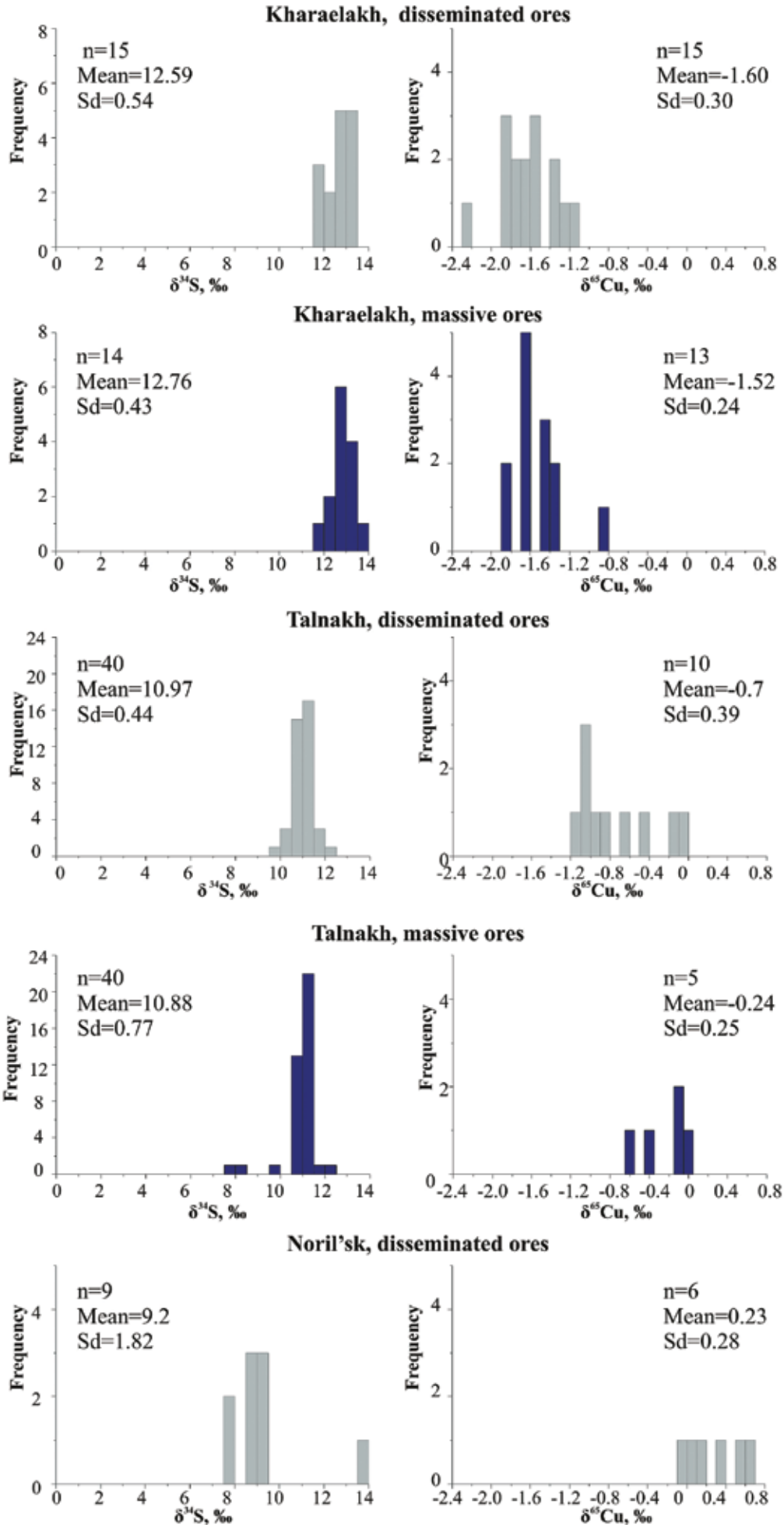

Fig. 27. Histograms showing the distribution of ^{34}S and ^{65}Cu values in disseminated (in grey) and massive (in blue) ores of economic Kharaelakh, Talnakh and Noril'sk-1 intrusions (modified after *Malitch et al*., 2014)

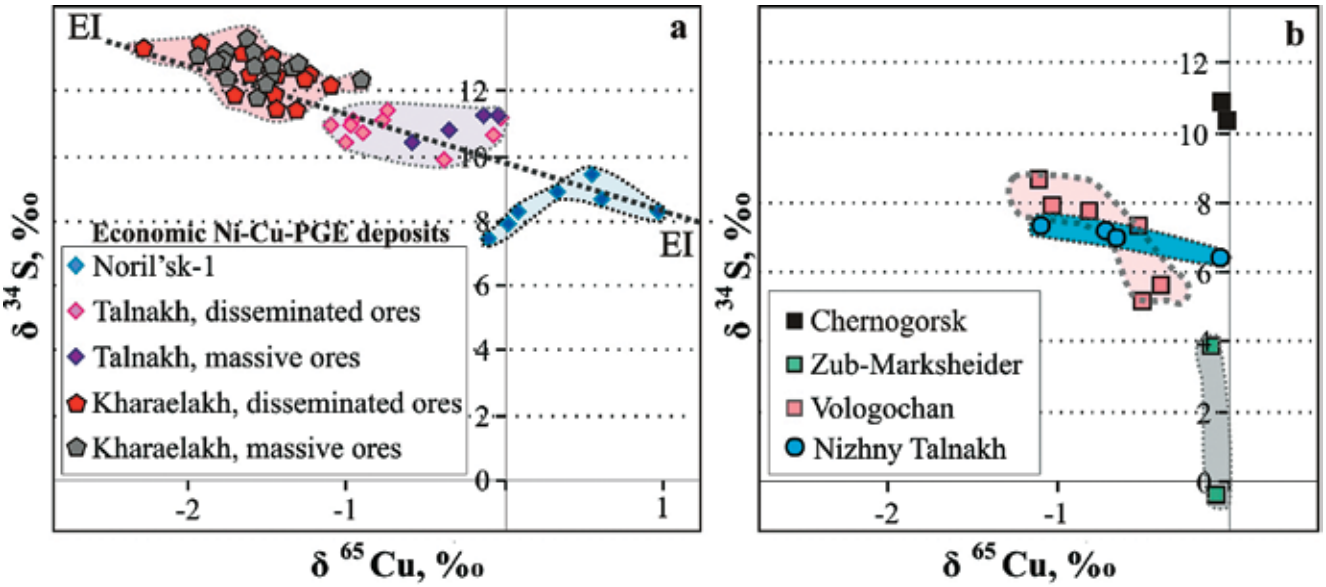

Fig. 28. ^{34}S–^{65}Cu systematics of Ni-Cu-PGE sulfide ores from (a) economic Kharaelakh, Talnakh and Noril'sk-1 intrusions; (b) subeconomic and non-economic intrusions of the Noril'sk Province (modified after *Malitch et al.*, 2014)

Phenocrysts are presented by prismatic crystals or grains of plagioclase, or their intergrowths 0.5-5 mm in size, which comprise 8-15% of the rock. Prismatic, isometric clinopyroxene crystals of 0.3-0.5 mm in size are observed in subordinate quantity, while olivine is almost always replaced by secondary minerals. The bulk rocks have a predominantly microdolerite structure that is replaced by tholeiitic and intersertal structure in thin flows and near amygdaloidal areas.

According to its composition (Tables 3-5, Figs. 31-33) the Nadezhdinsky Formation differs from the overlying basalts by higher levels of silica (up to 53%) and alkalis (especially K_2O> 1wt.%, Fig. 31) and lower levels of titanium (<1wt.% TiO_2). The enriched distribution spectra of trace elements are typical for its constituent basalts; in particular, they are characterized by elevated La/Sm (> 4) and La/Yb (>7) ratios. According to their copper content, the Formation rocks are subdivided into middle and upper subsuites (with concentrations of less than 80 and more than 80 ppm, respectively). The lower subsuite basalts (characterized by extremely low copper content of about 20-30 ppm) in this section are not exposed.

The Morongovsky Suite (T_1mr)

As part of the formation (Fig. 30) 13 lava flows and 9 horizons of tuffaceous rocks have been revealed. The total formation thickness is 300 m. It borders the Mokulaevsky Suite along the roof of the thickest aphyric basalt flow. Dominating in the Morongovsky suite are basalts with the aphyric structure: the lower part is dominated by thin (10-15 m) flows, and the top by thicker flows up to 30-40 m. Two lava flows with glomeroporphyry structure containing large phenocrysts and plagioclase splices have been established. The rock composition is typical for tholeiitic basalts: 30-52% plagioclase (An_{45-60}), 25-45% clinopyroxene (Mg# = 68-80), 3-7% olivine, 3-5% ore minerals, and 5-22% glass devitrification products. Tuffs contain angular and rounded fragments with psammitic, gravel and lapilli dimensions presented by variously altered basalts, volcanic glass, plagioclase, pyroxene or quartz grains, etc. Recent basalt fragments are observed in fragmental tuffs. Xenogenic fragments of sedimentary rocks underlying the tuff-lava strata are observed less frequently. Cement is composed of fine-clastic ash material, and often entirely chloritized and calcitated.

Compared with the Nadezhdinsky suite, the Morongovsky suite basalts differ in somewhat elevated titanium levels (TiO_2> 1 wt.%, typical for the Siberian Traps) and low potassium concentrations (0.4 wt.% of K_2O on average). Significantly higher alkaline content (both sodium and potassium, up to 5 wt.% in total) is inherent in tuffaceous rocks (Tables 3-5).

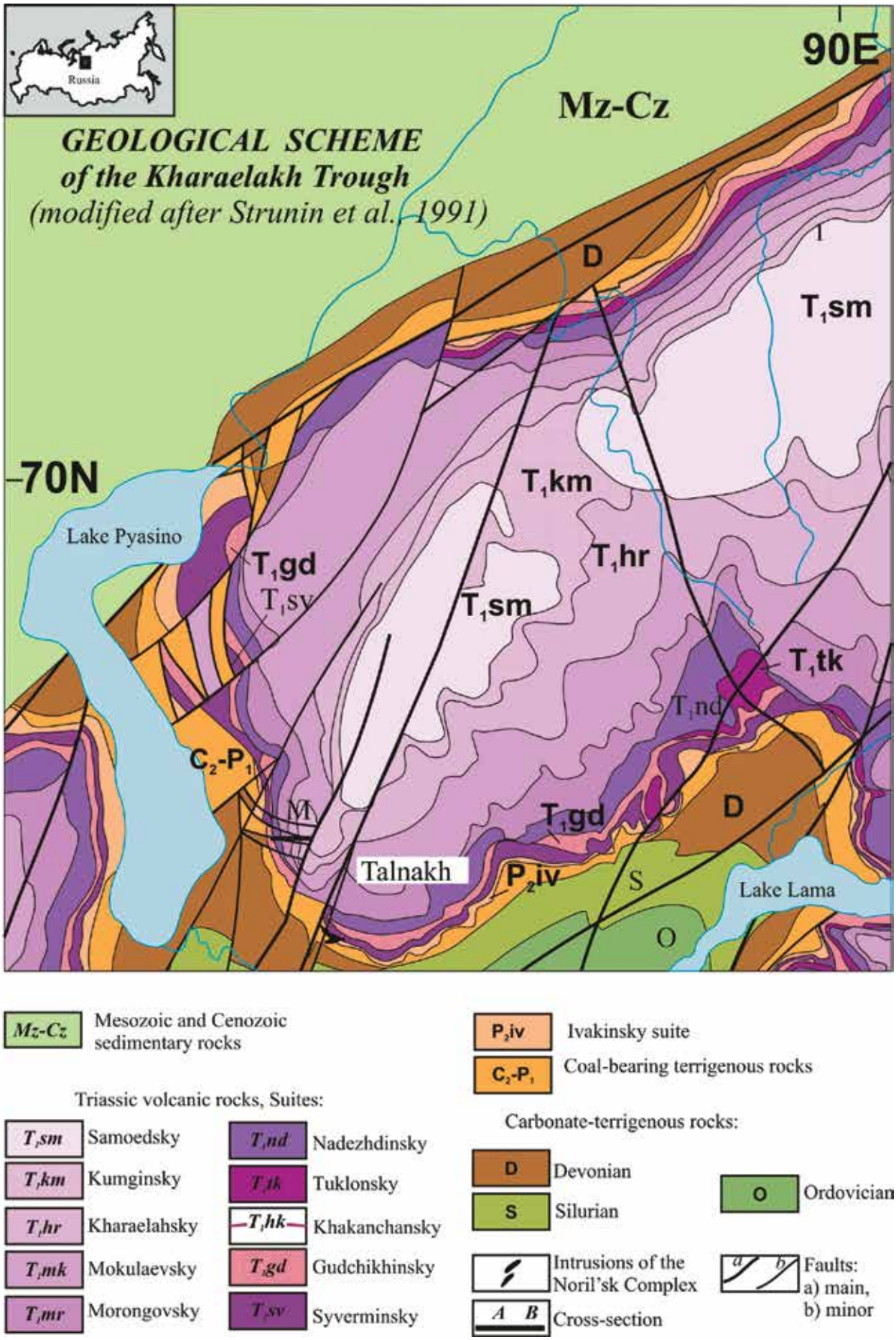

Fig. 29. Position of the Mokulaevsky section inside Kharaelakh Trough

The Mokulaevsky Suite (T_1mk)

There are 14 lava flows and 2 tuff horizons in the Mokulaevsky suite. It is characterized by the predominance of effusive rocks over tuffaceous rocks. Total thickness of the Mokulaevsky suite basalts is 240 ms. The upper boundary is on the roof of tuffaceous horizon, above which oligoglomeroporphyry basalts appear. The latter dominate dramatically in the section. Poikilophitic and aphyric basalt structural varieties are rarely observed. In thick flows the transition from aphanic structure in their marginal parts to fine- and medium-grain in the central part, from micro-grained to coarse-grained poikilophitic structure. The Mokulaevsky suite basalts are characterized by insignificant variations of their mineral composition without a great variety of microstructures. Among the latter, poikilophitic and doleritic textures are the most abundant, whereas ophitic, tholeiitic and intersertal are less frequent. Prevailing in porphyry phases are plagioclase (An_{65-80}) grains, which often form splices of 2-5 mm in size, with the maximum amount (10-15%) in the basalts of the upper unit of the Nizhny-Mokulaevsky subsuite. The bulk of the basalts consists of 35-53% plagioclase (An_{45-60}), 25-35% clinopyroxene (Mg # = 64-82), 12.3% olivine (Fo_{44-67}), ~ 3-7 % ore minerals, and 5-13% devitrification glass products.

By composition the Mokulaevsky formation rocks have elevated (compared to the Morongovsky basalts) titanium contents (above 1.2 wt.%), which allows distinguishing them in mapping even in the absence of the Nadayansky horizon allocated at the base of the Mokulaevsky formation and widely known within limits of the Siberian platform.

The Kharaelakhsky Suite (T_1hr)

As part of the Kharayelakh Formation (Fig. 30) 30 lava flows and 4 horizons of alevrite and psammite tuffs have been allocated. The total thickness of the suite is 475 m. Its boundary with the overlying Kumginsky Suite goes along the appearance of fine-grained aphyric basalts in the section. The basalts are characterized by aphyric and glomeroporphyry structures (in the lower and top parts of the section, respectively). Poikilophitic structure of the bulk, often coarse-grained, is typical for both of them. This helps diagnose formation rocks in the field conditions.

The present horizons of tuffaceous rocks occur in the upper section. Phenocrysts in porphyric basalts are presented by bytownite (An_{75}, up to 3%) sized 0.4-2 mm and olivine (Fa_{31}, 4%.) sized 0.5-0.8 mm. The groundmass is composed of 50% plagioclase (An_{65-60}), around 30% xenomorphic clinopyroxene grains and 3% olivine (Fa44) grains; 3% lamellar splices of ilmenite and magnetite, and 6% volcanic glass.

The Kumginsky Suite (T_1km)

The Kumginsky Suite has a simple structure: it consisted of 6 basalt sheaths/overthrusts with aphyric, porphyry, glomero- and oligoglomeroporphyry rock structures and prevailing thin-fine-grained microdolerite and micropoikilophitic textures. A characteristic distinctive feature of the Kumginsky suite glomeroporphyry basalts is a large number (10-15%) of plagioclase agglomerations of 3-5 mm in size. The visible thickness of the described Kumginsky Suite near the Mokulaevsky Creek is 40 m (its upper part is turfed). According to their textural and structural features, the basalts of the tuff-lava strata are very similar to each other. The flow borders can be established with enough confidence by the presence of the upper amygdaloidal zone, which sometimes has a complex structure (Fig. 31). This can be demonstrated by the example of one of their flows (observation point M-51). It is not always possible to identify the borders of the formations during geological trips. However, geochemical features of the formations (Tables 3-5, Figs. 32-34), especially the middle section part of the Nadezhdinsky, Morongovsky and Mokulaevsky suites are well manifested. This is observed in both major and rare elements. First, significant differences are characteristic of the Nadezhdinsky suites, i.e. the compositional points of its constituent basalts are distinct from those of other suites regarding SiO_2, TiO_2, Fe_2O_3, etc. (Fig. 32). It is clearly observed in La/Yb – U/Nb plots characterizing the gradient of the distribution spectrum of trace elements and the value of Ta-Nb anomalies (Figs. 33, 34). Compositional points of the Nadezhdinsky Suite rocks form a trend ($R^2 = 0.88$) with a negative correlation between the above ratios, while compositions of other rock formations are within the trend line of positive correlation.

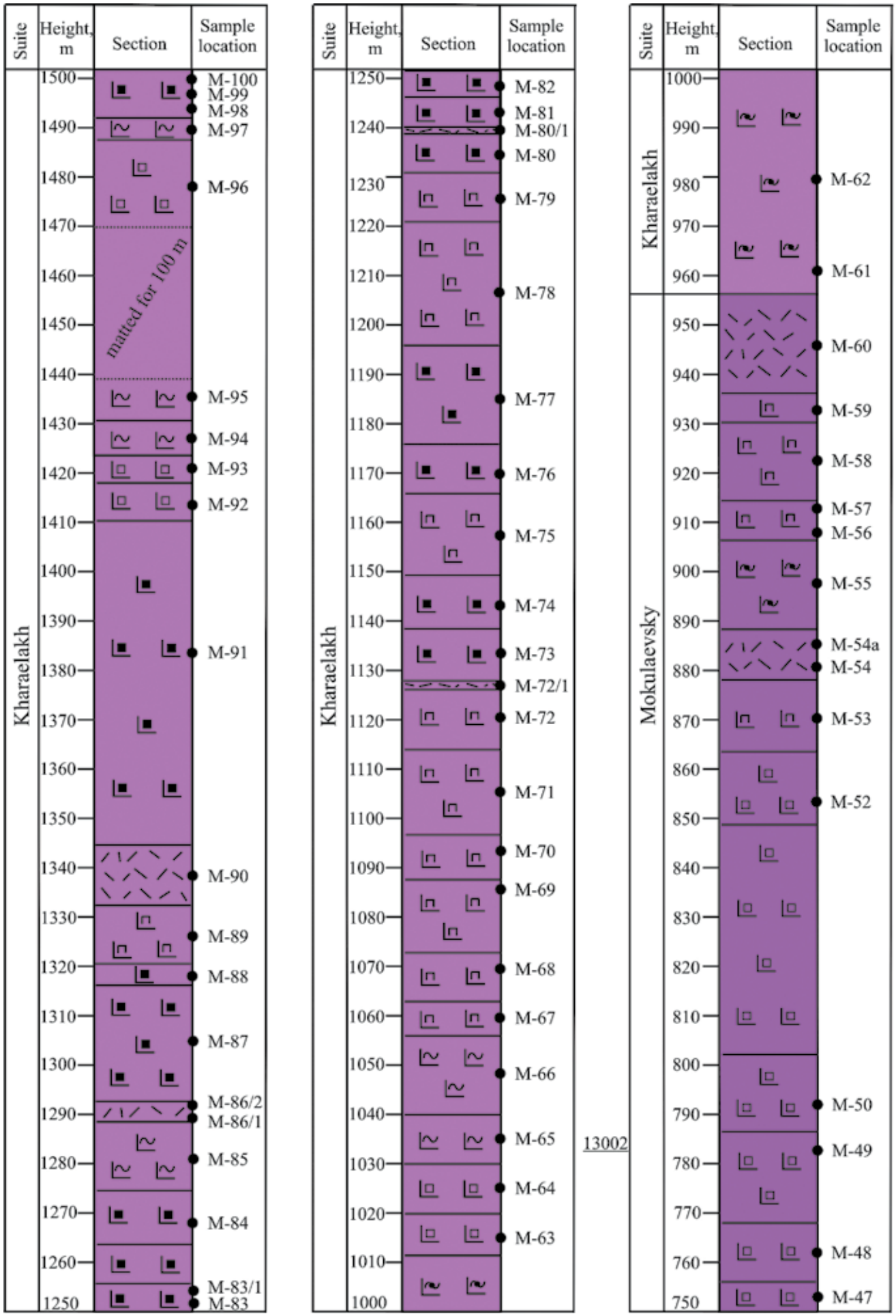

Fig. 30. Cross-section of the volcanic rocks at the Mokulaevsky Creek

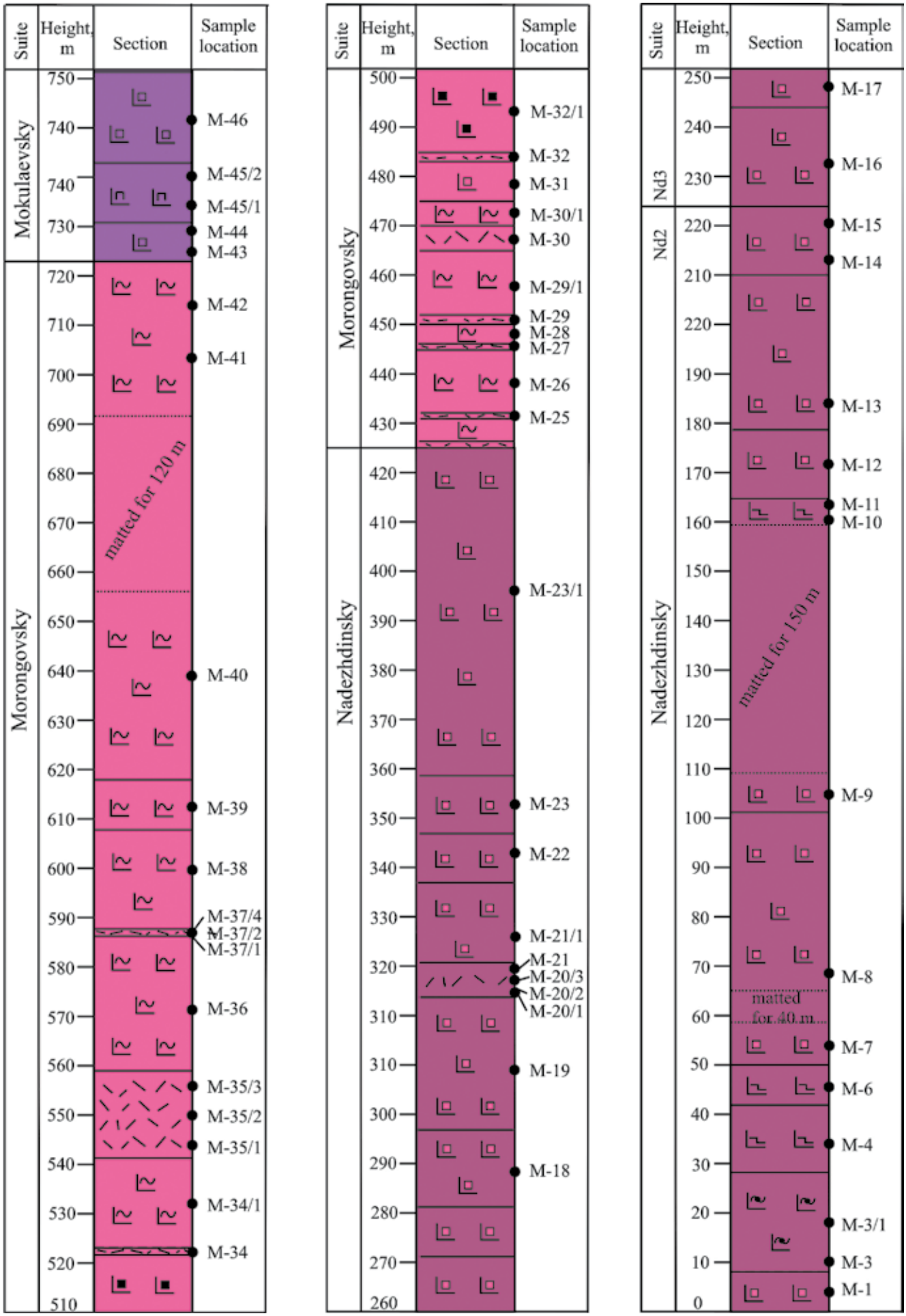
Suite
Height, m
Section
Sample location
Mokulaevsky
Morongovsky
Nadezhdinsky
Nd3
Nd2
matted for 120 m
matted for 150 m
matted for 40 m
M-46
M-45/2
M-45/1
M-44
M-43
M-42
M-41
M-40
M-39
M-38
M-37/4
M-37/2
M-37/1
M-36
M-35/3
M-35/2
M-35/1
M-34/1
M-34
M-32/1
M-32
M-31
M-30/1
M-30
M-29/1
M-29
M-28
M-27
M-26
M-25
M-23/1
M-23
M-22
M-21/1
M-21
M-20/3
M-20/2
M-20/1
M-19
M-18
M-17
M-16
M-15
M-14
M-13
M-12
M-11
M-10
M-9
M-8
M-7
M-6
M-4
M-3/1
M-3
M-1

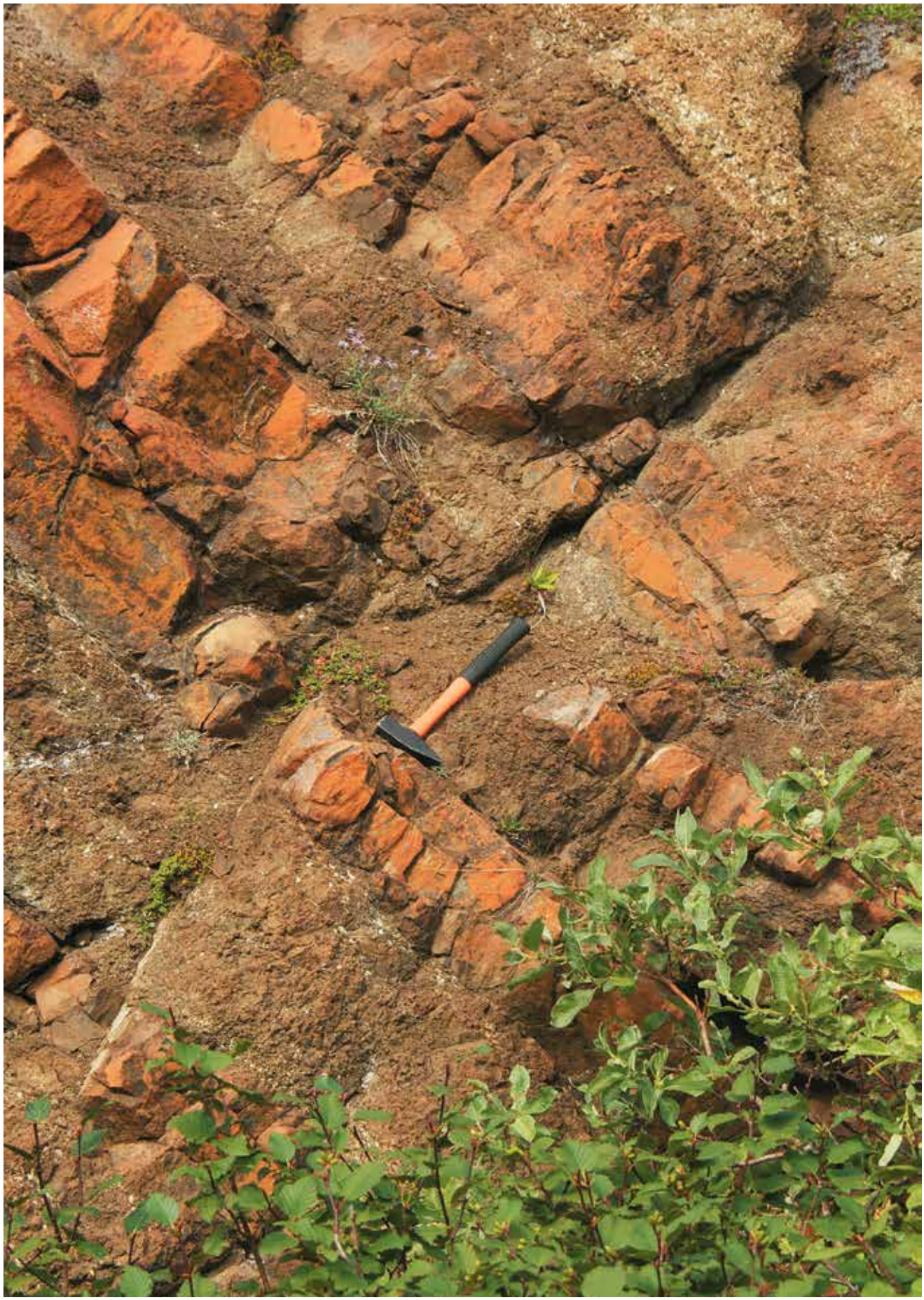

Fig. 31. Complex structure of the upper contact zone (observation point M-51)

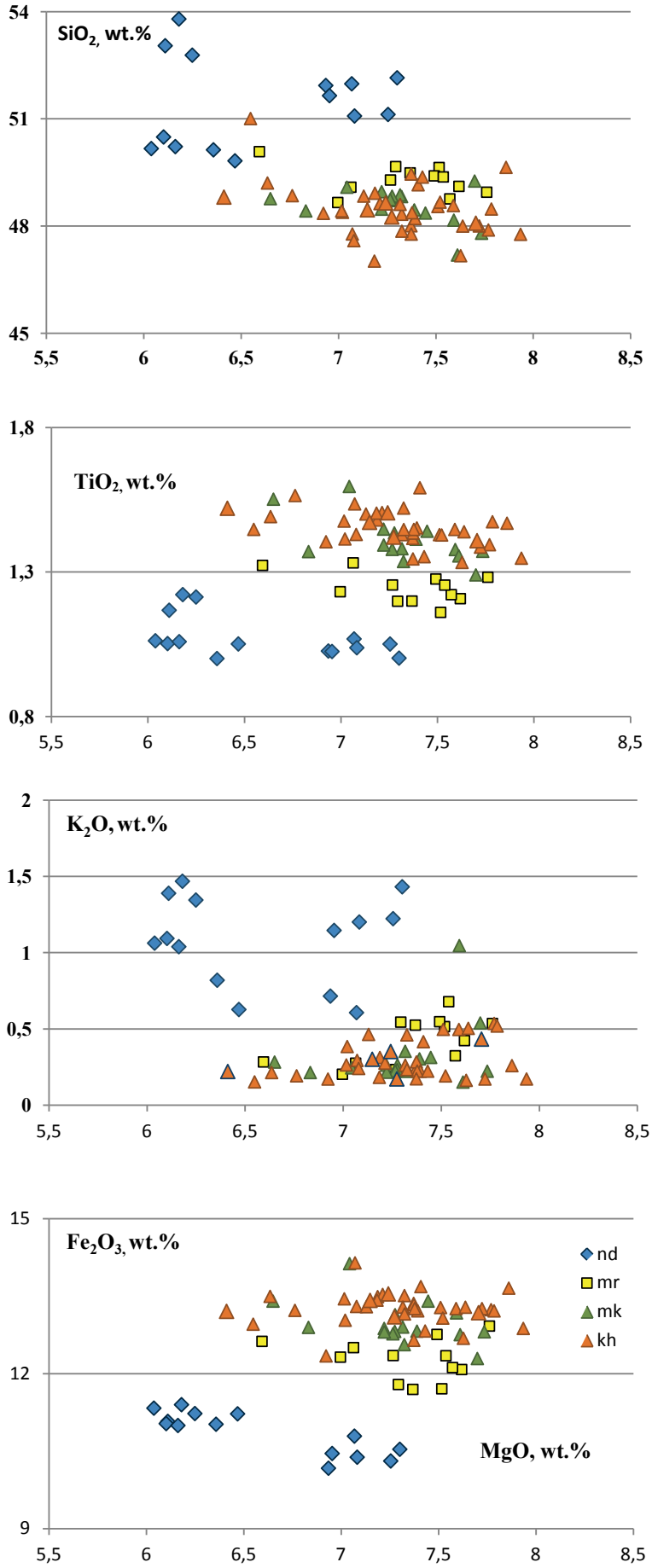

Fig. 32. Diagrams MgO vs SiO_2, TiO_2, K_2O, FeO for volcanic rocks for the Mokulaevsky section

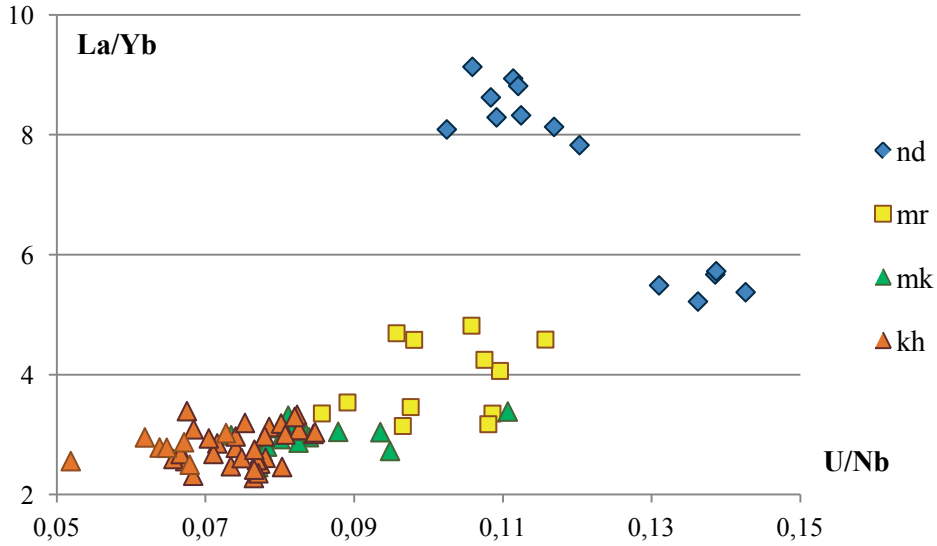

Fig. 33. Diagram La/Yb - U/Nb for volcanic rocks for the Mokulaevsky section

Volcanic rocks of the Morongovsky formation are also quite clearly distinguished by a number of components from the underlying and overlying rocks (Figs. 33, 34). The higher along the section, the more homogeneous are basalts of the Mokulaevsky, Kharayelakh and Kumginsky suites. They are subdivided effectively only by textural and structural features (Fig. 35).

STOP 3: Field trip to the Medvezhy Ruchei open pit of the Zapolyarny mine

The participants will be visiting the Medvezhy Ruchei open pit of the Zapolyarny mine. The open-pit uncovers the northern part of the Norilsk 1 intrusion and the related sulfide ores (Figs. 6, 36-39). The western side of the open-pit shows the whole section of the ore-bearing intrusion. In its lower part, disseminated sulfide ores in picritic and taxitic gabbrodolerites are exposed. In the upper endocontact of the intrusion, chromite-bearing taxitic gabbro hosts low-sulfide PGE ores. Norilsk-1 deposit is currently being developed by the Medvezhy Ruchei open pit of the Zapolyarny mine (Fig. 38). Zapolyarny mine operates mainly disseminated ores, but sometimes there are thin veins of highly enriched ores containing more than 100 g/t PGE (Fig. 39).

STOP 4: Field trips to the Oktyabrsky and Taymyrsky mines

During the excursion participants will be visiting the Oktyabrsky and Taimyrsky mines that process massive and copper-rich sulfide ores of the largest Oktyabrsky PGE-Cu-Ni sulfide deposit by underground mining (Fig. 40-44). The Oktyabrsk mine process the richest in Cu and PGE frontal part of the Kharaelakh main deposit One (X1-O), located in the lower exocontact of the Kharaelakh intrusion (Fig. 41), as well as cupper-rich sulfide ores injected into the upper exocontact (Fig. 43) of the main deposit (MO). The "Taimyr" mine processes massive sulfide ores of the eastern deposit part (X1-O) and north 2 (C-2) deposit merged into one body (Fig. 44). According to operational prospecting this joint mega reservoir (X1-O) + (C-2) + (C-1) has a length of 5.5 km, the maximum width of 1 km, with the maximum thickness of 50 m.

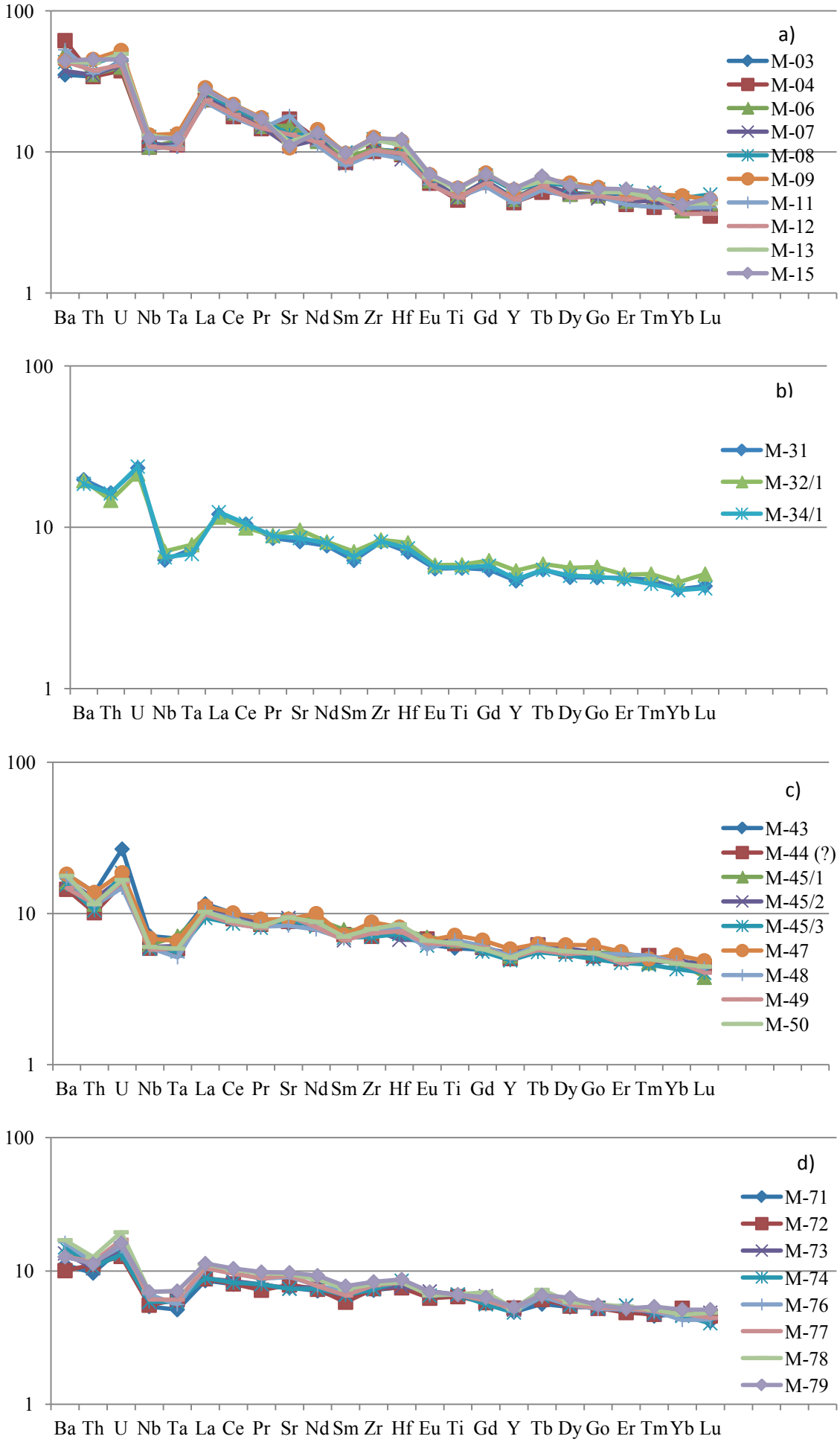

Fig. 34. Spider-diagrams for basalts of the Mokulaevsky Creek; Suites: a) Nadezhdinsky, b) Morongovsky, c) Mokulaevsky, d) Kharaelakhsky.

Fig. 35

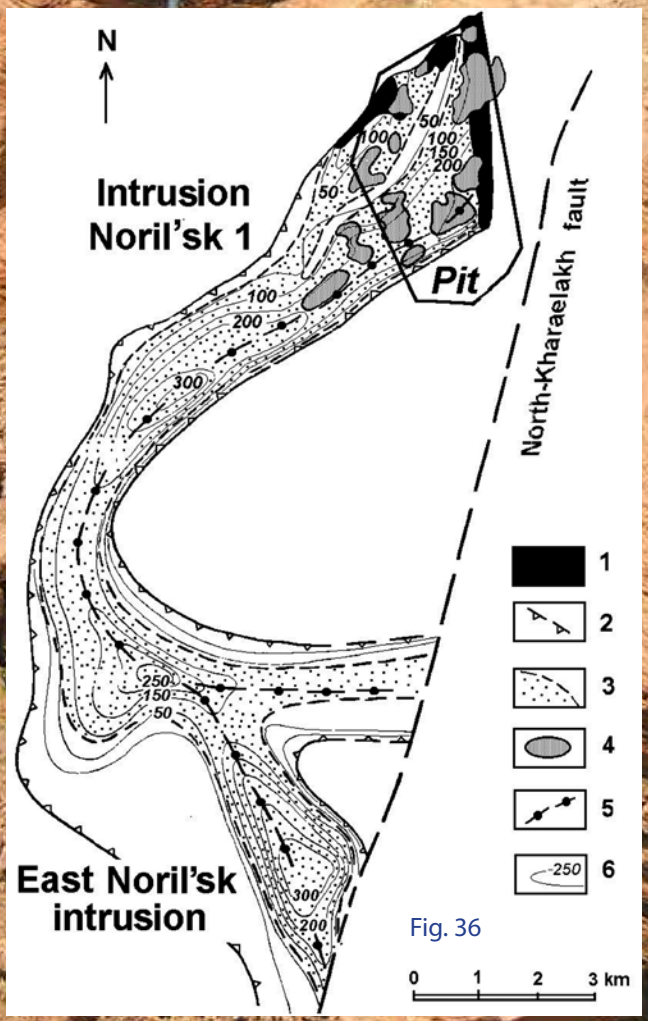
N
Intrusion
Noril'sk 1
Pit
North-Kharaelakh fault
East Noril'sk
intrusion
50
100
150
200
250
300
1
2
3
4
5
6
0 1 2 3 km

Fig. 36

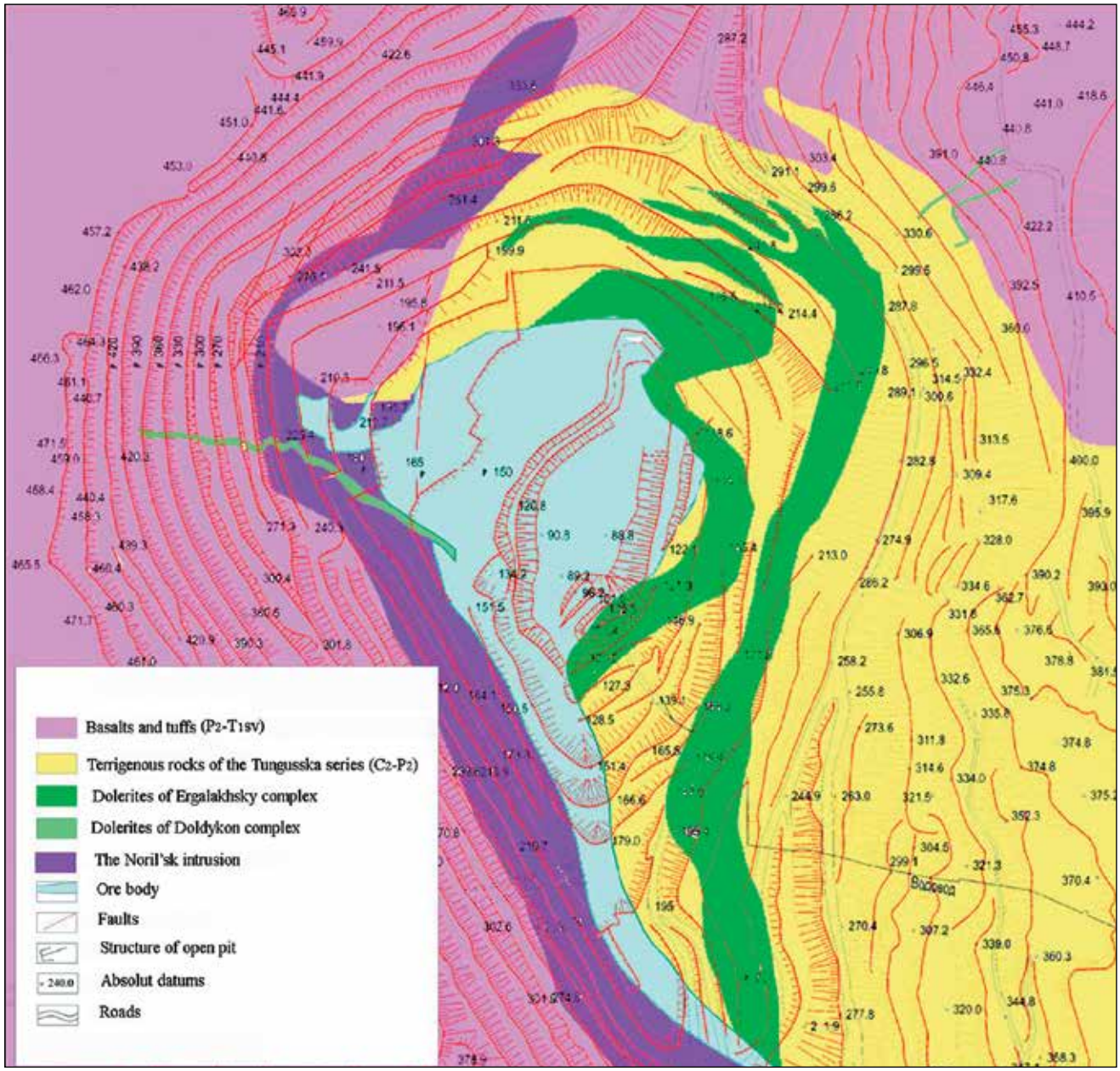

Fig. 37. Geological scheme of the Medvezhy Ruchei open pit

Fig. 35. Fluidal structure of the basalts from the Kharayelakh Suite (M-68)

Fig. 36. Geological and structural scheme of the Noril'sk 1 intrusion. 1) outcrops, 2) contour of the intrusion, 3) projection of gabbrodolertites, 4) massive sulfide ores, 5) axial line of the intrusion, 6) isopach, m; contour of the Medvezhy Ruchei open pit

Fig. 38. Open pit of the Medvezhy Ruchei mine, Norilsk-1 deposit

Fig. 39. Open pit of the "Medvezhy creek" mine showing a horizon 135 m, chalcopyrite-pyrrhotine vein in contact with the rocks of the Tunguska series in the fault zone

Fig. 40. Pit shafts of the Oktyabrsk and Taimyr mines

Fig. 41. The Oktyabrsky mine, X1-O deposit, pyrrhotine-pentlandite-chalcopyrite massive ore with galena and visible sperrylite

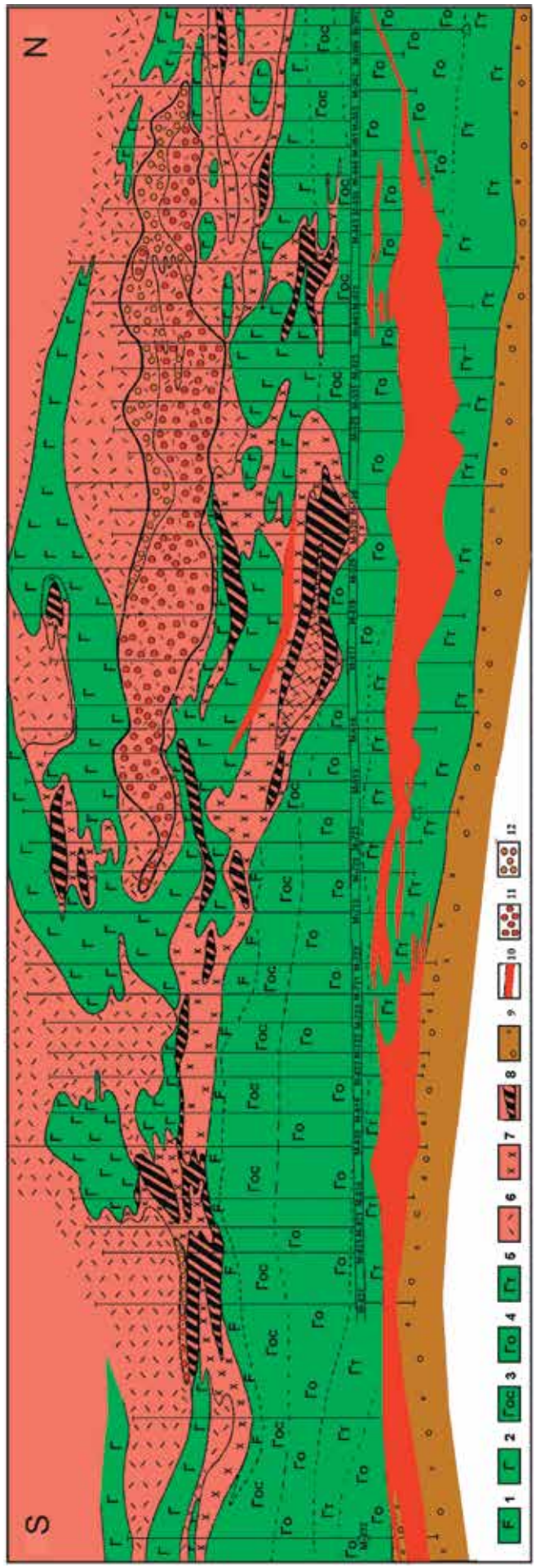

Fig. 42. Geological section of Oktyabrsky mine. 1) leucogabbro, 2) olivine-free, 3) olivine-bearing, 4) olivine, 5) taxitic, 6) pyroxene hornfels, 7) fassaite skarn, 8) forsterite and monticellite skarn, 9) pyroxene-fieldspar hornfels, 10) massive PGE-Cu-Ni ore, 11) pyrrhotite breccia-like ore, 12) breccia-like ore; 13) faults.

Fig. 43. The Oktyabrsky mine, MO deposit, Cu-rich brecciated pyrrhotine-chalcopyrite ore

Fig. 44. The "Taimyr" mine, C-2 deposit, massive pentlandite-chalcopyrite-pyrrhotite ore and relationship with hornfels

Table 3

Cross-section of volcanic rocks in the Noril'sk area

Suite	*Subsuite*	*Unit*	*Thickness (m)*
Samoedsky	–	Upper	260
		Middle	320
		Low	60-120
Kumginsky	–	–	170-190
Kharaelakhsky	Upper	Upper	200-295
		Low	180-230
	Low	Upper	5-40
		Low	32-110
Mokulaevsky	Upper	Upper	110-180
		Low	180-260
	Low	Upper	108-140
		Low	80-130
Morongovsky	–	–	350-450
Nadezhdinsky	–	Upper	10-110
		Middle	160-260
		Low	120-150
Tuklonsky	–	–	80-120
Khakanchansky	–	–	21-23
Gudchikhinsky	Upper	–	50
	Middle	–	50-400
	Low		48-112
Syverminsky	–	–	84-170
Ivakinsky	–	Upper	28-78
		Middle	40-70
		Low	40-80

Table 4

Contents of rock-forming oxides in basalts of the Kharaelakh trough (wt. %)

Suites / Oxides		Quantity of analyses	SiO_2	TiO_2	Al_2O_3	Fe_2O_3	FeO	MnO	MgO	CaO	Na_2O	K_2O	P_2O_5	Cr_2O_3	H_2O	Total
	1	2	3	4	5	6	7	8	9	10	11	12	13	14	15	16
T_1sm^3	⊓	23	48.39	1.64	14.94	4.90	8.16	0.21	6.9	10.98	2.14	0.23	0.16	0.00	1.97	100.62
	~	10	48.33	1.59	15.27	5.06	8.20	0.21	6.92	11.10	2.10	0.22	0.16	0.00	1.65	100.82
	■	2	48.41	1.50	15.60	4.08	8.08	0.21	6.97	10.94	2.08	0.28	0.16	0.00	1.76	100.07
T_1sm^2	■	8	48.59	1.48	15.28	4.40	8.04	0.21	4.06	10.77	2.17	0.28	0.15	0.00	1.68	100.11
	⊓~	6	48.88	1.49	15.29	4.22	7.82	0.21	7.18	10.97	2.10	0.45	0.15	0.00	1.85	100.61
	■⊓	4	48.63	1.54	15.84	5.32	6.82	0.20	6.72	10.79	2.11	0.14	0.17	0.00	1.90	100.18
	■~	1	47.55	1.26	17.20	5.94	5.72	0.18	5.81	10.81	2.13	0.78	0.15	0.00	2.05	99.58
T_1sm^1	□~	2	48.50	1.38	15.43	4.48	8.31	0.21	7.17	10.89	2.07	0.47	0.16	0.00	1.67	100.74
	~	5	47.77	1.62	14.71	5.74	7.87	0.23	6.35	10.41	2.18	0.39	0.23	0.00	2.25	99.75
	■~	2	48.61	1.39	16.10	4.83	7.80	0.20	6.36	10.59	2.07	0.32	0.18	0.00	1.76	100.21
T_1km	■~	16	48.85	1.52	15.29	4.63	7.78	0.21	6.47	10.73	2.17	0.32	0.19	0.00	1.96	100.12
$T_1hr_2^2$	□~	2	48.50	1.52	14.90	5.38	7.68	0.21	6.84	10.41	2.06	0.24	0.19	0.00	1.76	99.69
	⊓	9	47.54	1.43	15.24	6.05	6.43	0.16	7.16	11.38	2.29	0.15	0.12	0.03	1.36	99.34
	~	5	48.04	1.48	15.54	5.61	6.98	0.16	7.07	11.22	2.34	0.13	0.13	0.02	1.03	99.75
	■⊓	2	48.38	1.36	15.92	5.66	6.48	0.18	7.06	11.47	2.00	0.32	0.10	0.02	1.09	100.04
$T_1hr_2^1$	⊓	13	47.40	1.37	15.70	5.81	6.84	0.18	7.70	11.24	2.24	0.22	0.13	0.03	1.47	100.32
	□~	1	49.22	1.45	15.74	6.20	6.90	0.15	7.60	10.58	2.12	0.40	0.14	0.02	0.71	101.23
$T1hr_1^2$	■	1	47.88	1.43	15.74	7.66	5.41	0.19	6.58	12.05	2.18	0.11	0.13	0.02	1.34	100.72
$T_1hr_1^1$	□~	5	47.87	1.43	15.45	5.54	7.35	0.17	7.16	11.46	2.14	0.20	0.14	0.02	1.04	99.97
$T_1mk_2^2$	⊓	8	46.93	1.33	16.19	6.54	5.86	0.18	7.66	11.57	2.11	0.19	0.14	0.02	2.46	101.18
	~	1	48.66	1.31	15.84	5.07	6.98	0.15	7.64	10.58	2.00	0.13	0.13	0.02	1.34	99.85
$T_1mk_2^1$	⊓	7	47.29	1.38	15.72	6.53	6.01	0.18	7.42	10.76	2.25	0.21	0.14	0.02	2.57	100.48
	□⊓	7	48.63	1.50	15.22	6.90	6.13	0.17	7.00	10.54	2.22	0.25	0.16	0.02	1.61	100.35

Table 4. continuation

	1	2	3	4	5	6	7	8	9	10	11	12	13	14	15	16
		3	48.41	1.34	15.52	7.86	4.32	0.16	7.24	10.13	2.67	0.48	0.14	0.02	2.12	100.41
$T_1mk_1^2$		5	48.72	1.27	15.38	5.59	6.33	0.18	7.53	11.82	2.23	0.28	0.13	0.02	1.41	100.89
$T_1mk_1^1$		3	48.92	1.24	15.02	5.59	6.17	0.19	8.05	9.90	3.13	0.49	0.13	0.02	2.43	101.28
		2	48.44	1.22	15.68	4.45	7.44	0.18	6.98	10.82	1.89	0.15	0.13	0.01	1.46	98.85
T_1mr		4	49.06	1.17	15.64	4.53	7.18	0.18	7.43	10.76	1.47	0.32	0.12	0.02	1.07	98.95
		14	48.45	1.16	15.51	5.31	6.18	0.18	7.69	11.22	1.78	0.29	0.12	0.01	1.84	99.94
		10	48.69	1.18	15.47	4.84	6.84	0.18	7.49	10.78	1.98	0.26	0.12	0.01	2.11	99.95
		2	49.18	1.23	14.92	4.62	7.23	0.18	6.59	10.43	2.17	0.89	0.13	0.01	1.24	98.82
T_1nd^3		4	49.58	0.99	15.90	5.19	5.51	0.19	5.86	11.28	2.23	0.93	0.18	0.01	1.62	99.47
T_1nd^2		4	48.84	1.11	15.90	4.16	6.70	0.19	6.08	8.98	2.31	1.92	0.13	0.01	2.92	99.24
		7	51.76	1.04	14.83	3.42	6.63	0.18	6.07	9.98	2.18	1.21	0.11	0.01	2.06	99.48
T_1nd^1		8	49.57	0.96	15.04	3.48	5.91	0.16	6.77	9.64	2.57	1.27	0.10	0.01	3.96	99.44
		9	50.90	0.99	15.04	2.95	6.53	0.16	6.56	9.16	2.44	1.33	0.11	0.02	3.04	99.23
T_1tk		9	50.35	1.04	15.11	3.15	6.09	0.18	6.98	10.18	2.41	1.00	0.12	0.03	2.74	99.38
T_1hk		4	48.68	1.00	14.54	4.18	5.78	0.15	9.29	10.35	1.80	0.33	0.10	0.00	3.13	99.33
T_1gd_2		9	46.38	1.28	10.44	5.28	7.20	0.16	15.00	8.70	1.22	0.22	0.11	0.07	4.26	100.32
		69	47.94	1.52	12.26	5.23	6.59	0.17	10.21	9.53	1.84	0.31	0.14	0.05	4.01	99.80
T_1gd_1		26	50.07	1.84	14.51	4.38	6.52	0.16	6.16	9.44	2.61	0.85	0.28	0.03	3.00	99.85
T_1sv		17	50.41	1.69	15.10	4.33	6.01	0.14	6.32	6.34	3.55	1.19	0.22	0.03	3.67	99.00
P_1iv^3	2	2	52.32	2.35	13.69	6.84	6.15	0.16	3.39	5.81	3.07	2.39	0.78	0.00	1.84	98.79
P_1iv^{2-3}	A	29	51.55	2.42	13.95	5.39	7.60	0.19	3.57	6.71	2.99	1.96	0.72	0.01	2.15	99.21
P_1iv^2		3	52.98	2.56	14.01	5.80	6.96	0.18	3.52	5.36	3.27	2.06	0.75	0.00	1.29	98.74
P_1iv^1		25	47.04	2.13	15.81	5.95	6.81	0.16	6.02	7.70	2.93	1.20	0.39	0.00	3.48	99.62
P_1iv	T	30	45.35	3.36	14.45	7.03	8.11	0.20	4.52	7.25	2.93	2.28	1.20	0.01	3.18	99.87

Note. Samples have been grouped either from similar lithological variations of the same flow. or from microunits with similar structure arranged sequentially one over another. i.e. in the time sequence. The section from T_1tk to T_1hr is compiled along drill hole CD-24. and above it – along the original outcrops in the right upper side of the Upper Talovaya River. Compiled by V.A. Radko. The analyses/tests have been performed in the central laboratory of JSC Noril'skgeologiya. Legend: structural varieties of basalts.

Table 5

Contents of rock-forming oxides in basalts of the Mokulaevsky Creek cross-section (wt. %)

№	Sample number	Suite	Lithology	SiO_2	Al_2O_3	TiO_2	Fe_2O_3	MnO	MgO	CaO	Na_2O	K_2O	P_2O_5	H_2O	Total
1	M-3	T_1nd_2	Porphyric basalt	50.60	15.20	1.04	10.50	0.17	6.88	11.60	2.06	0.59	0.11	1.19	99.94
2	M-4	T_1nd_2	Tholeiite basalt	51.00	14.80	0.98	10.30	0.17	7.14	8.00	3.45	1.40	0.10	2.68	100.02
3	M-6	T_1nd_2	Tholeiite basalt	50.60	15.30	1.04	10.20	0.18	7.18	8.82	3.15	1.21	0.11	2.11	99.90
4	M-7	T_1nd_2	Oligoglomeroporphyric basalt	51.60	15.10	1.02	10.10	0.16	6.89	11.10	2.18	0.71	0.11	1.02	99.99
5	M-8	T_1nd_2	Lava breccia	51.88	14.57	1.05	10.95	0.15	6.73	8.94	2.84	1.33	0.16	2.21	100.81
6	M-9	T_1nd_2	Oligoglomeroporphyric basalt	52.40	14.70	1.19	11.10	0.17	6.02	9.86	2.35	1.43	0.13	0.64	99.99
7	M-11	T_1nd_2	Tholeiite basalt	50.20	15.40	1.02	10.20	0.19	6.96	8.79	3.35	1.18	0.11	2.60	100.00
8	M-12	T_1nd_2	Oligoglomeroporphyric basalt	51.40	14.90	1.02	10.40	0.16	6.92	9.35	2.87	1.14	0.11	1.69	99.96
9	M-13	T_1nd_2	Oligoglomeroporphyric basalt	52.70	14.60	1.16	11.00	0.17	6.07	10.00	2.31	1.38	0.12	0.37	99.88
10	M-15	T_1nd_2	Oligoglomeroporphyric basalt	52.20	14.60	1.20	11.10	0.17	6.18	10.10	2.33	1.33	0.13	0.60	99.94
11	M-17	T_1nd_3	Oligoglomeroporphyric basalt	49.60	15.60	0.99	10.90	0.17	6.29	12.00	2.35	0.81	0.18	0.96	99.85
12	M-19	T_1nd_3	Oligoglomeroporphyric basalt	49.90	15.60	1.04	10.90	0.17	6.03	11.60	2.44	1.08	0.17	1.01	99.94
13	M-20/1	T_1nd_3	Tuff	45.34	11.60	1.07	10.62	0.17	7.59	9.46	3.24	2.51	0.12	9.14	100.86
14	M-20/2	T_1nd_3	Tuff	46.38	11.14	0.92	8.82	0.14	6.59	10.63	2.31	2.46	0.14	11.02	100.55
15	M-20/3	T_1nd_3	Tuff	47.88	14.84	1.10	11.46	0.11	6.87	5.67	3.76	1.76	0.12	6.95	100.52
16	M-21	T_1nd_3	Tuff	48.81	13.15	1.17	12.01	0.17	7.98	7.66	2.67	1.45	0.11	5.15	100.33
17	M-22	T_1nd_3	Oligoglomeroporphyric basalt	49.30	15.40	1.04	11.10	0.18	6.40	12.30	2.30	0.62	0.18	1.11	99.93
18	M-23	T_1nd_3	Oligoglomeroporphyric basalt	49.60	15.60	1.05	11.20	0.16	5.97	11.70	2.43	1.05	0.18	1.06	100.00
19	M-23/1	T_1nd_3	Oligoglomeroporphyric basalt	49.80	15.60	1.05	10.90	0.17	6.11	11.60	2.42	1.03	0.18	1.04	99.90
20	M-25	T_1mr	Tuff	47.46	14.20	1.02	11.46	0.20	7.71	7.30	3.77	1.16	0.11	5.66	100.05
21	M-26	T_1mr	Basalt aphyric	49.10	15.00	1.19	11.60	0.21	7.31	12.10	2.00	0.52	0.12	0.69	99.84
22	M-27	T_1mr	Tuff	48.89	14.36	1.33	12.42	0.19	6.74	11.30	2.33	0.24	0.15	2.91	100.86
23	M-28	T_1mr	Basalt aphyric	49.30	14.80	1.19	11.70	0.17	7.24	12.10	2.05	0.54	0.12	0.71	99.92
24	M-29	T_1mr	Tuff	48.45	16.40	1.06	11.38	0.16	6.69	11.43	2.50	0.50	0.15	2.14	100.86
25	M-29/1	T_1mr	Basalt aphyric	49.20	15.10	1.15	11.60	0.17	7.45	12.00	1.97	0.51	0.11	0.76	100.02
26	M-30	T_1mr	Tuff	47.50	13.40	1.09	11.62	0.17	7.69	8.68	4.51	0.50	0.15	5.56	100.87
27	M-30/1	T_1mr	Basalt aphyric	49.60	14.30	1.31	12.50	0.19	6.53	12.20	2.06	0.28	0.14	0.91	100.02
28	M-31	T_1mr	Basalt aphyric	48.80	15.10	1.20	12.00	0.18	7.57	11.60	2.04	0.42	0.12	1.03	100.06

Table 5. continuation

№	Sample number	Suite	Lithology	SiO_2	Al_2O_3	TiO_2	Fe_2O_3	MnO	MgO	CaO	Na_2O	K_2O	P_2O_5	H_2O	Total
29	M-32/1	T_1mr	Basalt glomeroporphyric	48.80	15.20	1.26	12.60	0.19	7.40	11.10	2.14	0.54	0.13	0.62	99.98
30	M-34	T_1mr	Tuff	47.97	13.81	1.17	11.45	0.16	7.97	4.99	1.81	3.88	0.12	6.31	99.64
31	M-34/1	T_1mr	Basalt aphyric	48.30	15.30	1.21	12.00	0.18	7.50	11.90	1.94	0.32	0.12	1.18	99.95
32	M-35/1	T_1mr	Tuff	36.06	10.22	0.74	8.02	0.17	6.60	19.13	2.95	0.87	0.12	15.83	100.71
33	M-35/2	T_1mr	Tuff	38.39	10.05	0.88	8.41	0.18	7.09	17.29	1.20	2.00	0.11	15.04	100.64
34	M-35/3	T_1mr	Tuff	41.54	11.52	0.88	9.48	0.16	7.72	12.77	2.63	1.58	0.11	12.34	100.73
35	M-36	T_1mr	Basalt aphyric	48.50	14.90	1.27	12.80	0.19	7.69	11.00	2.04	0.53	0.13	0.92	99.97
36	M-37/1	T_1mr	Tuff	47.99	13.92	1.12	11.48	0.19	7.49	8.59	2.55	0.88	0.11	6.30	100.62
37	M-37/2	T_1mr	Tuff	35.81	10.08	0.95	9.87	0.22	7.80	18.81	1.33	1.52	0.17	14.09	100.65
38	M-37/4	T_1mr	Tuff	46.66	12.34	1.28	13.18	0.18	7.71	7.14	2.32	1.35	0.10	6.23	98.49
39	M-38/3	T_1mr	Basalt aphyric	48.70	15.10	1.24	12.20	0.20	7.18	12.00	2.10	0.23	0.13	0.77	99.85
40	M-38?	T_1mr	Basalt aphyric	48.30	15.40	1.31	12.30	0.19	6.95	11.90	2.04	0.27	0.14	1.00	99.80
41	M-39	T_1mr	Basalt aphyric	48.20	15.20	1.22	12.20	0.17	6.93	12.20	1.94	0.20	0.13	1.39	99.78
42	M-41	T_1mr	Basalt aphyric	48.80	15.10	1.24	12.20	0.18	7.45	11.20	2.08	0.67	0.13	0.88	99.93
43	M-43	T_1mk	Basalt glomeroporphyric	48.50	15.10	1.27	12.10	0.19	7.58	11.30	2.12	0.53	0.14	1.16	99.99
44	M-44	T_1mk	Basalt glomeroporphyric	47.40	15.20	1.36	12.70	0.26	7.67	11.50	2.02	0.22	0.12	1.51	99.96
45	M-45/1	T_1mk	Basalt poikiloophytic	48.20	15.10	1.42	13.00	0.18	7.20	11.50	2.17	0.26	0.13	0.75	99.91
46	M-45/2	T_1mk	Basalt poikiloophytic	48.20	15.10	1.44	12.80	0.18	7.18	11.50	2.14	0.26	0.14	1.01	99.95
47	M-45/3	T_1mk	Basalt poikiloophytic	48.00	15.70	1.40	12.70	0.21	7.32	11.50	2.17	0.30	0.13	0.58	100.01
48	M-47	T_1mk	Oligoglomeroporphyric basalt	48.40	15.20	1.54	13.30	0.20	6.60	11.10	2.29	0.28	0.15	0.75	99.81
49	M-48	T_1mk	Oligoglomeroporphyric basalt	48.00	15.20	1.43	13.30	0.19	7.39	11.10	2.18	0.31	0.14	0.62	99.86
50	M-49	T_1mk	Oligoglomeroporphyric basalt	48.60	15.00	1.33	12.50	0.19	7.29	11.90	2.08	0.22	0.13	0.84	100.08
51	M-50	T_1mk	Oligoglomeroporphyric basalt	48.50	15.30	1.37	12.80	0.19	7.26	11.50	2.13	0.35	0.13	0.56	100.09
52	M-52	T_1mk	Oligoglomeroporphyric basalt	48.30	14.70	1.57	13.90	0.20	6.93	11.10	2.15	0.24	0.14	0.86	100.09
53	M-53	T_1mk	Basalt poikiloophytic	47.90	14.90	1.37	13.10	0.18	7.55	10.30	1.92	1.04	0.13	1.67	100.06
54	M-54	T_1mk	Tuff	48.16	12.73	1.15	12.04	0.18	7.72	9.63	1.35	1.97	0.14	4.66	99.73
56	M-55	T_1mk	Basalt porphyric	48.40	15.30	1.41	12.70	0.20	7.21	11.70	2.16	0.23	0.13	0.70	100.14
55	M-56	T_1mk	Basalt poikiloophytic	48.10	15.60	1.36	12.60	0.19	7.17	11.60	2.13	0.22	0.13	0.82	99.92
57	M-57	T_1mk	Basalt poikiloophytic	47.70	15.90	1.35	12.70	0.16	6.73	11.70	2.10	0.21	0.13	1.32	100.00

Table 5. continuation

№	Sample number	Suite	Lithology	SiO_2	Al_2O_3	TiO_2	Fe_2O_3	MnO	MgO	CaO	Na_2O	K_2O	P_2O_5	H_2O	Total
58	M-58	T_1mk	Basalt poikiloophytic	47.80	15.60	1.36	12.50	0.18	7.05	11.60	2.07	0.21	0.13	1.47	99.97
60	M-59	T_1mk	Basalt poikiloophytic	47.00	15.40	1.35	12.70	0.19	7.58	11.20	1.93	0.15	0.12	2.04	99.66
61	M-61	T_1hr	Basalt porphyric	48.30	15.10	1.52	13.50	0.20	7.32	10.80	2.25	0.46	0.14	0.50	100.09
62	M-62	T_1hr	Basalt porphyric	48.60	15.10	1.47	13.40	0.21	7.14	11.30	2.27	0.31	0.13	0.11	100.04
63	M-63	T_1hr	Oligoglomeroporphyric basalt	48.50	15.10	1.47	13.30	0.20	6.54	11.70	2.19	0.21	0.13	0.80	100.14
64	M-64	T_1hr	Oligoglomeroporphyric basalt	47.30	14.90	1.52	14.00	0.20	7.00	11.10	2.11	0.29	0.14	1.28	99.84
65	M-65	T_1hr	Basalt aphyric	47.90	15.20	1.41	13.10	0.20	7.41	11.10	2.06	0.49	0.12	1.09	100.08
66	M-66	T_1hr	Basalt aphyric	47.40	15.20	1.38	13.10	0.20	7.69	10.80	2.23	0.53	0.13	1.30	99.96
67	M-67	T_1hr	Basalt poikiloophytic	47.80	15.10	1.41	13.30	0.19	7.34	11.40	2.06	0.24	0.13	1.04	100.01
68	M-68	T_1hr	Basalt poikiloophytic	48.00	15.20	1.42	13.20	0.19	7.60	11.40	2.17	0.25	0.13	0.46	100.02
69	M-69	T_1hr	Basalt poikiloophytic	46.57	14.94	1.32	12.52	0.18	7.53	11.05	2.28	0.16	0.14	3.93	100.62
70	M-70	T_1hr	Basalt poikiloophytic	47.30	15.30	1.42	13.20	0.17	7.30	11.50	2.12	0.28	0.13	1.32	100.04
71	M-71	T_1hr	Basalt poikiloophytic	47.90	15.40	1.40	12.90	0.21	6.95	11.60	2.13	0.38	0.13	0.98	99.98
72	M-72	T_1hr	Basalt poikiloophytic	47.80	15.00	1.38	13.20	0.19	7.69	11.40	2.04	0.17	0.12	0.90	99.89
73	M-73	T_1hr	Basalt glomeroporphyric	48.00	15.40	1.43	13.10	0.20	7.50	11.10	2.23	0.49	0.12	0.64	100.21
74	M-74	T_1hr	Basalt glomeroporphyric	47.70	15.00	1.43	13.20	0.20	7.59	11.00	2.07	0.50	0.12	1.27	100.08
75	M-75	T_1hr	Basalt poikiloophytic	47.50	15.60	1.34	12.80	0.20	7.89	11.60	2.15	0.17	0.12	0.55	99.92
76	M-76	T_1hr	Basalt glomeroporphyric	48.30	15.10	1.42	13.20	0.19	7.27	11.40	2.16	0.26	0.13	0.72	100.15
77	M-77	T_1hr	Basalt glomeroporphyric	48.40	15.00	1.42	13.00	0.19	7.48	11.40	2.15	0.19	0.13	0.78	100.14
78	M-78	T_1hr	Basalt poikiloophytic	47.80	15.60	1.44	13.10	0.21	7.33	11.50	2.10	0.22	0.14	0.56	100.00
79	M-79	T_1hr	Basalt poikiloophytic	47.80	15.40	1.43	13.10	0.21	7.29	11.50	2.05	0.22	0.14	1.04	100.18
80	M-80	T_1hr	Basalt glomeroporphyric	47.60	15.50	1.43	13.30	0.18	7.08	11.30	2.04	0.24	0.14	1.14	99.95
81	M-81	T_1hr	Basalt glomeroporphyric	48.50	14.90	1.57	13.50	0.22	7.31	11.20	2.26	0.41	0.14	0.10	100.11
82	M-82	T_1hr	Basalt glomeroporphyric	48.90	14.80	1.33	12.50	0.19	7.29	11.40	1.96	0.17	0.12	1.34	100.00
83	M-83	T_1hr	Basalt glomeroporphyric	48.90	14.70	1.34	12.70	0.19	7.36	11.30	2.04	0.22	0.12	1.10	99.97
84	M-83/1	T_1hr	Basalt glomeroporphyric	50.40	14.80	1.43	12.80	0.19	6.47	10.60	2.06	0.15	0.14	1.12	100.16
85	M-84	T_1hr	Basalt glomeroporphyric	48.40	15.20	1.55	13.10	0.20	6.70	11.10	2.21	0.19	0.15	1.16	99.96
86	M-85	T_1hr	Basalt aphyric	47.90	15.50	1.46	13.30	0.19	6.94	11.20	2.18	0.26	0.14	0.82	99.89
87	M-87	T_1hr	Basalt glomeroporphyric	47.70	15.40	1.45	13.00	0.18	7.66	10.80	2.08	0.51	0.13	1.18	100.09

Table 5. continuation

№	Sample number	Suite	Lithology	SiO_2	Al_2O_3	TiO_2	Fe_2O_3	MnO	MgO	CaO	Na_2O	K_2O	P_2O_5	H_2O	Total
88	M-88	T_1hr	Basalt glomeroporphyric	47.30	15.50	1.43	13.00	0.19	7.24	11.30	2.07	0.23	0.13	1.55	99.94
89	M-89	T_1hr	Basalt poikiloophytic	48.20	15.80	1.40	12.30	0.18	6.90	11.60	2.15	0.17	0.13	1.21	100.04
90	M-91	T_1hr	Basalt glomeroporphyric	48.50	15.50	1.49	13.20	0.20	7.08	10.90	2.21	0.46	0.13	0.63	100.30
91	M-92	T_1hr	Oligoglomeroporphyric basalt	47.80	15.80	1.48	13.30	0.21	7.09	11.00	2.21	0.27	0.14	0.70	100.00
92	M-93	T_1hr	Oligoglomeroporphyric basalt	46.60	16.30	1.49	13.30	0.18	7.12	10.80	2.18	0.18	0.14	1.71	100.00
93	M-94	T_1hr	Basalt aphyric	47.80	15.30	1.40	13.10	0.19	7.66	11.00	2.10	0.43	0.12	1.11	100.21
94	M-95	T_1hr	Basalt aphyric	47.90	15.60	1.41	13.00	0.20	7.22	11.70	2.09	0.17	0.12	0.79	100.20
95	M-96	T_1hr	Oligoglomeroporphyric basalt	48.80	15.10	1.52	13.20	0.19	6.41	11.50	2.19	0.22	0.13	0.81	100.07
96	M-98	T_1hr	Basalt aphyric	48.50	15.10	1.50	13.50	0.21	7.22	11.20	2.26	0.35	0.13	0.16	100.13
97	M-99	T_1hr	Basalt glomeroporphyric	48.40	15.20	1.47	13.40	0.20	7.14	11.20	2.25	0.30	0.13	0.39	100.08
98	M-100	T_1hr	Basalt glomeroporphyric	48.10	15.70	1.49	13.40	0.20	7.11	11.20	2.25	0.30	0.13	0.34	100.22

CONCLUDING REMARKS AND FUTURE OUTLOOK

The origin of ore-bearing mafic-ultramafic intrusions in the Noril'sk region, Russia has been hotly debated. Key hypotheses include differentiation of a single magma, emplacement of multiple magmas with distinct compositions, volcanic feeder systems, a crust-mantle interaction model, assimilation and metasomatic models. The disagreement about the ore genesis is due to the fact that many issues of the geological structure, petrology and mineralization in the Norilsk region still remain unresolved. These include (i) the relationship of ore-bearing intrusions and lavas, (ii) the composition of melts of the ore-bearing intrusions, (iii) the role of assimilation in the ore formation.

Understanding the processes leading to the formation of economically important ore deposits is crucial for recognizing new deposits in areas that have not been previously considered. It is commonly assumed that ultramafic-mafic intrusions and associated PGE-Cu-Ni sulfide deposits of Northern Siberia represent a small component of a major episode of mafic activity at ~250 Ma, which included formation of the most extensive flood-basalt province on Earth (*Campbell et al.*, 1992). Recent studies, however, advocated protracted evolution of the ore-forming magmas parent to the Noril'sk-type intrusions (*Malitch et al.*, 2010a; 2012 among others).

It is generally accepted that the mantle-derived ultramafic–mafic magmas and PGE-Ni-Cu deposits of the Noril'sk-Talnakh region are closely linked, implying that primitive mantle-derived materials are intrinsic to their petrogenesis. Nd-Sr-Os-Pb isotopic studies of the main units of the economic Noril'sk-type intrusions and their ores have contributed to a better understanding of the origin of Noril'sk-type intrusive hosts and associated ores. The Os- and Pb-isotope compositions of the PGE-Cu-Ni sulfide ores preserve mantle-like values, and it has been suggested that staged chambers played an important role in the evolution of the Noril'sk-type deposits (*Wooden et a*l., 1992; *Walker et al*., 1994; *Malitch & Latypov*, 2011, among others).

Hf-isotope data on zircon and baddeleyite, which serve as an explicit constraint on their source region, provided recently new set of constraints for the origin of the Noril'sk-type intrusions. A case study at Kharaelakh (*Malitch et al*., 2010b) showed a significant range in initial $^{176}Hf/^{177}Hf$ values of zircon, which favoured a model of mixing between mantle and lithospheric sources. For the Noril'sk 1 intrusion, in-situ Hf-isotope data of zircon and baddeleyite, combined with whole-rock Nd-isotope results (*Malitch et al*., 2013), identify three distinct clusters of Hf-Nd isotope values typical of different lithological units (e.g. unmineralised gabbroic rocks, mineralised ultramafic and taxitic-textured rocks with disseminated PGE-Cu-Ni sulfide ores, and gabbro-diorite). These groupings suggest the interaction of three distinct magma sources during the protracted evolution of the Noril'sk-1 intrusion: (1) a juvenile source equivalent to the Depleted Mantle, (2) a subcontinental lithospheric mantle source and (3) a minor crustal component. A prolonged period for concentration of the ore components in staging chambers during this interaction might be a key factor for formation of economic deposits. Similar conclusions, arising from different lines of reasoning, have been reached previously by, among others, *Godlevsky* (1959), *Distler et al.,* (1988) and *Tuganova* (1991).

The zircon and baddeleyite from economic intrusions show isotopic and geochemical features that are not usually expected for mafic and ultramafic rocks. They indicate a complex geological history for the economic ultramafic-mafic intrusions of the Noril'sk region. Therefore, models for the origin of the Siberian flood basalts and their relationships to the Norilsk-type intrusions (reviewed by *Arndt*, 2005; *Ivanov*, 2007; *Dobretsov et al.*, 2008; *Zhang et al.*, 2008, among many others) may be critically evaluated in light of new Hf-Nd isotopic constraints.

Acknowledgements

This study was partly supported by Russian Foundation for Basic Research (grant 13-05-00671-a) and by Program of Ural Division of RAS (projects 12-Y-5-1038 and 12-5-6-019-Arctic).

PROGRAM

of visiting Polar Division of OJSC "Mining & Metallurgical Company Norilsk Nickel"
as part of the XII International Platinum Symposium
31.07.2014 – 07.08.2014

Local time	Schedule
	July 31, Thursday
06.00-07.45	Arrival to Noril'sk airport
08.30-10.30	Transfer to Talnakh; accommodation at the Talnakh hotel
10.30-11.30	Breakfast at the hotel
11.30-13.00	Free time
13.00-14.00	Lunch at the hotel "Talnakh"
14.00-14.45	Transfer to the Polar Division of Mining & Metallurgical Co. Norilsk Nickel
15.00-16.00	Meeting with Director of Polar Division of Mining & Metallurgical Co. Norilsk Nickel; detalization of the program
16.00-19.00	Visit to the Museum of History of Norilsk Industrial Region, the first house in Norilsk (N.N. Urvantsev's House). City tour, visit to Norilsk Golgotha Memorial complex
19.00-19.45	Transfer to Talnakh
20.00	Dinner at the hotel
	August 1, Friday
08.00-09.00	Breakfast at the hotel
09.00-09.20	Transfer to the Mining and Geology Department
09.30-11.30	Visit of the Mining and Geology Department, presentation "An Overview of the deposits and factories of the Polar Division of OJSC "MMC Norilsk Nickel".
11.30-12.30	Visiting the viewing point BC-5 of the Taimyr Mine
12.30-13.30	Lunch at the hotel
13.30-13.45	Transfer to JSC Norilskgeologiya
13.45-18.00	Visit of JSC Norilskgeologiya, introduction to its activity, lecture about geology and minerageny of the Norilsk region, visit of the Geological Museum
20.00	Dinner at the hotel
	August 2, Saturday
08.00-09.00	Breakfast at the hotel
09.00-10.00	Transfer to the Mokulaevsky stream area
10.00-13.00	Studying and sampling the upper part of the tuff-lava strata section at the Mokulay stream
13.00-14.00	Picnic lunch (sandwiches, vegetables, fruits, juices)
14.00-18.00	Completion of studying and sampling the upper part of the tuff-lava strata section at the Mokulaevsky stream
18.00-19.00	Transfer to Talnakh
20.00	Dinner at the hotel

	August 3, Sunday
07.45-08.45	Breakfast at the hotel
08.45-09.00	Transfer to Oktyabrsky and Taimyrsky mines
09.00-14-00	Group 1. Introductory training, selection of clothes and way-down into the Oktyabrsky mine
09.00-14-00	Group 2. Introductory training, selection of clothes and way-down into the Taimyrsky mine
14.00-15.00	Lunch at the hotel
15.00-16.20	Transfer from the hotel "Talnakh" through Norilsk to Zapolyarny mine («Medvezhy Ruchei»)
16.20-18.30	Visit of Zapolyarny open-pit mine ("Medvezhy Ruchei"). Studying of the rocks and ores of differentiated ore-bearing intrusion of the Norilsk complex
18.30-19.50	Transfer to Talnakh
20.00	Dinner at the hotel
	August 4, Monday
08.00-09.00	Breakfast at the hotel
09.00-9.15	Transfer to JSC Norilskgeologiya
9.15-13.00	Investigation of sections of plateau basalts and the Norilsk-1 intrusion (Maslovskoye deposit) with help of drill cores OM-1 and OM-3
13.00-14.00	Lunch at the hotel
14.00-17.30	Investigation of rock lithologies of the Talnakh and Kharaelakh intrusions from drill cores OUG-2, ZF-39 and EM-6
20.00	Dinner at the hotel
	August 5, Tuesday
08.00-09.00	Breakfast at the hotel
09.00-10.00	Transfer to the area of Mount Gudchikha (or the Listvyanka stream as an alternative)
10.00-13.00	Investigation and sampling rock lithologies of the Noril'sk-2 intrusion (or lower part of the tuff-lava section along the Listvyanka stream as an alternative)
13.00-14.00	Picnic lunch (sandwiches, vegetables, fruits, juices)
14.00-18.00	Completion of studying and sampling the the Noril'sk-2 intrusion (or tuff-lava strata section at Listvyanka)
18.00-19.00	Transfer to Talnakh
20.00	Dinner at the hotel
	August 6, Wednesday
07.45-08.45	Breakfast at the hotel
08.45-09.00	Transfer to Oktyabrsky and Taimyrsky mines
09.00-14-00	Group 2. Introductory training, selection of clothes and way-down into the Oktyabrsky mine
09.00-14-00	Group 1. Introductory training, selection of clothes and way-down into the Taimyrsky mine
14.00-15.00	Lunch at the hotel
15.00-15.45	Transfer from the hotel "Talnakh" to the Polar Division of Mining & Metallurgical Co. Norilsk Nickel
17.50-18.10	Meeting with managers of Polar Division of Mining & Metallurgical Company Norilsk Nickel. Summary of the visit; presentation of memorable gifts
20.00	Farewell Dinner at the hotel
	August 7, Thursday
05.30	Transfer to Noril'sk airport
08.30	Flight to Yekaterinburg

REFERENCES

1. Arndt, N.T., 2005. The conduits of magmatic ore deposits, in: Mungall, J. (Ed.), Exploration for platinum-group element deposits. Mineralogical Association of Canada Short Course 35, Oulu, Finland, pp. 181-201.
2. Arndt, N.T., Czamanske, G.K., Walker R.J., Chauvel, C., Fedorenko, V.A., 2003. Geochemistry and origin of the intrusive hosts of the Noril'sk-Talnakh Cu-Ni-PGE sulfide deposits. Economic Geology 98, 495-515.
3. Butler, J., 2012. Platinum 2012. Johnsom Matthey PLC, UK. 60 p.
4. Campbell, I.H., Czamanske, G.K., Fedorenko, V.A., Hill, R.I., Stepanov, V., 1992. Synchronism of the Siberian traps and the Permian-Triassic boundary. Science 255, 1760-1763.
5. Czamanske, G.K., Wooden, J.L., Zientek, M.L., Fedorenko, V.A., Zen'ko, T.E., Kent, J., King, B.S., Knight, R.J., Siems, D.F., 1994. Geochemical and isotopic constraints on the petrogenesis of the Noril'sk-Talnakh ore-forming system, in: Lighfoot, P.C., Naldrett, A.J. (Eds.), Proceedings of the Sudbury-Noril'sk Symposium, Special Publ. 5, Geological Survey, Ontario, pp. 313-342.
6. Czamanske, G.K., Zen'ko, T.E., Fedorenko, V.A., Calk, L.C., Budahn, J.R., Bullock, J.H., Fries, T.L., King, B.S., Siems, D.F., 1995. Petrography and geochemical characterization of ore-bearing intrusions of the Noril'sk type, Siberia; with discussion of their origin. Resource Geology Special Issue 18, 1-48.
7. Dalrymple, G.B., Czamanske, G.K., Fedorenko, V.A., Simonov, O.N., Lanphere, M.A., Likhachev, A.P., 1995. A reconnaissance $^{40}Ar/^{39}Ar$ study of ore-bearing and related rocks, Siberian Russia. Geochimica et Cosmochimica Acta 59, 2071-2083.
8. Distler, V.V., Grokhovskaya, T.L., Evstigneeva, T.L., Sluzhenikin, S.F., Filimonova, A.A., Dyuzhikov, O.A., 1988. Petrology of magmatic sulfide ore formation. Nauka, Moscow. 232 p. (in Russian).
9. Distler, V.V., Sluzhenikin, S.F., Cabri, L.J., Krivolutskaya, N.A., Turovtsev, D.M., Golovanova, T.A. et al., 1999. Platinum ores of the Noril'sk layered intrusions: the proportion of the magma and fluid concentration. Geologiya Rudnykh Mestorozhdenii 41, 241-265 (in Russian).
10. Distler V.V., Smirnov A.V., Grokhovskaya T.L., et al., 1979. Stratification, cryptic layering of trap intrusions and formation conditions of sulphide ore formation, in: Formation conditions of magmatic deposits. Nauka, Moscow, pp. 211-269 (in Russian).
11. Dobretsov, N.L., Kirdyashkin, A.A., Kirdyashkin, A.G., Vernikovsky, V.A., Gladkov, I.N., 2008. Modelling of thermochemical plumes and implicationsfor the origin of the Siberian traps. Lithos 100, 66-92.
12. Dodin D.A., Batuev B.N., 1971. Geology and petrology of the Talhakh differentiated intrusions and their metamorphic aureole, in: Petrology and ore resource potential of the Talnakh and Noril'sk differentiated intrusions. Nedra, Leningrad, pp. 31-100 (in Russian).
13. Dyuzhikov O.A., Distler V.V., Strunin B.M., et al. 1988. Geology and ore resource potential of the Noril'sk district. Nedra, Moscow, 279 p. (in Russian).
14. Dyuzhikov, O.A., Distler, V.V., Strunin, B.M., Mkrtychyan, A.K., Sherman, M.L., Sluzhenikin, S.F., 1992. Geology and metallogeny of sulfide deposits, Noril'sk region, USSR. Society of Economic Geologists. Special Publication. 242 p.
15. Dyuzhikov O.A. 1971. Picritic basalts of the Noril'sk district. Dokl. Akad Nauk SSSR 197 (6), 1406-1409 (in Russian).
16. Egorkin, A.V., Zyuganov, S.K., Chernyshev, N.M., 1984. Upper mantle of Siberia. 27-th Intern. Geol. Congress, Moscow. Geophysics 8, 27-42.
17. Egorov, V.N., Sukhanova, E.N., 1963. Talnakh ore-bearing intrusion in northwestern Siberian Platform. Exploration and protection of natural resources 1, 17-21 (in Russian).
18. Fedorenko V.A. 1981. Petrochemical series of volcanic rocks in the Noril'sk district. Geologiya i Geofizika 22 (6), 78-88 (in Russian).
19. Fedorenko V.A. 1991. Tectonic control of magmatism and localization of Ni-bearing areas in the northwestern Siberian Platform. Geologiya i Geofizika 32 (1), 48-56 (in Russian).
20. Fedorenko V.A. 1994. Evolution of magmatism as reflected in the volcanic sequence of the Noril'sk region, in: Proceedings of the Sudbury-Noril'sk Symposium, Special Publ. 5, Geological Survey, Ontario, pp. 171-184.
21. Geological map of Norilsk ore region at a scale of 1:200,000., 1991. Strunin, B.M. (ed.). Explanatory note, Geoinformmark, Moscow, 118 p. (in Russian).
22. Genkin A.D., Distler V.V., Gladyshev G.D., et al. 1981. Sulphide copper–nickel ores of the Noril'sk deposits. Nauka. Moscow, 234 p. (in Russian).
23. Godlevsky, M.N., 1959. Traps and ore-bearing intrusions of the Noril'sk region. Gostekhmetizdat, Moscow, (in Russian).
24. Ivanov, A.V., 2007. Evaluation of different models for the origin of the Siberian traps, in: Fougler, G.R., Jurdy, D.M. (eds.) The origin of melting anomalies: Plates, plumes and planetary processes, Special Paper Geol. Soc. Am., Vol. 430, 669-691.
25. Kamo, S.L., Czamanske, G.K., Krogh, T.E., 1996. A minimum U-Pb age for Siberian flood-basalt volcanism. Geochimica et Cosmochimica Acta 60, 3505-3511.
26. Komarova, M.Z., Kozyrev, S.M., Lyul'ko, V.A., Vilinsky, S.A., 2000. Precious-metal mineralisation of the disseminated ores from the Noril'sk ore-bearing district, in: Simonov, O.N., Malitch, N.S. (Eds.), Natural Resources of Taimyr 4. VSEGEI Press, Noril'sk, pp. 122-136 (in Russian).

27. Komarova, M.Z., Kozyrev, S.M., Simonov, O.N., Lyul'ko, V.A., 2002. The PGE mineralization of disseminated sulfide ores of the Noril'sk-Taimyr Region, in: Cabri, L.J. (Ed.), The Geology, Geochemistry, Nineralogy and Mineral Beneficiation of Platinum-Group Elements. Canadian Institute of Mining, Metallurgy and Petroleum 54, pp. 547-567.
28. Korovyakov, I.A., Nelyubin, A.E., Raikova, Z.A., Khortova, L.K., 1963. Origin of the copper-nickel sulfide ore-bearing Noril'sk trap intrusions. Proceedings VIMS 9, Gosgeotekhizdat, 101 p. (in Russian).
29. Kotulsky, V.K., 1946. About the origin of magmatic copper-nickel deposits. Doklady USSR Academy of Sciences 51, 381-384 (in Russian).
30. Kravtsov, V.F., 2003. History discoveries of copper-nickel deposits in the Noril'sk area. Essays on the history of discoveries of mineral deposits of Taimyr. Publishing House of SB RAS, Novosibirsk, 21-40 (in Russian).
31. Krivolutskaya, N.A., 2014. Evolution of trap magmatism and processes producing Pt-Cu-Ni mineralization in the Noril'sk area. KMK, Moscow, 320 p. (in Russian).
32. Krivolutskaya, N.A. Gongalskiy, B.I., Yushin, A.A., Schlychkova, T.B., Kononkova, N.N., Tushentsova, I.N., 2011. Mineralogical and geochemical characteristics of PGE-Cu-Ni ores of the Maslovsky deposit in the Noril'sk area, Russia. Canadian Mineralogist 49, 1649-1674.
33. Krivolutskaya, N.A., Sobolev, A.V., Snisar, S.G., Gongalskiy, B.I., Hauff, B., Kuzmin, D.V., Tushentsova, I.N., Svirskaya, N.M., Kononkova, N.N., Schlychkova, T.B., 2012. Mineralogy, geochemistry and stratigraphy of the Maslovsky Pt-Cu-Ni sulfide deposit, Noril'sk Region, Russia: Implications for relationship of ore-bearing intrusions and lavas. Mineralium Deposita 47, 69-88.
34. Latypov, R.M., 2002. Phase equilibria constraints on relations of ore-bearing intrusions with flood basalts in the Noril'sk region, Russia. Contributions to Mineralogy and Petrology 143, 438-449.
35. Latypov, R.M., 2007. Noril'sk- and Lower Talnakh-type intrusions are not conduits for overlying flood basalts: insights from residual gabbroic sequence of intrusions. Applied Earth Science (IMM Transactions Section B) 116, 215-225.
36. Lightfoot P.C., Hawkesworth C.J., Hergt J., et al., 1993. Remobilisation of the continental lithosphere by a mantle plume: major-, trace-element, and Sr-, Nd-, and Pb-isotope evidence from picritic and tholeiitic lavas of the Noril'sk district, Siberian Trap, Russia. Contributions to Mineralogy and Petrology 114, 171-188.
37. Lightfoot P.C., Naldrett A.J., Gorbachev N.S., et al., 1990. Geochemistry of the Siberian trap of the Noril'sk area, USSR, with implication for the relative contributions of crust and mantle to flood basalt magmatism. Contributions to Mineralogy and Petrology 104, 631-644.
38. Lightfoot P.C., Naldrett A.J., Gorbachev N.S., et al., 1994. Chemostratigraphy of Siberian trap lavas, Noril'sk district, Russia: implications for the source of flood basalt magmas and their associated Ni-Cu mineralization, in: Lightfoot, P.C. and Naldrett, A.J. (Eds.), Proceedings of the Sudbury-Noril'sk Symposium. Special Publ. 5, Geological Survey, Ontario, pp. 283-312.
39. Likhachev, A.P., 1994. Ore-bearing intrusions of the Noril'sk region, in: Lightfoot, P. C. & Naldrett, A. J. (Eds.), Proceedings of the Sudbury-Noril'sk Symposium, Spec. Publ. 5. Geological Survey, Ontario, pp. 185-201.
40. Lishnevsky, E.N., Distler, V.V., Egorkin, A.V., 2006. New data on deep structure of the Noril'sk ore district. Byull. MOIP. Otd. Geol. No. 4 (in Russian).
41. Lyul'ko, V.A., 1971. Localization of deposits of copper-nickel ore in the Noril'sk district, in: Geology and mineral resources of the Krasmoyarsk krai. Krasnoyarsk Knizhnoe Izd., Krasnoyarsk. pp. 32-35 (in Russian).
42. Lyul'ko, V.A., Fedorenko, V.A., Distler, V.V., Sluzhenikin, S.F., Kunilov, V.E., Stekhin, A.I. et al., 1994. Geology and ore deposits of the Noril`sk region, in: Distler, V.V., Kunilov, V.E. (Eds.), Guidebook of the VII International Platinum Symposium Moscow-Noril`sk. Moskovsky contact Press, Moscow.
43. Lyul'ko, V.A., Amosov, Y.N., Kozyrev, S.M., Komarova, M.Z., Ryabikin, V.A., Rad'ko, V.A., Simonov, O.N., Rochev, N.V., 2002. The state of the ore base of non-ferrous and noble metals in the Noril`sk region, with guidelines of top-priority geological and exploration works. Rudy i Metally 5, 66-82 (in Russian).
44. Malitch, K.N., Badanina, I.Yu., Belousova, E.A., Tuganova, E.V., 2012. Results of U-Pb dating of zircon and baddeleyite from the Noril'sk-1 ultramafic-mafic intrusion (Russia). Russian Geology and Geophysics 53(2), 123-130.
45. Malitch, K.N., Badanina, I.Yu, Tuganova, E.V., 2010a. Magmatic evolution of the ultramafic-mafic intrusions of the Noril'sk Province (Russia): Insights from compositional and geochronological data. Litosphera 10 (5), 37-63 (in Russian).
46. Malitch K.N., Belousova E.A., Griffin W.L., Badanina I.Yu., 2013. Hafnium-neodymium constraints on source heterogeneity of the economic ultramafic-mafic Noril'sk-1 intrusion (Russia). Lithos 164-167, P. 36-46.
47. Malitch, K.N., Belousova, E.A., Griffin, W.L., Badanina, I.Yu., Pearson, N.J., Presnyakov, S.L., Tuganova, E.V., 2010b. Magmatic evolution of the ultramafic-mafic Kharaelakh intrusion (Siberian Craton, Russia): insights from trace-element, U-Pb and Hf-isotope data on zircon. Contributions to Mineralogy and Petrology 159, 753-768.
48. Malitch, K.N., Latypov, R.M., 2011. Re-Os and S-isotope constraints on timing and source heterogeneity of PGE-Cu-Ni sulfide ores: a case study at the Talnakh ore junction (Russia). Canadian Mineralogist 49, 1653-1677.
49. Malitch, K.N., Latypov, R.M., Badanina, I.Yu., Sluzhenikin, S.F., 2014. Insights into ore genesis of Ni-Cu-PGE sulfide deposits of the Noril'sk Province (Russia): evidence from copper and sulfur isotopes. Lithos 204, 172-187.
50. Malitch, N.S., Grinson, A.S., Tuganova, E.V., Chernyshev, N.M., 1988. Rifting of the Siberian platform. 28th session of International Geological Congress. Tectonic processes. Nauka Press, Moscow, pp. 184-193 (in Russian).
51. Malitch, N.S., Mironyuk, E.P., Tuganova, E.V., Grinson, A.S., Masaitis, V.L., Surkov, V.S. et al., 1987. Geological structure of the USSR and regularities of distribution of mineral deposits, in: Malitch, N.S., Masaitis, V.L., Surkov, V.S. (Eds.), The Siberian Platform 4. Nedra Press, Leningrad.

52. Mitrofanov F.P., Bayanova T.B., Korchagin A.U., Groshev N.Yu., Malitch K.N., Zhirov D.V., Mitrofanonov A.F., 2013. East Scandinavian and Noril'sk plume mafic large igneous provinces of Pt-Pd ores: geological and metallogenic comparison. Geology of Ore Deposits 55 (5), 305-319 (translated from Geologiya Rudnykh Mestorozhdenii 55 (5), 357-373).
53. Naldrett, A.J., 2004. Magmatic sulphide deposits. Geology, geochemistry and exploration. Springer, Berlin Heidelberg New York. 727 p.
54. Naldrett, A.J., Lightfoot, P.C., Fedorenko, V. A., et al., 1992. Geology and geochemistry of intrusions and flood basalts of the Noril'sk region, USSR, with implications for the origin of the Ni–Cu ores. Economic Geology 87, 975-1004.
55. Natorkhin I.A., Arkhipova A.I., Batuev B.N. 1977. Petrology of the Talnakh intrusions. Leningrad, Nedra, 236 p. (in Russian).
56. Petrov, O.V., Malitch, K.N., Tuganova, E.V., Pushkarev, Yu.D., Badanina, I.Yu., Krymsky, R.S., Kapitonov, I.N., Distler, V.V., Sluzhenikin, S.F., Knauf, V.V., Belousova, E.A., Griffin, W.L., Romanov, A.P., Tuganova, S.M., Bocharov, S.N., Bogomolov, E.S., Prasolov, E.M., Khalenev, V.O., Lokhov, K.I., Matukov, D.I., 2009. Test-methodical investigations on elaborating isotope-geochemical criteria for prospecting platinum-group metals, gold, copper, nickel and cobalt in the layered intrusions of the northern Siberia (Krasnoyarsk region). Proceedings of VSEGEI – Year 2008, VSEGEI Press, St. Petersburg 8(56), 248-262 (in Russian).
57. Ramberg, I., Morgan, P., 1984. Physical characteristics and evolutionary trends of continental rifts, in: 27th International Geological Congress. Tectonics, Nauka Press, Moscow, pp. 78-109.
58. Rogover, G.B., 1959. Norilsk deposit 1. Gosgeoltechizdat, Moscow. 168 p.
59. Ryabov, V.V., Shevko, A.Ya., Gora, M.P., 2000. Igneous rocks of the Noril'sk district. V.1. Petrology of traps. Nonparel. Novosibirsk. 408 p. (in Russian).
60. Ryabov, V.V., Zolotukhin, V.V., 1977. Minerals of differentiated traps. Novosibirsk, Nauka. 392 p. (in Russian).
61. Sluzhenikin, S.F., Distler, V.V., Dyuzhikov, O.A., Kravtsov, V.E., Kunilov, V.E., Laputina, I.P., Turovtsev, D.M., 1994. Low sulfide platinum mineralization in the Noril'sk differentiated intrusive bodies. Geologiya Rudnykh Mestorozhdenii 36, 195-217 (in Russian).
62. Sotnikov, A.A., 1919. About operation of the Noril'sk (Dudinsky) deposits of coal and copper ore in connection with the practical implementation and development of the Northern Sea Route. Tomsk, 98 p. (in Russian).
63. Stepanov, V.K., Turovtsev, D.M., Avgustinchik, I.A., Zemskova, G.V., 1985. Geological and genetic model of sulphide copper-nickel ore magmatic system of the Noril'sk district, in: Abstracts of conference on genetic models of endogenic ore deposits. V. 1. UIGGM, Novosibirsk, pp. 104-105 (in Russian).
64. Sukhanova, E.N., 1968. Zoning of orebodies, intrusions, and tectonomagmatic clusters and its applied implications. In: Geology and mineral resources of the Noril'sk mining district. NTO Tsvetmet. Noril'sk, pp. 139-142 (in Russian).
65. Tuganova, E.V., 1991. Petrological geodynamical model of formation of sulfide copper-nickel deposits. Soviet Geology and Geophysics 32, 1-7.
66. Tuganova, E.V., 2000. Petrographic types, genesis and regularities of distribution of PGE-Cu-Ni sulfide deposits. VSEGEI Press, St. Petersburg (in Russian).
67. Tuganova, E.V., Shergina, Yu.P., 2003. Isotope-geochemical rock heterogeneity in ore-bearing Noril'sk-type intrusions: genetic considerations. Regional Geology and Metallogeny 17, 140-146 (in Russian).
68. Turovtsev, D.M., 2002. Contact metamorphism of the Noril'sk intrusions. Nauchny Mir, Moscow, 293 p. (in Russian).
69. Vaulin, L.L., Sukhanova, E.N., 1970. Oktyabrskoe copper-nickel deposit. Protection and prospecting 4, 48-52.
70. Walker, R.J., Morgan, J.W., Horan, M.F., Czamanske, G.K., Krogstad, E.J., Fedorenko, V.A., Kunilov, V.E., 1994. Re-Os isotopic evidence for an enriched-mantle source for the Noril'sk-type, ore-bearing intrusion, Siberia. Geochimica et Cosmochimica Acta 58, 4179-4197.
71. Wooden, J.L., Czamanske, G.K., Bouse, R.M., Likhachev, A.P., Kunilov, V.E., Lyul'ko, V., 1992. Pb isotope data indicate a complex mantle origin for the Norilsk-Talnakh ores, Siberia. Economic Geology 87, 1153-1164.
72. Wooden J.L., Czamanske, G.K., Fedorenko, V.A., et al. 1993. Isotopic and trace-element constraints on mantle and crustal contributions to Siberian continental flood basalts, Noril'sk area, Siberia. Geochimica et Cosmochimica Acta 57, 3677-3704.
73. Yakubchuk, A., Nikishin, A., 2004. Noril'sk-Talnakh Cu-Ni-PGE deposits: A revised tectonic model. Mineralium Deposita 39, 125-142.
74. Yang, J.-H., Wu, F.-Y., Chung, S.-L., Wilde, S.-A., Chu, M.F., 2006. A hybrid origin for the Qianshan A-type granite, northeast China: Geochemical and Sr-Nd-Hf isotopic evidence. Lithos 89, 89-106.
75. Zhang, M., O'Reilly, S.Y., Wang, K-L., Hronsky, J., Griffin, W.L., 2008. Flood basalts and metallogeny: The lithospheric connection. Earth-Science Reviews 86, 145-174.
76. Zolotukhin, V.V., Ryabov, V.V., Vasil'ev, Yu.R., Shatkov, V.A., 1975. Petrology of the Talnakh ore-bearing differentiated trap intrusion. Nauka, Novosibirsk, 432 p. (in Russian).
77. Zolotukhin, V.V., Vilensky, A.M., Nemenenok, T.I., et al., 1978. Petrology and outlook for ore resource potential of traps in the northern Siberian Platform. Nauka, Novosibirsk, 217 p. (in Russian).

Sluzhenikin S.F., Krivolutskaya N.A., Rad'ko V.A., Malitch K.N.,
Distler V.V., Fedorenko V.A.

Ultramafic-mafic intrusions, volcanic rocks and PGE-Cu-Ni sulfide deposits of the Noril'sk Province, Polar Siberia. Field trip guidebook.
12th International Platinum Symposium.
Edited by Simonov O.N.

Scientific publication

Managing editor: K.N. Malitch

Design and layout: I.M. Amromin, Compass Press

IGG UB RAS
620075, Yekaterinburg, Pochtovy 7

Signed in print 20.07.2014. Format 60x84 $^{1}/_{8}$. Offset Paper.
Conventional printed sheets 10.0.
Circulation 50 copies. Order number 1011.

Printed from the original layout in the AMB printery
620026, Yekaterinburg, Rosa Luxemburg, 59